Biochemical studies of enzymes involved in glycolysis of the thermoacidophilic crenarchaeon *Sulfolobus solfataricus*

Dissertation

zur Erlangung des akademischen Grades eines
Doktors der Naturwissenschaften
– Dr. rer. nat. –

vorgelegt von

Patrick Haferkamp

geboren in Essen

Institut für Molekulare Enzymtechnologie und Biochemie
der
Universität Duisburg-Essen

2011

Die vorliegende Arbeit wurde im Zeitraum von Januar 2008 bis August 2011 im Arbeitskreis von Prof. Dr. Bettina Siebers am Institut für Molekulare Enzymtechnologie und Biochemie der Universität Duisburg-Essen durchgeführt.

Tag der Disputation: 18.11.2011

Gutachter: Prof. Dr. Bettina Siebers
Prof. Dr. Daniel Hoffmann

Table of contents

1 Introduction

Since 1990, the leading opinion on the evolution of Life is that there are three major lines of living organisms: the Eukarya, and the two prokaryotic domains of the Bacteria and Archaea (Woese et al., 1990, Fig.1) based on studies of the universal small ribosomal RNA subunit (SSU rRNA). Archaea exhibit bacterial and eucarya-like features as well as (Archaea-) specific characteristics, absent in either of the two other domains. For example primases, helicases and replicative polymerases are part of the DNA replication apparatus in Archaea and Eukarya, but are completely unrelated to the bacterial system (Olsen and Woese, 1996). In contrast, archaeal cell size, presence of polycistronic transcription units as well as utilisation of Shine-Dalgarno sequences for translation are similar to the bacterial system (Londei, 2005). A unique feature of Archaea is the composition of the glycerol backbone of their membrane phospholipids, consisting of reduced ether-linked isoprenyl groups instead of ester bonds of fatty acids as in Bacteria and Eukarya (Kates, 1993).

Within the archaeal domain, three phyla (Fig.1) are accepted: Euryarchaeota, Crenarchaeota (Gribaldo and Brochier-Armanet, 2006) Korarchaeota (Barns et al., 1996) and the possible fourth phylum Nanoarchaeota is still under debate (Huber et al., 2002). Brochier-Armanet et al. (2008) proposed a re-classification of Archaea into only three phyla. Combined phylogenetic analyses of archaeal small subunit (SSU)/large subunit (LSU) rRNA sequences led to a proposed classification of Archaea into Eury-, Cren- and the newly proposed phylum called Thaumarchaeota. Archaea categorized as Thaumarchaeota are mesophilic and previously belonged to the Crenarchaeota (Brochier-Armanet et al., 2008).

The kingdoms of the Crenarchaeota and Korarcheaeota mostly consist of hyperthermophilic and thermoacidophilic organisms, whereas the Euryarchaeota include also halophilic and methanogenic species.

Archaea often live in extreme habitats. Psychrophilic Archaea are found at sites exhibiting temperatures between -10°C to 20°C, whereas thermophilic Archaea thrive in habitats with temperatures of 60°C to 80°C. Hyperthermophilic Archaea require temperatures of above 80°C to 120°C for growth. There are aerobic, microaerophilic and strictly anaerobic members and certain Archaea prefer low-salt freshwater habitats, while halophilic Archaea thrive at salt concentrations of up to 1.5 M NaCl (Grant and Larsen, 1989). According to their extreme lifestyle these Archaea are referred to as “extremophiles”. However, the extreme habitats are not only populated

by Archaea. Also very few extremophilic Bacteria and Eukarya (and even metazoans), like the thermotolerant “water bear” (tardigrades), which tolerates extreme conditions regarding temperature, pressure and radiation (Budd, G.E. 2001), are found.

Although Archaea are abundant in extreme environments, recent studies revealed that they are much more widespread in mesophilic habitats, such as marine plankton or soils, than previously thought (Broichier-Armanet, 2008).

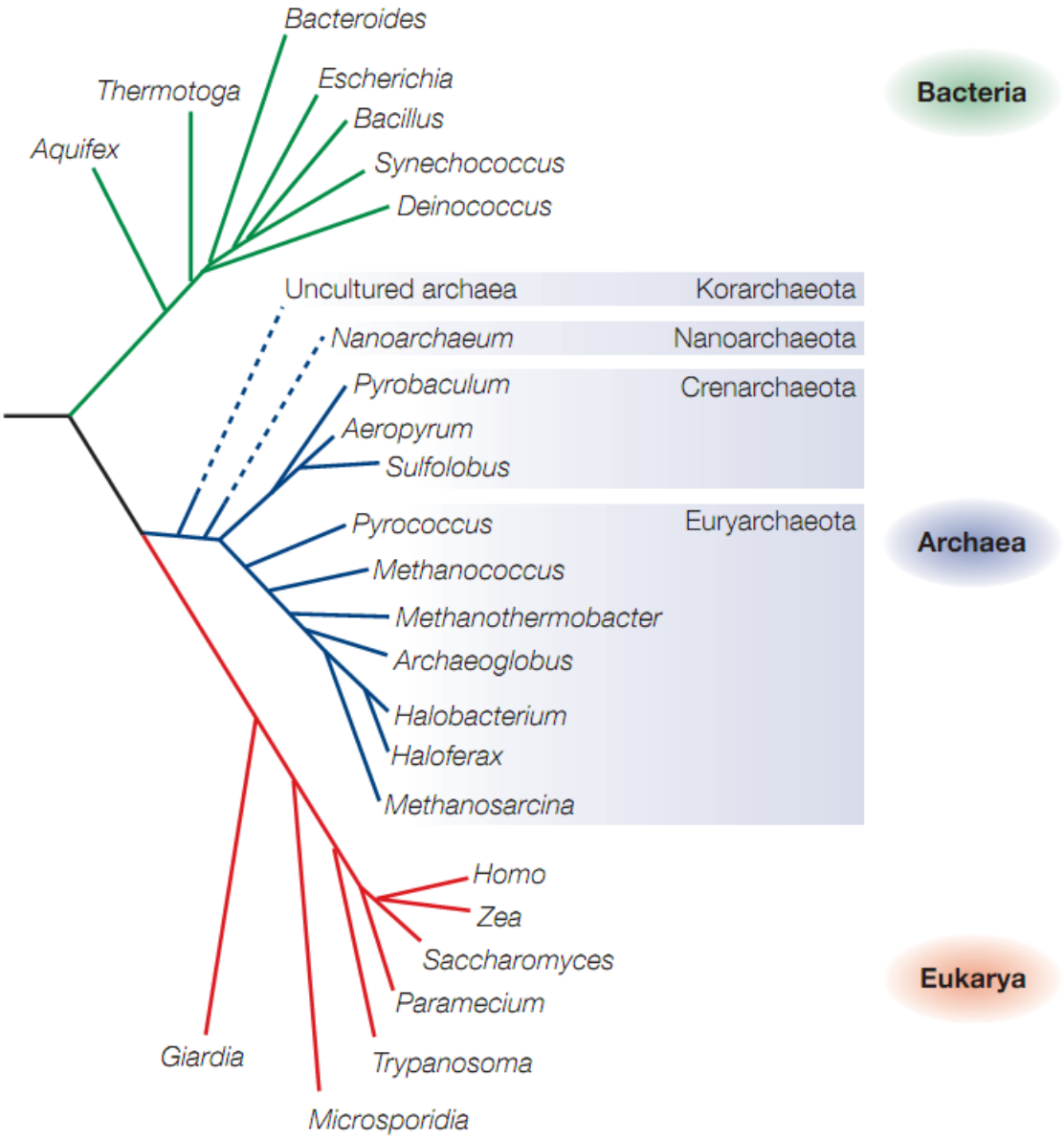

Fig. 1: Phylogenetic tree of the three domains of life: Eukarya, Bacteria and Archaea. The latter is devided in four phyla: The Crenarchaeota and Euryarchaeota next to the Nanoarchaeota and Korarchaeota. (T. Allers and M. Mevarech, 2006).

A wide diversity of archaeal physiology is known (Koonin, 2003), which correlates with the diversity of the archaeal metabolism. Comparative analyses of glycolytic pathways in hyperthermophilic Archaea show a variety of differences from the classical Embden-Meyerhof-Parnas (EMP) and the Entner-Doudoroff (ED) pathways that are present in Bacteria and Eukarya (Siebers and Schönheit, 2005). These variations of the classical bacterial and eukaryal routes are characterized by many novel archaeal enzymes. Most of the catalyzed reactions of the modified archaeal pathways match the classical glycolytic pathways in Bacteria and Eukarya, but most of the archaeal enzymes exhibit no similarity to their respective counterparts. Additionally, a large diversity of alternative (new) enzymes from different enzyme families is found in Archaea (Siebers and Schönheit, 2005).

The thermoacidophilic crenarchaeon *Sulfolobus solfataricus* (strain P2) is growing optimally at 80°C (60 – 92°C) and pH 2 – 4 (Zillig et al., 1980), but is able to maintain an intracellular pH at around 6.5 (Moll and Schäfer, 1988). The organism uses a variation of the classical ED pathway for sugar degradation (Ahmed et al., 2005). *S. solfataricus* is the archaeal model organism, because it unites several relevant properties: The genome of the P2 strain is completely sequenced and consists of a single 2,992,245 bp chromosome comprising a total of 3,032 annotated genes. It encodes 2,977 proteins, of which 40% appear to be Archaea-specific, whereas 12% and 2.3% are exclusively shared with the Bacteria and Eukarya, respectively (She et al., 2001). *S. solfataricus* is easily culturable under defined growth conditions (Grogan, 1989). Furthermore, and probably most important, the organism is genetically tractable. Methods for the generation of gene deletion mutants and proteinexpression have been established (Albers et al., 2009).

Additionally, heat stable proteins from thermo(acido)philes are of special interest for some biotechnological applications, since they outcompete enzymes of mesophiles in terms of resilience and production of heat stable bioproducts (Albers et al., 2009).

A modified version of the ED pathway that is generally referred to as the semi-phosphorylative ED pathway was firstly reported in the Bacterium *Rhodobacter sphaeroides* (Szymona and Doudoroff, 1958).

In the thermoacidophile *S. solfataricus* and the hyperthermophile *Thermoproteus tenax, both* member of the Crenarchaeota, the operation of both a semi-phosphorylative (sp) and a non-phosphorylative (np) ED branch (Fig.2), the so called "branched ED pathway", was verified by the combination of comparative genomic approaches and *in vitro* reconstruction experiments (Ahmed et al., 2005).

In *S. solfataricus*, the pathway is promiscuous not only utilized for the degradation of glucose but also of galactose. In the sp as well as in the np ED pathway, glucose or galactose is metabolized yielding 2-keto-3-deoxygluconate/-galactonate (KDG/KDGal) catalyzed by glucose dehydrogenase (GDH) and gluconate dehydratase (GAD), respectively (Ahmed et al., 2005). Following the np ED branch, KDG/KDGal is cleaved into one molecule of pyruvate and one glyceraldehyde (GA), by a bifunctional KD(P)G aldolase (KDPGA; Ahmed et al., 2005; Lamble et al., 2005). Glycerate is subsequently formed from GA to gain another molecule of pyruvate via 2-phosphoglycerate (2-PG) and phosphoenolpyruvate (PEP) formation (Selig et al., 1997; Kardinahl et al., 1999; Kehrer et al., 2007).

KDG metabolism via the sp ED branch is continued via the formation of 2-keto-3-deoxy-6-phosphogluconate/-galactonate (KDPG/KDPGal) catalyzed by KDG kinase (Ahmed et al., 2005; Lamble et al., 2005). KDPG/KDPGal is cleaved into pyruvate and glyceraldehyde-3-phosphate (GAP) catalyzed by the bifunctional KD(P)GA (Theodossis et al., 2004). From the formed GAP a second molecule of pyruvate is formed via the lower shunt of the EMP pathway. Further, 1,3-bisphosphoglycerate (1,3-BPG) is formed from GAP by GAP dehydrogenase (GAPDH) and further metabolized by phosphoglycerate kinase (PGK) to yield 3-phosphoglycerate (3-PG). Encoding a non-phosphorylating GAP dehydrogenase (GAPN), *S. solfataricus* is competent to directly form 3-PG from GAP in a non-phosphorylative one-step oxidation, which omits the formation of one molecule adenosine triphosphate (ATP). 3-PG is converted to 2-PG by phosphoglycerate mutase (PGAM). PEP formation from 2-PG is catalyzed by enolase; pyruvate kinase (PK) catalyzes pyruvate and ATP formation from PEP.

From kinetic data it has been suggested that, in general, the semi-phosphorylative ED pathway is favoured over the non-phosphorylative branch in *S. solfataricus*. However, under starvation conditions, i.e. lack of ATP necessary for KDG/KDGal phosphorylation, KD(P)G aldolase bifunctionality enables the organism to maintain pyruvate production for ATP synthesis via the citric acid cycle (Lamble et al., 2005).

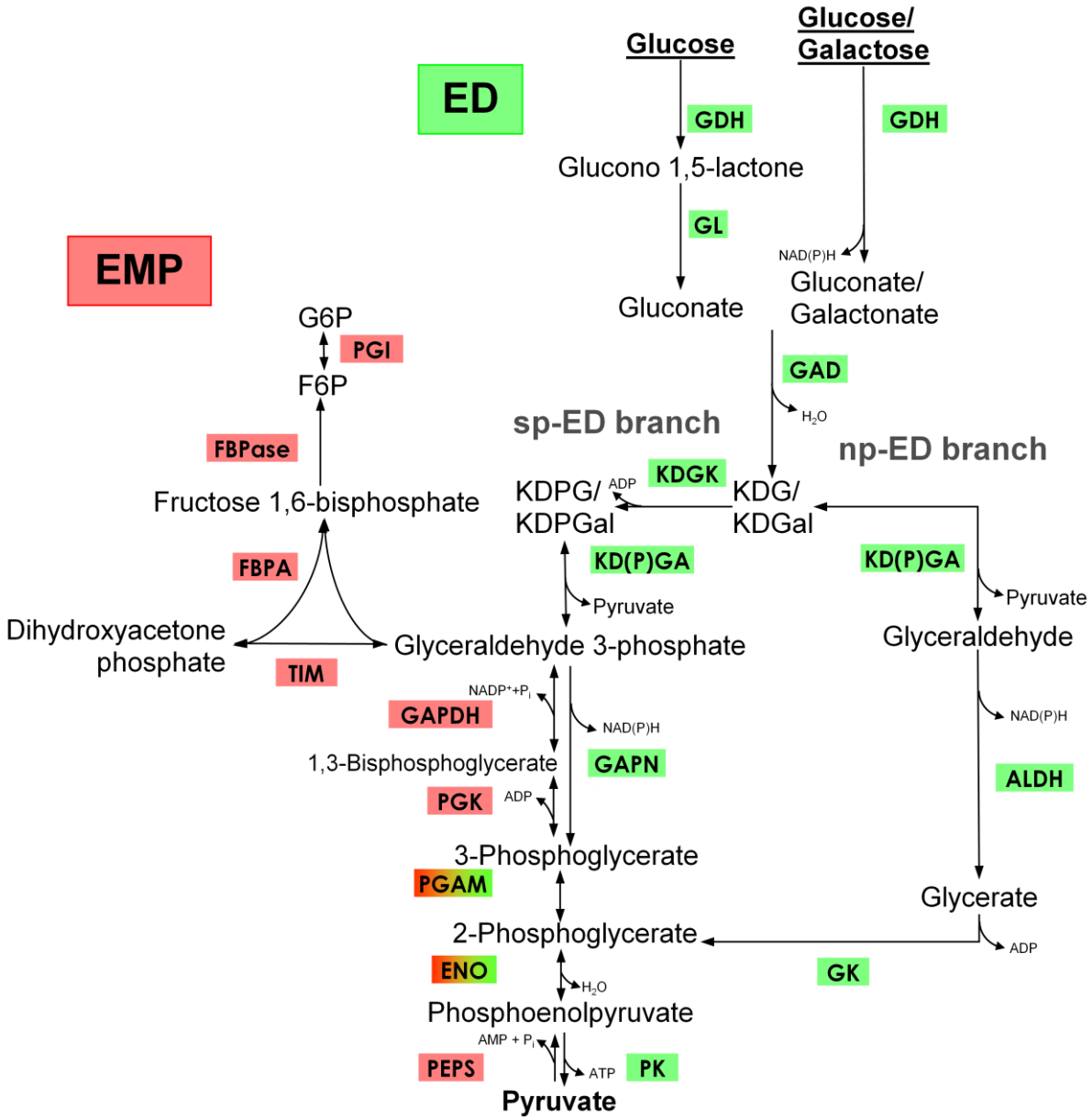

Fig. 2: Overview of the modified, branched ED pathway (green) and the EMP variant (red) pathway in *S. solfataricus* (abbreviations see appendix).

Life at high temperature requires a very efficient adaptation to temperature changes and it is unclear how biological networks can withstand and respond to such changes (Albers et al., 2009). The regulation of the CCM in Archaea e.g. in *S. solfataricus* is still unclear, including DNA, RNA, protein expression and kinetic properties.

In course of a transnational Systems Biology (SysMO) project called “Sulfolobus Systems Biology” (SulfoSYS) (http://www.sysmo.net/), 10 European partners collaborate in order to study the central carbohydrate metabolism (CCM), in particular the branched ED pathway, of *S. solfataricus* and its regulation under temperature variation by the integration of genomic, transcriptomic, proteomic, metabolomic, kinetic and biochemical information as well as modeling (Albers et al., 2009). The aim of SulfoSYS is the construction of a silicon cell model of the CCM network in *S. solfataricus*. The project is a systems biology approach to get insights into how the organisms metabolism is regulated at the different levels. The aim of the biochemistry workpackage is to contribute biochemical and kinetic information of enzymes to fill the CCM model of *S. solfataricus* with life. The major focus lies on the enzymes of the branched, promiscuous ED pathway.

An important prerequisite for the SulfoSYS project represents the reconstruction of the *S. solfataricus* CCM by the identification of “players”, i.e. enzymes playing a role in *S. solfataricus* glycolysis.

The first enzyme of the pathway, GDH SSO3204 (EC 1.1.1.47), catalyzes the $NAD(P)^+$ dependent oxidation of glucose to gluconate. The enzyme has been purified previously from cell extracts of *S. solfataricus* and has been shown to possess dual co-substrate (NAD^+/$NADP^+$) and broad substrate specificity (Giardina1986). Detailed enzymatic characterization of the recombinant enzyme (SSO3003, Lamble et al., 2003) and the available crystal structure (Milburn et al., 2006) allowed for further insights into the catalytic activity and promiscuity of GDH.

GDH belongs to the medium-chain alcohol/polyol dehydrogenase/reductase (MDR) branch of the pyridine nucleotide dependent alcohol/polyol/sugar dehydrogenase superfamily (Riveros-Rosas, 2003). In course of the pathway reconstruction (Zaparty et al. manuscript in preparation) several members of this superfamily were identified, raising questions about possible GDH isoenzymes in *S. solfataricus*. In previous studies, two alcohol dehydrogenases have been characterized (SSO2536 and SSO0764) (Chong, 2007).

Since it is difficult to predict function by sequence alone, the additional GDH candidate (SSO3204) was analyzed (Haferkamp et al., 2011).

The protein shows high similarity (61% amino acid sequence identity) to the previously characterized GDH of *S. solfataricus* (SSO3003) (Lamble et al., 2003, Milburn et al., 2006, Zaparty et al., manuscript in preparation).

Pyruvate kinase SSO0981, another key enzyme (EC:2.7.1.40) (PK) catalyzes the final step in glycolysis (Boyer P.D., et al 1962) the conversion of PEP to pyruvate with phosphorylation of ADP to ATP. Pyruvate is an essential intermediate that channels into several metabolic pathways and its conversion via PK and PEPS displays a typical control point in the classical EMP pathway of Bacteria and Eukarya. The enzyme requires magnesium or other divalent metalions for activity (Susan-Resiga D. and Nowak T., 2004). In vertebrates, four tissue-specific isozymes are found in liver (L) , red cells (R), muscle, heart and brain (M1), and early foetal tissue (M2). In plants, PK exists as cytoplasmic and plastid isozyme, while most Bacteria, lower Eukarya and Archaea possess only one enzyme, except in certain Bacteria, such as *Escherichia coli* that harbour two isoenzymes. All PK isoenzymes exhibit a homotetrameric structure with subunits of ~50 kDa residues. The structure of several PKs from various organisms has been determined (Strominger J.L., 1955). The protein comprises three to four domains: a small N-terminal helical domain (absent in bacterial PK), a beta/alpha-barrel domain, a beta-barrel domain (inserted within the beta/alpha-barrel domain), and a 3-layer alpha/beta/alpha sandwich domain. PK helps to control the rate of glycolysis, along with phosphofructokinase (PFK) and hexokinase (HK) in Bacteria and most Eukarya. Bacterial L-type PK possesses allosteric sites for numerous effectors, the activity is increased by fructose1,6-bisphosphate (F1,6BP) and lowered by ATP as well as alanine, therefore, when glucose levels are high, glycolysis is promoted, and when glucose levels are low, gluconeogenesis is promoted.

To date, only a few PKs from the archaeal domain of have been biochemically characterized, i.e. of the hyperthermophile *T. Tenax*, the moderate thermophile *Thermoplasma acidophilum* and *Archaeoglobus fulgidus*. In contrast, to bacterial and eukaryal PKs, archaeal PKs exhibit only a reduced regulatory potential (Siebers and Schönheit, 2005). For the *T. tenax* PK no response to allosteric effectors were found (Schramm et al., 2000), whereas, the PK from *T. acidophilum* is shown to be activated by AMP and the PK from *A. fulgidus* is inhibited by ATP, which could be reversed by higher PEP concentrations, suggesting a competitive inhibition (Johnsen, 2004; Potter, 1992).

The activity of a PEP synthetase (SSO0831, EC 2.7.9.2), the synthesis of PEP from pyruvate and ATP, was already shown in the 1960s in *E. coli* (Cooper and Kornberg, 1965). Since then, PEPS activity was shown for a lot of bacterial and archaeal

species. Deletion mutant experiments in *E. coli* and *Salmonella typhimurium* showed that the enzyme is crucial for growth on C3 substrates like pyruvate, lactate and alanine (Cooper and Kornberg, 1974). Further, for the archaeon *Methanothermobacter thermoautotrophicus*, PEPS plays an essential role for autotrophic growth in presence of CO_2 (Eyzaguirre et al., 1982). In *Pyrococcus furiosus* PEPS is required for growth on pyruvate (Schäfer and Schönheit, 1993). Multiple alignments of PEPS sequences show that those parts of the sequence are highly conserved that harbour the catalytic histidine group, which is located in the C-terminal domain of the enzyme and within the PEP/pyruvate binding site, as shown by computational and biochemical studies (Tjaden et al., 2006).

So far, little is known about the PEP/pyruvate formation, the initial step of the gluconeogenic EMP pathway, in *S. solfataricus*. PEPS is a member of the PEP-utilizing enzyme family, which also comprises pyruvate, phosphate dikinase (PPDK, EC 2.7.9.1). Additionally to a PEPS (SSO0883), also a putative PPDK (SSO2820) was annotated in the *S. solfataricus* genome.

Enolase (2-phospho-D-glycerate hydrolase, SSO0913, EC 4.2.1.11) catalyzes the reversible conversion of 2-PG to PEP and thus represents a gluconeogenic and a glycolytic enzyme. Enolases from a wide range of organisms have been studied and characterized. The *S. solfataricus* enzyme encoded by SSO0913 belongs to the enolase subfamily of the enolase superfamily (Gerlt and Babbitt, 2001). Enolases are members of the β-barrel class of enzymes (Farber and Petsko, 1990). They are dimeric and exhibit a weakly basic active site mediated by the amino acid lysine. The two enolase subunits are identical and require two divalent cations per active site for functionality (Qin et al., 2006; Sims et al., 2003). Enolases catalyse the β-elimination reaction of H_2O from 2-PG to form PEP (Babbitt et al., 1996) and vice versa (Pal-Bhowmick et al., 2004). Sequence alignments of three members of the enolase superfamily revealed divalent metal ions to be essential for the function of the enzymes (Babbitt et al., 1996). Mg^{2+}, Zn^{2+}, Mn^{2+} (Warburg and Christian, 1942) as well Fe^{2+} (Malmström, 1955) were found to be activating *Saccharomyces cerevisiae* enolase.

Warburg and Christian (1942) also showed an inhibitory effect of F^- on the activity of *S. cerevisiae* enolase. In several organisms enolases have been shown to possess diverse non glycolytic biological functions (moonlighting, Pal-Bhowmick, 2007), e.g. the degradation of RNA (Evguenieva-Hackenberg, E., 2008).

Phosphoglycerate mutase (PGAM; EC 5.4.2.1) belongs to the histidine phosphatase superfamily and is involved in both glycolysis and gluconeogenesis. PGAM catalyzes the essential interconversion of 2-PG and 3-PG of the reversible EMP pathway. The histidine phosphatase superfamily is separated into two branches, branch I and branch II. Archaea only contain members of branch I, indicating that their common ancestor must have completely lacked histidine phosphatases. Branch I members of the histidine phosphatase superfamily usually are cytoplasmic in Eukarya. Acquirement of branch I PGAMs might be due to lateral gene transfer (Rigden, 2008). PGAMs are either 2, 3-bisphosphoglycerate (2.3-BPG) independent (iPGAM) or 2.3-BPG dependent (dPGAM).

Co-factor dependent dPGAMs require small amounts (10µM) of 2.3-BPG for the interconversion of 3-PG and 2-PG as the enzyme has to be rephosphorylated after the substrate leaves the active site (Johnsen et. al., 2007).

PGAM from *S. solfataricus* is an cofactor-independent phosphoglycerate mutase (iPGAM) (Potters et al., 2003), which comprises one domain homologous to alkaline phosphatases (Jedrzejas M. J., 2000) and β-phosphoglucomutase, which is closely related to the phosphatase branch of the HAD (haloalkanoic acid dehalogenase) enzyme superfamily (Zhang G. et al.,2005). In all cases, transient phosphorylation of the enzyme is involved in catalysis (Rigden et al., 2008). Further, iPGAMs are structurally unrelated to dPGAMs and therefore, must have evolved separately (Johnsen et al., 2007) and only one example of a dPGAM in Archaea, in *T. acidophilum*, is known to date (Johnsen et. al., 2007). A possible cofactor dependent dPGAM (SSO2236) has also been predicted for *S. solfataricus* (Van der Oost et al., 2002) in addition to iPGAM (SSO0417), but this was not confirmed by functional analysis yet.

1.2 Aims of this study

The presented work shall contribute missing enzymatic information of the CCM of SSO in order to gain further insights into the effect of temperature changes on the network. Therefore, the identification of the enzymes involved in the network is necessary and will be performed by the biochemical analysis of the following predicted candidate enzymes: GDH-2 (SSO3204), PGAM (SSO0417), ENO (SSO0913), PK (SSO0981), PEPS (SSO0831), PPDK (SSO2820) dPGAM (SSO2236). The respective encoding genes of the *S. solfataricus* glycolysis (branched ED pathway) will be cloned, heterologously expressed in *E.coli*, purified and if the activity is confirmed will be charcterized in detail at different temperatures (50°C-88°C). Additionally, cell free extracts of *S.solfataricus* cells grown at three different temperatures (65°C, 70°C and 80°C) will be analyzed regarding the respective enzyme activities to provide data for modelling purposes and to confirm in vivo activity. Further, the temperature dependent stability of metabolic intermediates will be analyzed by the determination of half-lifes at different temperatures. The final goal of this study will be to provide data for the above mensioned silicon cell model in course of the SulfoSYS project.

2 Materials and Methods

2.1. Materials

2.1.1 Laboratory equipment

Agarose gel electrophoresis system	B1A EasyCast™, Owl Separation Systems (Portsmouth (USA)); Power supply: Consort E835 (MS Laborgeräte)
Autoclave	VARIOKLAV® Dampfsterilisator (H+P Labortechnik AG)
Balances	KERN EW 4200-2NM (Kern & Sohn GmbH) TE124S (Sartorius AG, Goettingen) TE601 (Sartorius AG, Goettingen)
Centrifuges	Mini Spin plus (Eppendorf AG, Hamburg) 5415 R (Eppendorf AG, Hamburg) SORVALL® RC6 (Kendro Laboratory Products GmbH, Langensbold)
Container	Medico 6 (LAUDA GmbH & Co. KG)
Diafiltration cups	Vivaspin 20, 10,000 MWCO PES (Sartorius Stedim Biotech S.A., Aubagne Cedex)
Dialysis membrane	Spectra/Por 3, MWCO: 3,500 Daltons (Spectrum® Laboratories, Inc.)
Fermenter	Infors HT Benchtop Bioreactor Minifors, (Infors AG, Bottmingen-Basel)
FPLC	BioLogic Duo Flow Pathfinder 20 system (BioRad Laboratories GmbH, Munich); System: F10 work station, MX-1 Mixer, 3-Tray rack, AVR7-3 Auto-injection valve, AVR9-8 Auto-selection-Valve AVR9-8, QuadTec UV/VIS Detektor mit 3 mm PEEK flow cell, System cable 25 (RS-232), BioFrac fraction collector
Gel documentation	Molecular Imager Gel Doc XR+ System (Bio-Rad Laboratories GmbH, München); Video copy processor: Mitsubishi P91W (Mitsubishi Electric Europe B.V., Ratingen); Software: Quantity One 4.6.5 (Bio-Rad Laboratories GmbH, München)

Gel filtration column	HiLoad 26/60 Superdex™ 200 prep grade (GE Healthcare, Munich)
Heated stirrer plate	POWERTHERM VARIOMAG® (H+P Labortechnik AG); agitator: MR 3001 (Heidolph Instruments GmbH & Co. KG, Schwabach)
Incubation shaker	Multitron Standard (Infors AG, Bottmingen-Basel)
Membrane vacuum pump	LABOPORT Typ:N816.3KN.18 (KNF Neuberger GmbH, Freiburg)
Microwave	Typ HF1612 (Siemens AG, Munich)
pH-electrode	SenTIX 81 pH 0-14/0-100°C/3mol/KCl (WTW GmbH, Weilheim)
pH-meter	WTW Series inoLab pH 720 (WTW GmbH, Weilheim)
Photometer	BioPhotometer Plus (Eppendorf AG, Hamburg); Specord® 200 (Analytik Jena, Jena) Controller: JUMO dTRON 308 (Analytik Jena, Jena)
SDS-PAGE system	Hoefer Mighty small II Model SE250-10A-75 (Hoefer Pharmacia Biotech Inc., San Francisco); Power supply: Consort E835 (MS Laborgeräte)
Shaker	POLYMAX 1040 (Heidolph Instruments GmbH & Co. KG, Schwabach)
Sterile bench	HERAsafe® KSP Class II Bio-safety Cabine (Kendro Laboratory Products GmbH, Langensbold)
Table top thermostate	Thermostat 5320 (Eppendorf AG, Hamburg)
Thermal cycler (for PCR)	C-1000 (Bio-Rad, Munich)
Thermostation	THERMOBOY (LAUDA GmbH & Co.KG)
Ultrasound processor	UP 200s (Hielscher Ultrasonics GmbH, Stuttgart, Deutschland)
UV light	UV-Flächenstrahler, Faust
Vortexer	MS 2 Minishaker (IKA® Werke GmbH & Co. KG)
Waterbath	THERMOMIX® UB (B. Braun Melsungen AG, Melsungen)

2.1.2. Chemicals and Plasmids

All chemicals and enzymes were purchased from Amersham Pharmacia Biotech Europe GmbH, Applied Biosystems, ARK Scientific, Bio-Rad Laboratories GmbH, Biometra, Difco Laboratories, Fermentas Life Science, Gerbu Biotechnik GmbH, Life Technologies, MBI Fermentas GmbH, Merck, QIAGEN, Roche Diagnostics GmbH, Roth GmbH, Schleicher & Schuell, SERVA Electrophoresis GmbH, Sigma-Aldrich, Tropix and VWR International in analytical grade. For heterologous expression the pET vector system (pET-15b, pET-11c; Novagen, pET302, pET-324; Albers et al., 2003) was used.

2.1.3 Antibiotics

Ampicillin	Sigma-Aldrich Chemie, Deisenhofen
Chloramphenicol	Sigma-Aldrich Chemie, Deisenhofen

2.1.4 Enzymes

*Bam*HI	Fermentas, St. Leon-Rot
CIP (intestinal alkaline phosphatase)	Promega GmbH, Mannheim
Enolase from rabbit muscle	Sigma-Aldrich Chemie, Deisenhofen
Glyceraldehyde-3-phosphate dehydrogenase from rabbit muscle	Sigma-Aldrich Chemie, Deisenhofen
KOD HIFI polymerase	Merck KGaA, Darmstadt
L-Lactic dehydrogenase from rabbit muscle	Sigma-Aldrich Chemie, Deisenhofen
*Nco*I	Fermentas, St.Leon-Rot
*Nde*I	Fermentas, St. Leon-Rot
Phosphoglycerate kinase from baker's yeast (*S. cerevisiae*)	Sigma-Aldrich Chemie, Deisenhofen
Pyruvate kinase from rabbit muscle	Sigma-Aldrich Chemie, Deisenhofen
T4 DNA ligase	Fermentas, St. Leon-Rot
Taq-polymerase	Promega GmbH, Mannheim
*Xho*I	Fermentas, St. Leon-Rot

2.1.5 Oligonucleotide sets for mutagenesis PCR

Construct/Primer	Sequence(5`- 3`)	Tm
PGAM _pET11c		
FP SSO0417NdeIF	gggggaatt**catatg**aagcaatataaaattc	56°C
RP SSO0417BglIIR	ggcggctcg**agatct**tcatgaaccgtatttctctgc	68°C
GDH_pET11c		
FP SSO3204NdeIF	gggggaatt**catatg**aaggcaatagtag	53°C
RP SSO3204BamHIR	ggcg**ggatcc**tcaaacccatgaaattactg	58°C
PK_pET324		
FP SSO0981BspHIF	ggggctcgag**tcatga**gaaagactaaaatagttgc	54°C
RP SSO0981XbaIR	ggcgg**tctaga**tcatttcttttgttgttctag	56°C
ENO_pET11c		
FP SSO0913NdeIF	ggggaagctt**catatg**attaaccgtttttcc	62°C
RP SSO091BglIIR	ggcggctcg**agatct**tcaaagataaaaatattttcc	56°C
SSO2820_pET11c		
FP SSO2820NdeIF	gggggaatt**catatg**aactatacatacttac	54°C
RP SSO2820BamHIR	ggcgg**ggatc**ctcaaaattcgggatacaatcg	57°C
SSO2236_pET11c		
FP SSO2236NdeIF	gggggaattcatatggagaaatataacaac	60°C
RP SSO2236BamHIR	ggcggggatcctcaaataatattaatatcgag	57°C

PEPS_pET11c SSO_0883 PEPS was synthesized by Eurofins MWG

2.1.6 Kits

DNA extraction from agarose gels	Promega Wizard SV Gel and PCR Clean-Up System (Promega)
Nucleotide removal	QIAquick Nucleotide Removal Kit (Qiagen)
Plasmid purification	QIAprep Spin Miniprep Kit (Qiagen)
	QIAfilter Plasmid Midi Kit (Qiagen)
	GeneJET™ Plasmid Miniprep Kit (Fermentas)
	innuPREP Plasmid Mini Kit (Analytik Jena)
Genomic DNA Extraction	DNEasy Blood and Tissue (Quiagen)

2.1.7 Strains and growth conditions

Escherichia coli K12 DH5α strain; DSMZ 6897 (Hanahan, 1983)

Escherichia coli Rosetta (DE3); Novagen (Studier and Moffatt, 1986)

Escherichia coli BL21(DE3); Novagen (Studier and Moffatt, 1986)

Escherichia coli BL21-CodonPlus(DE3)-RIL; Stratagene (Carstens and Waesche, 1999)

E. coli K12 strains DH5α and Rosetta (DE3) were grown under aerobic conditions in 5 – 100 ml batch cultures in reaction tubes and Erlenmeyer flasks, respectively, at 37°C with shaking (180 rpm). Cultures grown in a fermenter (4500 ml) were stirred at 750 rpm and aerated (1 bar). Cultures were grown in lysogeny broth (LB) medium. Foam generation due to stirring and aeration was prevented via addition of antifoam (25 µl/L of culture; Sigma). For preparation of solid medium plates 1.5% (w/v) agar-agar was added to the LB medium. Antibiotics were added according to the encoded plasmid resistance in the following concentrations: Ampicillin 100 µg/ml and chloramphenicol 34 µg/ml. Growth in liquid cultures was monitored spectrophotometrically at 600 nm (OD_{600}).

2.1.8 Bioinformatics

Clone Manager (Sci-Ed Software):	Location of appropriate restriction sites for design of oligonucleotides
OriginPro 8 (OriginLab Corporation):	Michaelis Menten curve fitting; Determination of parameters for enzyme characterisation
WINASPECT® (Analytik Jena, Jena):	Enzyme assay performance
Emboss (**E**uropean **M**olecular **B**iology **O**pen **S**oftware **S**uite)	DNA and aminoacid sequence analysis
Bio Edit (Ibis Therapeutics, Carlsbad,CA)	Sequence analysis and alignments

2.1.9 Internet databases and tools

Braunschweig Enzyme Database (BRENDA)	Electronic information resource comprising molecular and biochemical information on enzymes which have been classified by the IUBMB
UniProt	Resource of protein sequence and functional information http://www.uniprot.org/
NEBcutter V2.0	Programme from New England BioLabs® Inc. to find restriction sites in gene sequences
ClustalX 2.0.12	Multiple alignment of protein sequences (Larkin et al., 2007)
LALIGN	Local similarity comparison of two sequences (Huang and Miller, 1991)
BLAST	Database serach and comparison of DNA and protein sequences (Altschul et al., 1997) www.ncbi.nih.nlm.gov/blast
TIGR (The Institute for Genomic Research)	Microbial DNA and protein database http://www.jcvi.org/

2.2 Techniques Molecular Biology

2.2.1 Qualitative and quantitative analysis of DNA

DNA quantification was performed spectrophotometrically at a wavelength of λ = 260 nm. An absorbance (A_{260}) of 1.0 corresponds to 50 µg of double stranded (ds) DNA per ml (Sambrook and Russell, 1989). DNA size was analysed via digestion using restriction enzymes and subsequent agarose gel electrophoresis.

2.2.2 Purification of DNA fragments

In order to extract and purify DNA fragments from agarose gels the Promega Wizard SV Gel and PCR Clean-Up System (Promega) was applied. Gene fragments subjected to restriction via restriction enzymes were purified using the QIAquick Nucleotide Removal Kit (Qiagen). DNA purification was performed following manufacturer's instructions.

2.2.3 Agarose gel electrophoresis of DNA

Agarose gel electrophoresis was used for many applications, such as the quick estimation of DNA yield and purity, determination of the size of PCR reaction products and DNA gel extraction. Agarose gels with an agarose concentration of 1 % prepared in 1X TAE-buffer (50X TAE-buffer: 2 M Tris-HCl, 1 M acetic acid, 50 mM EDTA, pH 8.0) were used for all applications. The DNA samples were mixed with loading buffer (6X: 0.21 % bromophenol blue, 0.21 % orange G, 50 % glycerol and 0.2 M EDTA (pH 8)) and applied to the gel. Depending on the designated segregation quality of DNA bands and the chosen size of the gel chamber (distance of the electrodes) voltage was adjusted at 100-120 V and the gel run was performed at room temperature (RT). DNA samples were run in parallel with a size marker (GeneRuler^{TM} 1kb DNA Ladder, ready-to-use; Fermentas). For visualisation of fluorescing DNA under UV light, the gels were incubated in an ethidium bromide bath (500 µg/l) at room temperature for ca. 30 min and destained in an H_2O bath for 5 min. The results were documented using the Molecular Imager Gel Doc XR+ System (Bio-Rad).

2.2.4 Amplification of genomic and plasmid DNA via polymerase chain reaction (PCR)

PCR is used for specific amplification of DNA and for the introduction of restriction sites at the beginning and at the end of specific DNA fragments (PCR mutagenesis). During PCR, DNA is denatured at high temperature, specific oligonucleotide primers anneal to the DNA, which is subsequently elongated by a DNA polymerase in cyclic manner at lower temperature. For DNA amplification 50–100 ng genomic DNA template, 0.4 µM each of the forward and the reverse primer (Invitrogen, 2.5), 200 µM dNTPs (Novagen), 10X Buffer #1 (Novagen) and 1 unit (u) of DNA polymerase (KOD HiFi DNA Polymerase; Novagen) were used. The PCR reaction was performed using the thermocycler C-1000 (Bio-Rad). Standard PCR amplification conditions were set as specified below (annealing temperature was adjusted to primer sets; 2.1.5):

95°C, 2 min		
95°C, 15 s	Denaturing	34 cycles
55°C, 30 s	**Annealing**	
72°C, 50 s	Elongation	
72°C, 5 min	Final elongation	
8°C, ∞		

The denaturing, annealing and elongation steps were repeated 34 times. PCR products were analysed via agarose gel electrophoresis (2.11.3).

2.2.5 Amplification of genomic DNA and plasmid DNA by PCR

For PCR amplification, 50–100 ng genomic DNA template, 1 µM each of forward and reverse primers (Invitrogen), 1.5 mM $MgCl_2$, 200 µM dNTPs (Life Technologies) 10 x reaction buffer (Novagen) and 1 unit of DNA polymerase (KOD polymerase) (Novagen) was used. The PCR reaction was performed using a thermocycler T-1000 (BioRad).

2.2.6 DNA and vector restriction

PCR products were restricted applying 500-1000 ng of dsDNA. The DNA was incubated with 10 units (10 U/µl) of restriction endonuclease (Fermentas) each in 1X restriction buffer O (Fermentas) at 37°C overnight. Restriction was performed in a total volume of 20 µl. Restricted fragments were isolated via agarose gel electrophoresis and recovered from the gel using the Promega Wizard SV Gel and PCR Clean-Up System (Promega) following manufacturer's instructions.

Vector (1500 ng) was digested applying one unit of restriction enzyme (Fermentas) each in 2X buffer Tango (Fermentas) at a total volume of 20 µl incubated at 37°C overnight.

2.2.7 5`-Dephosphorylation of the linearized vector DNA

In order to avoid the self-ligation of restricted vector DNA, the 5'phosphate group was eliminated by treatment with calf intestinal alkaline phosphatase (CIP) (Promega), by which 0.05 units of CIP/pmol DNA was added to the restriction reaction and incubated at 37°C for 1 hour.

2.2.8 Ligation of vector DNA and insert

DNA ligation was performed by incubating the restricted DNA inserts with the restricted linearized dephosphorylated vector in the presence of T4 DNA ligase [BANKIER et al. 1987]. DNA ligase catalyses the formation of a phosphodiester bond between the 3' hydroxyl of one nucleotide and the 5' phosphate of another nucleotide. For ligation, equimolar amounts of restricted plasmid DNA and insert at the ratio of 1:3 were used. DNA (8 µl total volume) was incubated at 45°C for 5 minutes and chilled on ice. 1 µl of 10 x reaction buffer (400 mM Tris-HCl, 100 mM MgCl2, 100 mM DTT, 5mM ATP, pH 7.8) and 1 µl T4 DNA ligase (1unit/µl) (MBI Fermentas) were added to a final volume of 10 µl. Ligation was carried out overnight at 4°C or for 2 hours at 16°C and subsequently T4 DNA Ligase was inactivated by incubation at 70°C for 10 minutes. Ligated DNA was stored at –20°C.

2.2.9 Preparation of competent *E. coli* cells

In order to enable *E. coli* strains DH5α and Rosetta (DE3) to take up recombinant plasmid DNA, cells have to be in a competent state. Preparation of chemocompetent and electrocompetent cells, respectively, is described in the following.

Chemocompetent cells ($CaCl_2$ method):

A volume of 100 ml LB medium was inoculated with 1 ml overnight culture of the respective *E. coli* strain. Incubation was performed at 37°C, 180 rpm until an OD_{600} of 0.6 was reached. Cells were incubated on ice for 5 min, centrifuged (6000 x g, 6 min, 4°C) and were kept on ice throughout the following steps. The cell pellet was gently re-suspended in 40 ml ice cold buffer I (30 mM KAc, 10 mM $CaCl_2$, 50 mM $MnCl_2$, 100 mM KCl, glycerol (87%) 15 % (v/v), cells were incubated on ice for 5 min and centrifuged (6000 x g, 6 min, 4°C). The resulting pellet was resuspended in 4 ml ice

cold Buffer II (10 mM MOPS, 75 mM $CaCl_2$, 10 mM KCl, glycerol (87%) 15 % (v/v), pH 7.0). The suspension was stored in aliquots of 80 µl at a temperature of - 80 °C.

2.2.10 Electrocompetent cells:

A volume of 100 ml LB medium was inoculated with 1 ml overnight culture of the respective *E. coli* strain. Incubation was taken out at 37°C, 180 rpm until an OD_{600} of 0.7 - 1 was reached. Cells were incubated on ice for 15 min, centrifuged (6000 x g, 10 min, 4°C) and kept on ice throughout the following steps. Cells were washed with 200 ml H_2O bidest. (4°C) and centrifuged (6000 x g, 10 min, 4°C). The resulting cell pellet was resuspended in 3 ml H_2O bidest. The cell solution was centrifuged (6000 x g, 10 min, 4°C) and the resulting cell pellet was resuspended in 4 ml of glycerol (10 %, 4°C). The electrocompetent cells were quick-frozen in liquid nitrogen in aliquots of 40 µl.

2.2.11 Transformation of competent *E. coli* strains DH5α and Rosetta (DE3)-RIL

A volume of 80 µl of competent cells of *E. coli* strain DH5α and Rosetta (DE3)-RIL, respectively, was gently mixed with plasmid DNA and incubated on ice for 45 min. After a 45 s heat shock at 42°C, the cells were incubated again on ice for 2 min and afterwards at 37 °C for 45 min, 180 rpm in 600 µl of LB-medium. Cells were centrifuged and the supernatant was discarded. Cell pellet was resuspended in remaining LB-medium and plated on a LB agar plate containing the antibiotic ampicillin (amp; 100 µg/ml). After overnight incubation at 37°C single colonies were checked for positive clones via colony PCR (2.11.10) and plasmid restriction.

For electroporation 40 µl of electrocompetent *E. coli* DH5α cells were gently mixed with 1 µl of plasmid DNA and transferred to a cooled (-20°C) electroporation cuvette (Gene Pulser Cuvette, 0.1 cm gap, Bio-Rad). For electroporation using the Gene Pulser Xcell System (Bio-Rad) a preset protocol for transformation of *E. coli* cells was used (1800 V, 25 µF, 200 Ω, 4.8 ms time constant). A volume of 600 µl of LB-medium was added to the cells, transferred to a 1.5 ml reaction tube and incubated at 37°C, 180 rpm for 45 min and the cells were plated on LB agar plates containing the antibiotic amp (100 µg/ml) as described above. After incubation overnight at 37°C single colonies were checked for positive clones via colony PCR (2.11.10) and plasmid restriction.

2.2.12 Colony PCR

Colony PCR is based on standard PCR using genomic DNA from a colony as template and the respective specific oligonucleotides (forward and reverse). This method allows for a rapid screening of ligation success. For colony PCR GoTaq® Polymerase (Promega) was used. DNA was amplified with cell material from positive clones picked with a sterile pipette tip as a template. 0.5 µM of the forward and the reverse primer (Invitrogen, see 2.5) each, 200 µM dNTPs (Novagen), 5X Green GoTaq® Reaction Buffer (Promega) and two units of GoTaq® Polymerase (Promega) were applied. The PCR reaction was performed via the thermal cycler C-1000 (Bio-Rad).

2.2.13 Plasmid preparation

Plasmid-DNA used for restriction analyses, cloning procedures and transformation of the expression strain was isolated by the QIAprep Spin Miniprep Kit (Qiagen), the QIAfilter Plasmid Midi Kit (Qiagen), the GeneJET™ Plasmid Miniprep Kit (Fermentas) and the innuPREP Plasmid Mini Kit (Analytik Jena), respectively, according to manufacturers' instructions.

2.2.14 DNA sequencing

DNA sequencing was performed to verify the sequence information of genes cloned prior to transformation of *E. coli* Rosetta (DE3) RIL for protein expression. Automated DNA sequencing (Sanger et al., 1977) was done by AGOWA (Berlin).

2.2.15 Heterologous gene expression in *E. coli* Rosetta (DE3) pRIL

The constructs were transformed into competent cells. The cells were cultivated in a 5 l fermenter (Minifors, Infors HT) containing 4.5 L of LB-medium, 100 µg/ml ampicilin (amp), 34 µg/ml chloramphenicol (camp) and 25 µl/l LB-medium of antifoam 204 (Sigma). The LB-medium was inoculated with 90 ml (2 % (v/v)) of a 100 ml overnight culture of the expression strain *E. coli* Rosetta (DE3) RIL or *E.coli* BL21 (DE3). Fermentation was performed at 37°C, 750 rpm, aeration (1 bar).

Gene expression was induced at an OD_{600} of 0.5 to 0.8 (exponential phase) adding isopropyl-beta-D-thiogalactopyranoside (IPTG) to a final concentration of 1 mM. The cells were grown until stationary phase was reached and were harvested by centrifugation (5465 x g, 20 min, 4°C), subsequently. The clones (DH5α, Rosetta (DE3) RIL and BL21 (DE3)) were also stored as glycerol stocks (25 % (v/v) glycerol) at -20°C and -70°C, respectively.

Constructs (see 2.1.5) were transformed into competent cells of *E. coli* Rosetta (DE3) RIL. The cells were cultivated in a 500 ml Erlenmeyer flask containing 200 ml of LB-medium, 100 µg/ml amp and 34 µg/ml camp. The medium was inoculated with a 5 ml overnight culture (2 % (v/v)) of the expression strain *E. coli* Rosetta (DE3) RIL. The culture was incubated at 37°C, 180 rpm. Gene expression was induced at an OD_{600} of 0.5 to 0.8 (exponential phase) adding isopropyl-β-D-1-thiogalactopyranoside (IPTG) to a final concentration of 1 mM. The cells were grown for 3 hours and harvested (5000 x g, 20 min, 4°C). The clones (DH5α, Rosetta (DE3) RIL and BL21 (DE3)) were also stored as glycerol stocks (25 % (v/v) glycerol) at -20°C and -70°C, respectively.

2.3 Techniques Biochemistry

2.3.1 Determination of protein concentration

Protein concentrations (mg/ml) were determined with the Bio-Rad Protein assay based on the method of Bradford (Bradford, 1976) following the manufacturer's instructions. Bovine serum albumin (BSA) was applied as a standard (2-10 mg/ml).

2.3.2 SDS-Polyacrylamide gel electrophoresis (SDS-PAGE)

Enrichment, purification and the size of proteins was monitored by SDS-PAGE according to Laemmli (1970). In the presence of sodium dodecylsulfate (SDS) polypeptides denature into their primary structure. This is achieved by the anionic character of SDS. SDS binds, unfolds and confers an almost uniform negative charge to the polypeptide along the entire peptide strand. The denatured, negatively charged proteins are separated, travelling from cathode to anode, through the gel matrix with different velocities depending on their size but independent of their native charge and shape. SDS-gels were composed of a 4 % stacking gel (4.0 % (w/v) acrylamide-bisacrylamide (30 %), 125 mM Tris-HCl, pH 6.8 (RT), 0.1 % (w/v) SDS (10%), 0.45 % (w/v) ammoniumpersulfate (APS, 100 mg/ml), 0.1% (v/v) N,N,N´,N´-Tetramethylethylenediamine (TEMED)) and a 12.5 % resolving gel (12.5 % (w/v) acrylamide-bisacrylamide (30 %), 375 mM Tris-HCl, pH 8.8 (RT), 0.1 % (w/v) SDS, 0.7 % (w/v) APS (100 mg/ml), 0.067 % (v/v) TEMED). Gel runs were performed in a continuous buffer system (25 mM Tris-HCl, 192 mM glycine, 3.5 M SDS (pH 8.3, RT)). For electrophoresis either the Mighty Small II (SE250/SE260) System (Amersham Pharmacia Biotech AB, 10 × 8 cm) or the Mini-PROTEAN Tetra Electrophoresis System (Bio-Rad) was used. SDS-gel runs were performed at 20 mA. Prior to application the protein samples were mixed with loading buffer to a final concentration of 62.5 mM Tris-HCl, pH 6.8, 10% glycerol, 2% SDS, 5% DTT and 0.005% bromophenol blue. The samples were incubated at 95°C for 4 minutes for denaturation and applied to the SDS gel along with 5 µl of protein marker (PageRuler^{TM} Prestained Protein Ladder, Fermentas), covering a molecular size range of 10-170 kDa. After electrophoresis protein gels were stained with a staining solution (0.05% Serva BlueR, 40% methanol, 10% acetic acid) for 30 - 45 min at RT (Weber and Osborn, 1969). Preliminary de-staining of the protein gels was performed in tap water and boiling using a microwave (800w, 2 min). This step was repeated three times using fresh tap water. For complete de-staining the gels were incubated

in tap water overnight at room temperature. Gel documentation was performed using the Molecular Imager Gel Doc XR+ System (Bio-Rad) in combination with the Quantity One Software Package (Bio-Rad).

2.3.5 Preparation of *S. solfataricus* crude extracts (Zaparty et al 2010)

Resuspension of 0.5 g (wetweight) cells in 1.5 ml 0.1 M HEPES/KOH buffer, pH 7 at room temperature, containing 5 mM DTT and 250 µl Protease Inhibitor (Roche). Cell disruption is carried out by sonication (2 min pulse/1 min cooling). After centrifugation (1h, 21,000g, 4°C) the supernatant is dialyzed overnight against 100 mM Hepes-KOH, pH 7 (RT). For determination of protein concentration the BioRad Protein Assay based on the Bradford protein quantitation method (Bradford 1976, modified) is used. Between 0.25–1 mg total protein is used for the different enzyme assays using crude extracts.

2.3.4 Crude extracts and heat precipitation

Recombinant *E. coli* cells harvested after gene expression (10 g, wet weight;) were re-suspended in 30 ml (3 ml/g) 100 mM Hepes-KOH, pH 7 (RT). Cell disruption was performed applying ultrasound (ultrasound processor UP 200s (Hielscher Ultrasonics GmbH)) at an intensity of 50% for 4 x 5 min interrupted by intervals of 30 s on ice to avoid temperature increase. The solution was kept on ice during sonication. Cell debris and unbroken cells were removed by centrifugation (21,000 x g, 1 h, 4°C). The resulting crude extract was diluted 1:1 with 100 mM Hepes-KOH, pH 7 (RT). *S. solfataricus* proteins were enriched via heat precipitation for 20 min at 80°C. Precipitated proteins were removed via centrifugation (21,000 x g, 1 h, 4°C).

2.3.6 Dialysis

Dialysis was performed in order to remove salts and low molecular weight substances from protein extracts interfering with subsequent purification steps and/or in order to change buffer conditions. Protein extracts to be purified were transferred to dialysis tubes pre-incubated in respective dialysis buffer. In preparation for ion exchange chromatography (IEC) the protein solution was dialysed against 20 mM Hepes-KOH, pH 7 (RT). Protein extracts subjected to gel filtration were dialysed against 50 mM Hepes-KOH, 300 mM KCl, pH 7 (RT). Dialyses were performed using Spectra/Por 3 (Spectrum® Laboratories, Inc.) dialysis membranes with a 3,500 Dalton molecular weight cut-off (MWCO) in dialysis buffer (100 to 500 times sample volume) at 4°C, stirring. After 2 h the dialysis buffer was exchanged for fresh dialysis buffer. Dialysis was continued overnight at 4°C.

2.3.7 Ion exchange chromatography

The supernatant obtained from centrifugation following heat precipitation was dialysed against 4 L of 20 mM Hepes-KOH, pH 7 (RT) at 4°C (see 2.12.4). The following steps were used as standard procedur for all recombinant proteins in this work. Ion chromatography was performed using a continuous bed ion exchange column (Q-Sepharose Fast Flow, GE Healthcare, column volume 17.7 ml, column dimensions: 15 x 68 mm). The column was washed using filtered (Sartorius stedim biotech,

0.2 µm cellulose acetate filter) double distilled water (H_2O bidest.) and equilibrated with five column volumes of running buffer (20 mM Hepes-KOH, pH 7 (RT)). The protein sample was applied to the column (68 ml). Sample application was followed by a washing step applying 10 column volumes of running buffer. The protein was eluted via a continuous gradient of 0 – 1 M NaCl in 20 mM Hepes-KOH, pH 7 (RT) (336 ml, flow rate: 5 ml/min). Enzyme containing fractions were pooled and dialysed against 5 L of 20 mM Hepes, pH 7 (RT) for 2 h. The sample volume was reduced to 4.5 ml via centrifugation (3000 x g, 4°C) using Vivaspin 20 diafiltration cups (10,000 MWCO PES, Sartorius Stedim Biotech). The protein solution was stored at 4°C.

2.3.8 Gel filtration

The protein solution obtained from ion exchange chromatography was dialysed against 4 L of 50 mM Hepes-KOH, 300 mM KCl, pH 7(RT) at 4°C (see 2.12.4). The following steps were used as standard procedur for all recombinant proteins in this

work. Gel filtration was performed using a matrix consisting of dextran covalently bound to highly cross-linked agarose (HiLoad 26/60 Superdex^{TM} 200 prep grade, GE Healthcare, column volume 320 ml, average particle size 34 µm, Mr $1x10^3$ – $1x10^5$). The column was washed using filtered distilled water (H_2O dest.; ca. 0.75 column volumes) prior to equilibration with 50 mM Hepes-KOH, 300 mM KCl, pH 7 (RT; 2 column volumes) running buffer. The protein sample was applied to the column and eluted via one column volume of running buffer at a flow rate of 2 ml/min. Protein containing fractions were pooled and the protein sample was stored at 4°C. The column was washed with 2 column volumes of H_2O dest. Subsequently, 2 column volumes of 20 % EtOH were applied for storage of the column.

2.4 Enzyme assays

2.4.1 Glucose dehydrogenase (GDH)

GDH (SSO3204) catalyzes the oxidation of glucose yielding gluconate. GDH activity was determined spectrophotometrically in a continous assay by following the increase in absorbance at 340 nm due to the reduction of NAD^+/$NADP^+$ at 70°C. The standard assay (0.5 ml) contained 0.5 mM NAD^+/$NADP^+$, 10 mM glucose or alternative sugars, 10 mM $MgCl_2$ in 100 mM HEPES buffer (pH 6.5, at the respective temperature). Enzyme characterization was performed in the presence of 10 mM NAD^+/$NADP^+$ at different glucose concentrations and enzyme concentrations from 0.5 - 2mg/ml. Kinetic parameters were determined via Hanes-Woolf-Plots using Origin 8.1. The measured range of substrate and co-substrate concentrations [S] was 0.02 mM - 40 mM for glucose, 0.02 mM – 30 mM for NAD^+ and 0.02 mM – 10 mM for $NADP^+$.

2.4.2 Enolase (ENO)

Enolase (SSO0913) catalyses the interconversion of 2-PG to PEP. Enzymatic activity was measured in catabolic direction (conversion of 2-PG to PEP) via photometric detection of conversion of NADH to NAD^+ using two auxiliary enzymes. Pyruvate kinase (PK) catalyses pyruvate formation from PEP. L-lactic dehydrogenase (LDH) catalyses a redox reaction, the reduction of pyruvate to lactate and the resulting oxidation of NADH to NAD^+ is detectable photometrically at a wavelength of 340 nm (Bernt and Bergmeyer, 1974). Overall, one molecule of 2-PG is converted into one molecule of lactate, yielding one molecule of NADH. Continuous measurements were performed at 50°C as PK and LDH from rabbit muscle (Sigma) were not stable at exceeding temperature. The 500 µl enzyme assay contained 100 mM Hepes-KOH, pH 6.5 (50°C), 10 mM $MgCl_2$, 2 mM ADP, 0.5 mM NADH, 10 U PK, 6.5 U LDH, 0.16 mM or 0.28 mM 2-PG, respectively and 3.68 µg of enolase.

For characterisation purposes, PEP and 2-PG formation due to enolase activity was followed photometrically in a continuous assay from 50°C to 88°C at a wavelength of 240 nm according to Warburg and Christian (1941). The assay consists of 0.1 M HEPES/KOH (pH 6.5 at 80°C),10 mM $MgCl_2$, 2 µg of enolase in a total volume of 500 µl. Reactions arstarted by the addition of 2PG/PEP (0,01-5 mM). The produced PEP is detected directly at 240nm in 0.1 M HEPES/KOH (pH 6.5 at the respective temperature).

2.4.3 Pyruvate kinase (PK)

The standard assay was performed at 50 ,60, and 65°C with 100 mM HEPES buffer (pH 6.5) at the respective temperature, 0.5 mM NADH, 4U of LDH (rabbit muscle; Sigma), 20 mM PEP, 5 mM ADP, and 10 mM MgCl2. Enzyme activity was measured by monitoring the decrease in absorption at 340 nm. Reactions were started by adding the substrate PEP. Enzyme concentrations ranged from 0,75 to 2 mg/ml of protein. The enzyme reaction was monitored for the first 1 to 2 min. PK activity for 70°C and 80°C is measured in a discontinuous enzyme assay, performed in 0.1 M HEPES buffer (pH 6.5 at 70-80°C) containing 0,75-2 µg of protein in a total volume of 120µl. Reactions are started by the addition of phosphoenol pyruvate (PEP, final concentration 0.02 10 mM).The detection of the produced pyruvate is performed in a second step at 37°C and 340 nm in 0.1 M HEPES/KOH (pH 7, RT) containing NADH (0.5 mM), ADP (5 mM), $MgCl_2$ (10 mM), LDH (4U). The measured range of substrate and co-substrate concentrations [S] was 0.01 mM - 10 mM for pyruvate and 0.01 mM – 10 mM for ADP.

2.4.4 Phosphoglycerate mutase (PGAM)

Anabolic activity, the conversion from 2-PG to 3-PG, of the enzyme is measured in a continuous assay at 65, 70 and 80°C. The assay is performed in 0.1 M Tris/HCL (pH 6.5 at the respective assay temperature) containing NADPH (0,2 mM), ATP (20mM), $MgCl_2$ (10mM), GAPDH (SSO, HP 80°C 25µg), PGK (*T. Tenax*, HP 80°C) and 6µg PGAM in a total volume of 500 µl. Reactions are started by the addition of 2PG (0.02-10mM. Enzymatic activity is determined by monitoring the decrease of NADPH at 340 nm. For each assay three independent measurements are performed.

Katabolic activity, the conversion of 3-PG to 2-PG, of iPGAM is measured in a continuous enzyme assay at 65, 70 and 80°C. The assay is performed in 0.1 M HEPES/ KOH (pH 6.5 at the respective assay temperature) containing $MgCl_2$ (10 mM), 20 µg Enolase (HP 80°C) and 6 µg of PGAM in a total volume of 500 µl. The reaction is started by the addition of 3PG (0.02-10mM). Enzymatic activity is determined by monitoring the increase of PEP at 240 nm. For each assay three independent measurements are performed.

2.4.5 Phosphoenolpyruvate synthase (PEPS)

PEPS activity was determined at 70°C using a discontinuous assay according to Eyzaguirre et al. (1982). The standard assay (total volume 25–50 µl) was performed in 100 mM Tris/HCl, pH 7.0 (at 70°C), in the presence of 30 mM β-mercaptoethanol, 0.1-10 mM pyruvate, 0.1-10 mM ATP, 10 mM $MgCl_2$ and 20 µg of enzyme. The amount of PEP formed by PEPS activity after 60–300 s was determined at room temperature in 0.5 ml 100 mM Tris/ HCl, pH 7.0, 20 mM $MgCl_2$, 1 mM ADP and 0.8 mM NADH by calculating the decrease in absorption at 366 nm (Bergmeyer, 1975) using 10 U lactate dehydrogenase (LDH, rabbit muscle) and 5 U PK (rabbit muscle) as auxiliary enzymes.

2.4.6 Pyruvate, phosphate dikinase (PPDK)

For monitoring PPDK activity in the anabolic direction (PEP formation), the discontinuous assay described for PEPS was modified in that the standard assay contained 100 mM Tris/ HCl, pH 7.0 (55°C or 70°C), 20 mM β-mercaptoethanol, 6 mM pyruvate, 15 mM ATP, 10 mM MgCl2 and 5 mM KPi. Pyruvate formation by PPDK (catabolic direction) was measured either at 70°C using a discontinuous assay or at 55°C in a continuous assay. In both cases, standard assays were performed in 100 mM Tris/HCl, pH 7.0 (55°C or 70°C) in the presence of 3 mM PEP, 5 mM AMP and 4 mM Mg-EDTA. The reaction was started by addition of 1 mM PP_i. In the continuous assay, the reaction mixture additionally contained 0.8 mM NADH and 10 U LDH, and pyruvate formation was followed directly by the decrease in absorption at 366 nm [$\in$55°C = 3.33 mM^{-1} cm^{-1}(Fabry and Hensel, 1987)]. At 70°C, the amount of pyruvate formed by PPDK after 20–120 s (sample volume 25–50 µl) was determined at room temperature in 0.5 ml 100 mM Tris/HCl, pH 7.0, 0.8 mM NADH using 10 U LDH as auxiliary enzyme.

2.4.7 Metabolite stabilities

2-PG halflife

Thermal stability of 2-PG was determined at 88°C. Three stock solutions consisting of 20 mM 2-PG dissolved in 100 mM Hepes-KOH, pH 6.5 (88°C) were prepared. The solutions were heated to 88°C in a heating block. Samples with a volume of 60 µl each were taken after 0, 23.5, 33 and 72 h of incubation from all three stock solutions, transferred to one pre-chilled 1.5 ml cup each and stored on ice immediately. 2-PG degradation was quantified via the enzyme assay applied for enolase characterisation.

3-PG halflife

Determination of 3-PG stability was performed at 88°C. Three stock solutions consisting of 10 mM 3-PG dissolved in 100 mM Hepes-KOH, pH 6.5 (88°C) were prepared. The solutions were heated to 88°C in a heating block. Samples with a volume of 60 µl each were taken after 0, 27.08 and 72.33 h of incubation from all three stock solutions, transferred to one pre-chilled 1.5 ml cup each and stored on ice immediately. 3-PG degradation was quantified via the enzyme assay described earlier (2.13.3).

PEP halflife

The stability was determined by incubating PEP (10mM) at 65°C, 70°C, 80°C and 88°C. Three solutions consisting of 10 mM PEP dissolved in 100 mM Hepes/KOH, pH 6.5 were prepared. Samples with a volume of 60 µl each were taken after 0, 27.08 and 72.33 h of incubation from all three stock solutions, transferred to one pre-chilled 1.5 ml cup each and stored on ice immediately. Further, resedual PEP was detected via the PK enzyme assay (MM).

NAD(P)H halflife

Determination of NAD(P)H stability was performed at 65°C, 70°C, 80°C and 88°C. The solution consisting of 10 mM NAD(P)H dissolved in 100mM Hepes/KOH pH 6.5

was incubated in 500µl cuvettes and the heat induced degradation was followed directly at 340nm.

2.4.8 Calculation of specific activity

Enzyme activity was determined via change in absorption (ΔE) in each measurement. Continuous activity tests allow for determination of the absorption change per time (ΔE/min) from the extinction curve. Therefore the linear section of the extinction curve has to be analysed. The absorption change per time allows for the calculation of specific activity A:

$$\text{Specific activity}\,[\text{U/mg protein}] = \frac{\Delta E/\min * V_{Total}}{\varepsilon * d * c * V_{Protein}}$$

ΔE/min	Extinction change per minute
V_{Total}	Total volume of the assay [mL]
ε	Extinction coefficient [$mM^{-1}cm^{-1}$]
d	Cuvette diameter [cm]
c	Protein content [mg/mL]
$V_{Protein}$	Volume of protein solution [mL]

2.4.9 Michaelis Menten kinetics and Hanes-Woolf plot

The kinetics parameters (k_m and v_{max}) were determined through the relationship between initial velocity and substrate concentration following the

Michaelis-Menten equation: $$v = \frac{v_{max} * [S]}{k_m + [S]} ,$$

where S is the concentration of substrate, v is the initial reaction velocity, v_{max} is the maximal reaction velocity and k_m the Michaelis-Menten constant. Enzymes following the Michaelis-Menten kinetics display a hyperbolic curve when v is plotted against S with v reaching v_{max} when S -> ∞. When S is at k_m the reaction velocity is ½ v_{max}.
Calculation of the kinetic parameters (k_m and v_{max}) was performed by iterative curve-fitting (Hill 1 equation) using the program Origin 8 (Microcal Software Inc.). By this

way, also the Hill-Coefficients have been determined. The Hill equation considers allosteric enzymes and the Hill-coefficient gives an approximation for the amount of active sites present in the enzyme.

Hill-equation: $$v = \frac{Vmax*[S]^n}{K' + [S]^n} \quad ,$$

where S is the concentration of substrate, v is the initial reaction velocity, v_{max} is the maximal reaction velocity, K' a constant comprising the interaction factors of cooperative subunits in an enzyme and the intrinsic dissociation constant of the active site-substrate complexes and n the number of substrate binding sites per molecule of enzyme.

Also for k_m the Hanes Woolf plot (S/v versus S) has been used. The Hanes Woolf is a linearization model which enables one to detect deviations from the classical Michaelis-Menten kinetics. Also can k_m and v_{max} hardly be determined from the Michaelis-Menten curve.

The equation for the Hanes Woolf plot is achieved through mathematical conversions of the Michaelis-Menten equation.

Hanes: $$\frac{[S]}{v} = [S] * \frac{1}{v_{max}} + \frac{k_m}{v_{max}}$$

The intercept in Hanes plot is k_m/v_{max} and the slope is $1/v_{max}$.

The turnover number (k_{cat}) was calculated using the following formula:

$$k_{cat}[s^{-1}] = \frac{v_{max} * [E]_0^{-1}}{60}$$

It was necessary to divide through 60 to maintain the unit s^{-1}. $[E]_0$ is the enzyme concentration at the beginning of the reaction.

The catalytic efficiency (k_{cat}/k_m) was calculated according to the following formula:

$$\text{Catalyticefficiency } [\text{mM}^{-1}\text{s}^{-1}] = \frac{\text{k}_{\text{cat}}}{\text{k}_{\text{m}}}.$$

2.4.10 Sequence analysis

Sequence alignments of enzymes were performed using the software “ClustalX” (Larkin et al., 2007) with default settings. Protein sequences were obtained from UniProtKB and TIGR database. Unrooted phylogenetic networks were calculated from the sequences aforementioned using the software “SplitsTree4” (Huson and Bryant, 2006).

3 Results

3.1 Heterologous Expression of the *S.solfataricus* ED Proteins in *E.coli*

The GDH, dPGAM, iPGAM, ENO, PK, PPDK and PEPS genes of *S.solfataricus* were cloned into the pET expression system and expressed in *E.coli* Rosetta (DE3)-RIL. The annotated ED genes from *S.solfataricus* (Snijders et al., 2006; She et al. 2001; Zaparty *et al* in prep.) were amplified by PCR mutagenesis using the primer sets shown in tab 2.1.5. *S.solfataricus* genomic DNA was used as a template with PCR conditions reported previously (2.1.5). The following annealing temperature was used for the different amplified genes; 58°C GDH, 52°C PGAM, 55°C ENO and 55°C PK. For recombinant expression the amplified genes GDH (cloning was performed by J. Treichel), ENO, PEPS, and PGAM (cloning was performed by T. Kipper) were cloned into the vector pET11c, the PK gene was cloned into pET324. The PEPS gene was cloned into Vectors pET324, pET302, pET11c and pET15b, but no expression in *E.coli* was observed. Therefore the codons of the DNA sequence were altered to bacterial codon usage by gene synthesis (Eurofins MWG) the vector pET11c.

3.2 Enzyme Enrichment and Purification

For further biochemical studies, the recombinant proteins from *S.solfataricus* were purified to homogeneity from crude extracts. Cells (10g wet weight) were suspended in 30 ml of 100 mM HEPES/KOH (pH 7.0, 70°C), in the case of PEPS 30 mM β-mercaptoethanol was added and the cells were disrupted by sonication. Cell debris and unbroken cells were removed by centrifugation to gain cell free crude extracts. The recombinant enzymes were enriched from crude extracts by heat precipitation at the following temperatures: GDH at 80°C, iPGAM and dPGM at 80°C, ENO at 70°C, PK at 80°C, PPDK at 70°C and PEPS at 75°C.

Further, enrichment was achieved by heat precipitation as indicated above and due to the high temperatures (65°C, 70°C and 80°C) used for heat precipitation the presence of residual contaminating *E.coli* proteins was very unlikely. The possibility of a contamination was eliminated by analyzing a precipitated extract of the expression host with expression plasmid without insert as a control. To confirm enzyme activities, the depence of the enzyme activity on the amount of the respective recombinant protein was demonstrated.

Further purification of all recombinant proteins was achieved by ionexchange chromatography and subsequent gel filtration (2.1.7; 2.1.8). After dialysis overnight (50mM HEPES/KOH pH 7, RT), in case of the PEPS additionally containing 30mM ß-mercaptoethanol, recombinant proteins were subjected to the respective columns. Fractions containing the enriched enzyme solution were pooled and used for enzymatic studies (2.4). All expressed enzymes revealed a good expression and sufficient enrichment was observed from SDS-PAGE. The molecular masses approximately corresponded to the calculated mass for the respective *S. solfataricus* proteins. The differences of 3-5 kDA are in agreement with generally observed minor deviations.

3.3 Biochemical Characterization

3.3.1 Glucose dehydrogenase

The *S. solfataricus* GDH catalyzes the oxidation of glucose yielding gluconate (Fig. 4). In course of the ED-pathway reconstruction in *S.solfataricus* (Zaparty et al., manuscript in preparation), several members of the MDR superfamily were identified raising questions about possible GDH isoenzymes in *S. solfataricus*. The protein SSO3204 (Haferkamp et al., 2011) shows high similarity (61% amino acid identity) to the previously characterized GDH-1 (SSO3003).

The gene (SSO3204) encodes a functional GDH as confirmed by the activity of the recombinant protein. As seen in Fig.4 GDH-2 (SSO3204) exhibits a molecular mass of 39 kDa, which corresponds well with the calculated molecular mass of 39.97 kDa.

For purification ion exchange chromatography was performed and GDH-2 eluted at a concentration of 200 mM NaCl. After following gel filtration GDH-2 was sufficiently purified, and no other dominant protein band was visible (Fig. 7). The total yield of purified protein is 1.5 mg out of 8 g of cell mass (wet weight).

The *S. solfataricus* GDH-2 activity was determined in a continous assay at 70°C monitoring the formation of NADPH or NADH at 340 nm. All enzyme properties of GDH-2 were characterized with enzyme fractions after gel filtration. GDH activity was followed in response to different substrate concentrations at three different temperatures 65°C, 70°C and 80°C. The enzyme follows classical Michaelis Menten kinetics for D-glucose (0-30 mM) at all three temperatures.

In addition, the GDH activity was also analyzed in response to different concentrations of the two possible cosubstrates NAD^+ (0-20 mM) and $NADP^+$ (0-5 mM) (Fig.5; 6). Although a higher specific activity (V_{max}) was observed with NAD^+, 158.58 U/mg compared with 66.53 U/mg for $NADP^+$, the catalytic efficiency for $NADP^+$ is distinctly higher with 294.46 $mM^{-1}s^{-1}$ compared to 31.95 $mM^{-1}s^{-1}$ for NAD^+ (Tab.1).

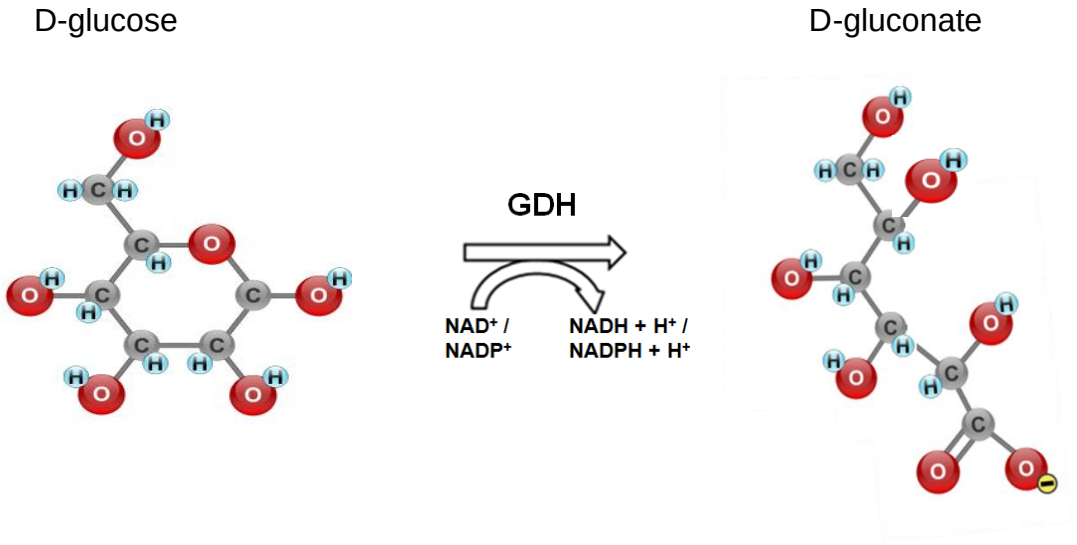

Fig. 4: *S. solfataricus* GDH catalyzes the oxidation of D-glucose yielding D- gluconate.

Several C5 and C6 sugars were tested as substrate for GDH-2: D-allose, D-mannose, L-arabinose, D-ribose, D-arabinose, L-xylose, D-glucosamine, 2-deoxy-D-glucose, D-fucose, D-lactose, D-maltose, D-fructose and ethanol were tested as substrate. Initial studies revealed, that GDH-2 (SSO3204) is specific for D-glucose and does not exhibit activity with any of the other tested substrates. However, currently performed more detailed analysis revealed also activity with D-xylose and D-galactose in the presence of the cosubstrate $NADP^+$. For glucose, higher GDH-2 activity was observed in the presence of NAD^+ with a V_{max} of 102.42 U/mg compared to 29.03 U/mg in the presence of $NADP^+$. Despite this, in the presence of $NADP^+$, GDH-2 exhibits a significantly higher affinity (lower K_m) towards glucose (0.17 mM, $NADP^+$; 4.59 mM, NAD^+), which results in a higher catalytic efficiency (k_{cat}/k_m) of 115.17 $s^{-1}mM^{-1}$ (NAD^+) in contrast with 14.86 $s^{-1}mM^{-1}$ ($NADP^+$).

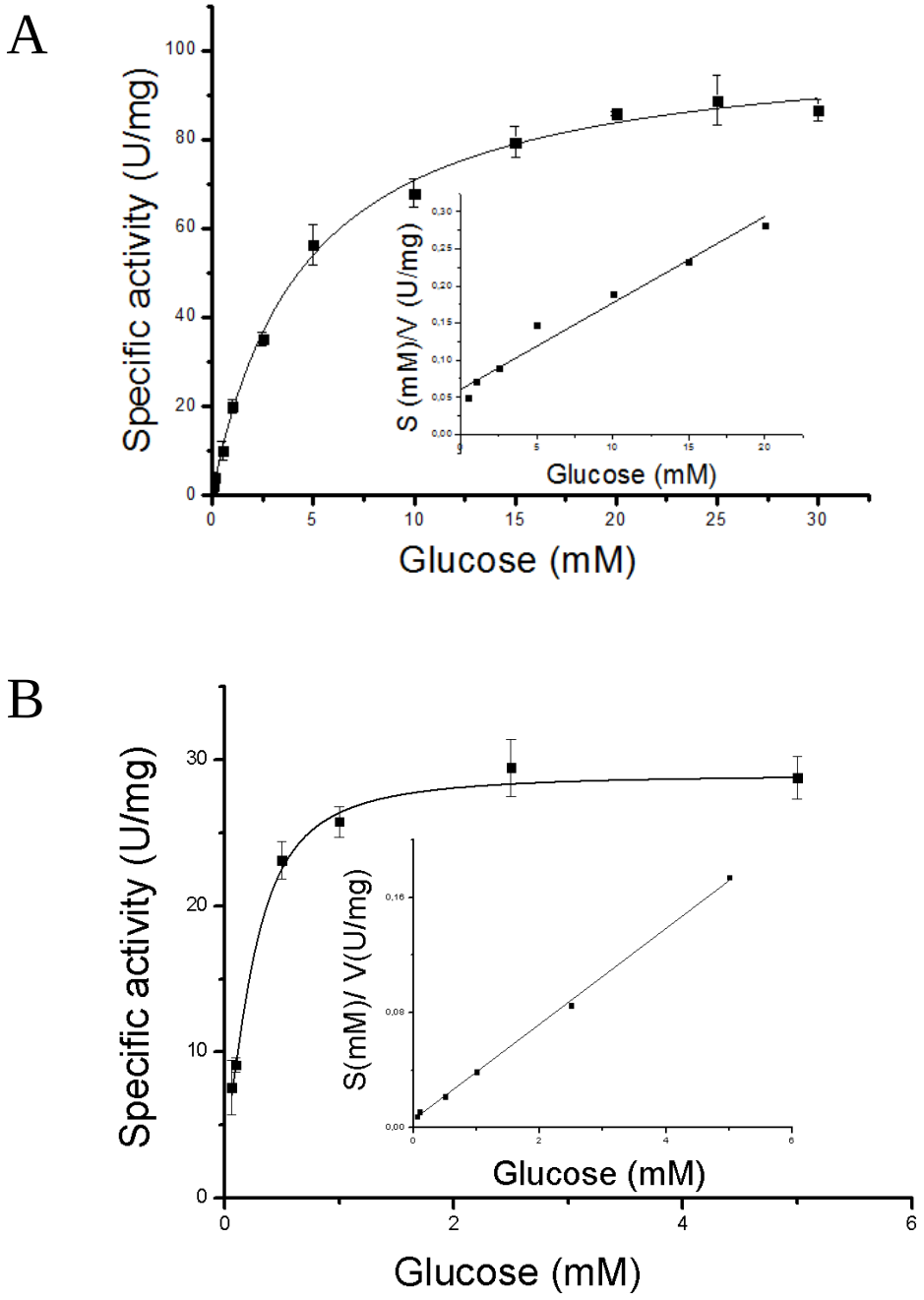

Figure 5: GDH-2 (SSO3204) activity assayed at 70°C with either NAD^+ (A) or $NADP^+$ (B) as co-substrate (10 mM). Inserts show the respective Hanes Woolf plot.

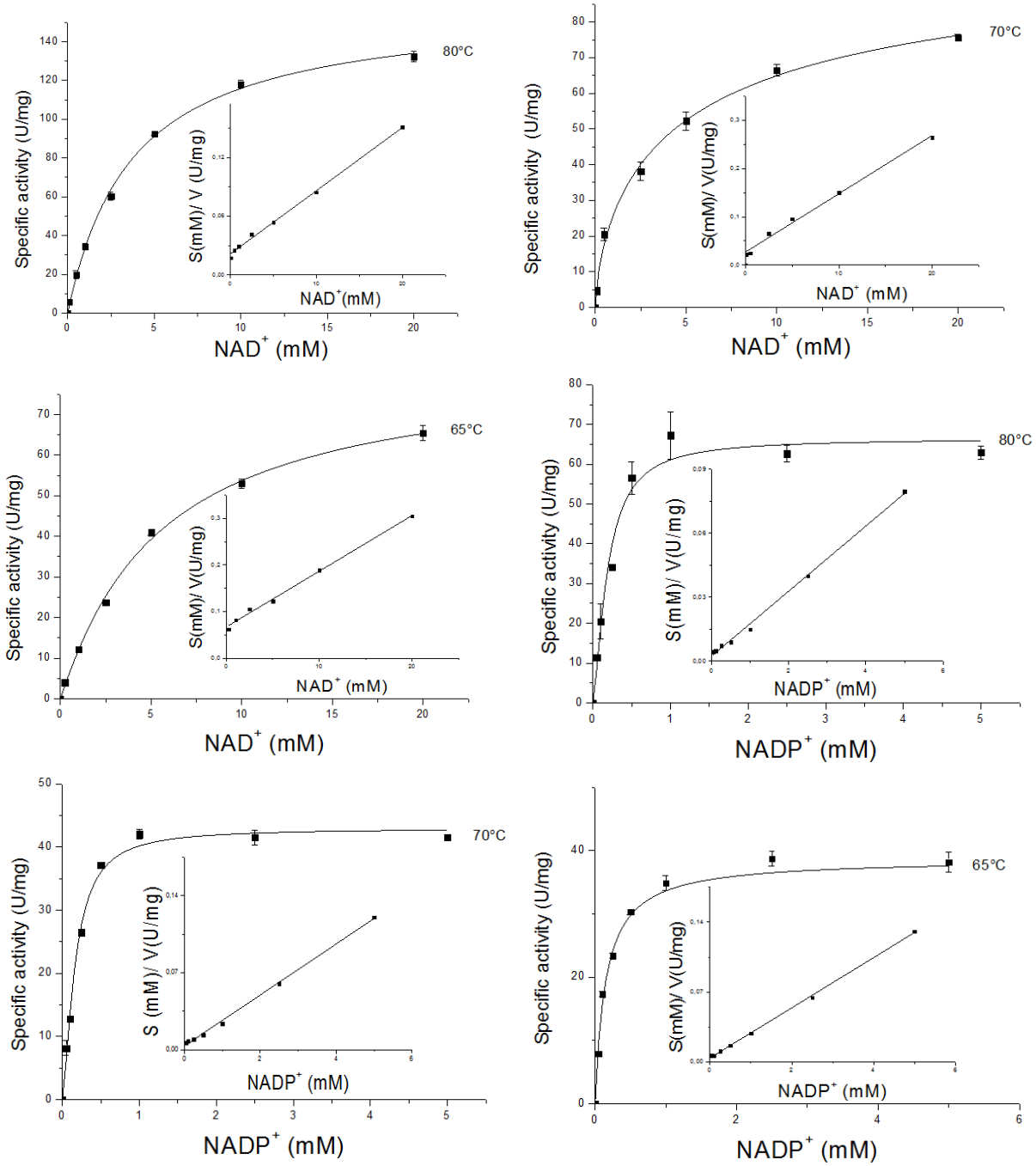

Fig. 6: Rate dependence of GDH-2 on NAD^+ and $NADP^+$ concentration assayed at 50°C, 65°C, 70°C and 80°C. The enzyme follows classical Michaelis Menten kinetics for the co-substrates NAD^+ and $NADP^+$ (20 mM and 6 mM glucose respectively). Insets show the respective Hanes-Woolf plots. All measurements were performed as triplicates and are means ± S.D. Kinetic parameters are given in Tab. 1.

Tab. 1: Kinetic parameters of SSO_GDH-2 (SSO3204) for D-glucose with NAD^+/ $NADP^+$ as co-substrate.

GDH-2 D-glucose 70°C	K_m (mM)	V_{max} (U/mg)	K_{cat} (s^{-1})	K_{cat}/K_m ($mM^{-1}s^{-1}$)
NAD^+	4.59	102.42	68.23	14.86
$NADP^+$	0.17	29.03	19.34	115.17

Tab. 2: Kinetic parameters of SSO_GDH-2 (SSO3204), for NAD^+ and $NADP^+$ and with glucose as substrate assayed at different temperatures.

GDH-2 $NADP^+$	K_m (mM)	V_{max} (U/mg)	K_{cat} (s^{-1})	K_{cat}/K_m ($mM^{-1}s^{-1}$)
80°C	0.15	66.43	44.17	294.46
70°C	0.14	42.94	28.52	203.71
65°C	0.15	40.22	26.74	178.26
GDH-2 NAD^+	K_m (mM)	V_{max} (U/mg)	K_{cat} (s^{-1})	K_{cat}/K_m ($mM^{-1}s^{-1}$)
80°C	3.3	158.58	105.45	31.95
70°C	2.23	106.89	70.49	31.6
65°C	5.59	81.92	54.47	9.74

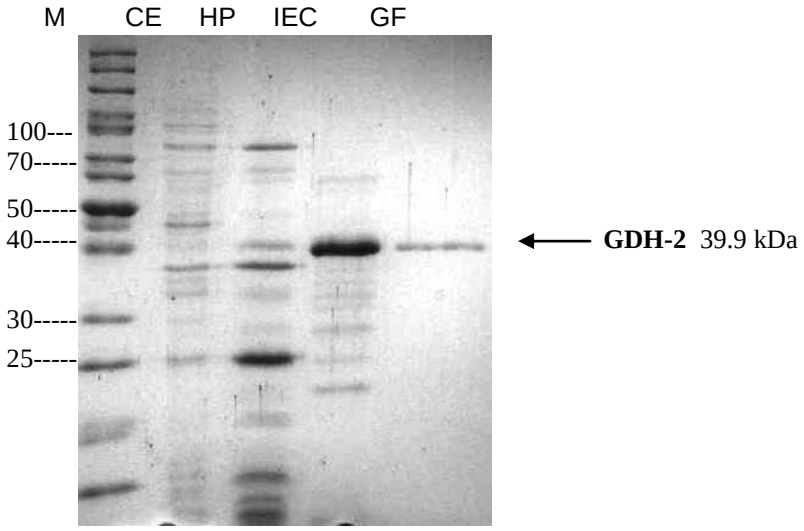

Fig. 7: Purification of the recombinant GDH-2 from *S. solfataricus* (BA thesis S. Kutschki); gel after SDS-page coomassie stained; M: Page ruler ™; CE: crude extract (10 µg); HP: heat precipitation 70°C (5 µg); IEC: enzyme fractions after ion exchange chromatography UNO-Q12 (2 µg); GF: purified enzyme fraction after gel filtration (1 µg).

3.3.2 Phosphoglycerate Mutase

The enzyme PGAM catalyzes the reversible interconversion of 3-PG and 2-PG in the commen part of the sp-ED branch and the EMP-pathway:

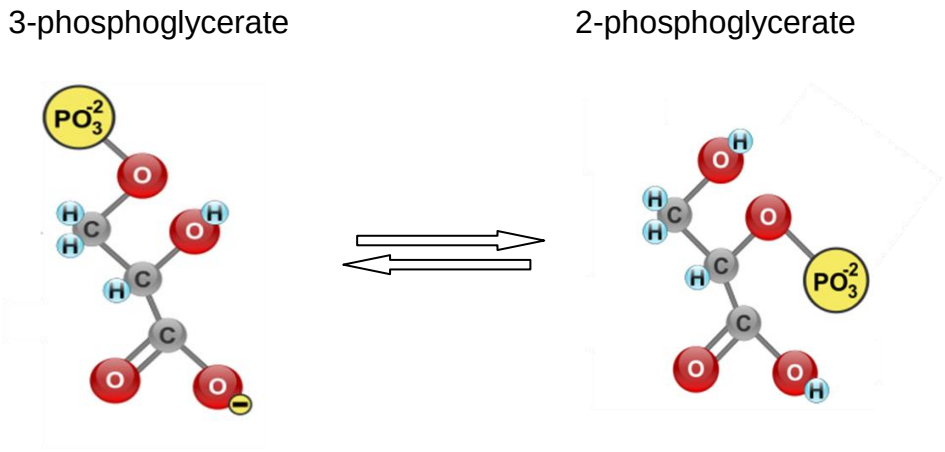

Fig. 8: Interconversion of 3-PG and 2-PG by *S.solfataricus* iPGAM

In *S. solfataricus* two genes encoding a dPGM (SSO2236) and iPGM (SSO0417) were identified. The putative dPGAM gene (SSO2236) was cloned into the vector pET11c and the recombinant protein was heterologously expressed in *E. coli* BL21 (DE3)-pRIL using the pET expression system. The recombinant enzyme was purified by heat precipitation (30 min at 75°C) of *E. coli* crude extracts to confirm the respective enzyme activity. For the predicted dPGAM (SSO2236) activity (conversion of 3-PG to 2-PG), the cofactor 2.3 BPG is essential (van der Oost et al.2002). Only small amounts of 2.3 BPG are required for the reaction, additionally it is a known contaminant of the substrate 3-PG. Commercially available 3-PG (5- 50 mM) (Sigma) was used as substrate without removing the contaminating 2.3-BPG to test for dPGAM activity (Johnsen et al., 2007). No enzyme activity could be detected under the given conditions, suggesting the gene encoding SSO2236 does exhibit neither dPGAM nor iPGAM activity. Further on, additional tests with 2.3-BPG were performed and showed no activity, but also the positive control with the enzyme from *A.fulgidus* failed, suggesting that further optimization might be required.

The gene encoding the *S. solfataricus* iPGAM (SSO0417 van der Oost et al., 2002) was cloned into the vector pET11c and heterologously expressed in *E. coli* Rosetta (DE3) using the pET expression system (Kipper T., Master Thesis). The enzyme was purified, first by heat precipitation (30 min at 80°C) and further by ion-exchange

chromatography followed by gel filtration. During ion-exchange chromatography, the protein did not bind to the column and was detected in the flow-through fractions. As most of the *E. coli* proteins bound to the column the protein was significantly enriched and applied to the gelfiltration column. After gel filtration the enzyme was sufficiently purified. As visible in Fig. 10 iPGM (SSO0417) exhibits a molecular mass of 46- 48 kDa which matches the calculated molecular mass of 46.8 kDa. However, the protein appeared on the SDS-PAGE as a double band. Upon, incubation with several phosphate containing intermediates the pattern of the band on the SDS-PAGE did not change. The following substances were tested: ATP, ADP, AMP, 3-PG, 2-PG, PP_i.

The total yield of protein was 2.2 mg out of 7.8 g of cells wet weight. The *S. solfataricus* iPGAM (SSO0417 van der Oost et al., 2002) was characterized regarding both, the anabolic and the katabolic reaction. Enzyme activity of *S.solfataricus* PGAM with 3-PG (0-6 mM) was followed in a continuous assay by coupling the formation of 2-PG (0-5 mM) to the formation of PEP via ENO as auxiliary enzyme at 240 nm. The activity with 2-PG was followed in a continous assay by coupling the formation of 3-PG to the formation of 1.3 BPG by PGK and the formation of GAP via GAPDH.

The enzyme follows Michaelis Menten kinetics at the three measured temperatures: 65°C, 70°C and 80°C with both substrates. The kinetic parameters were determined to analyze the enzymes catalytic properties of the enzyme in respect to temperature change (Tab3,4; Fig.9).

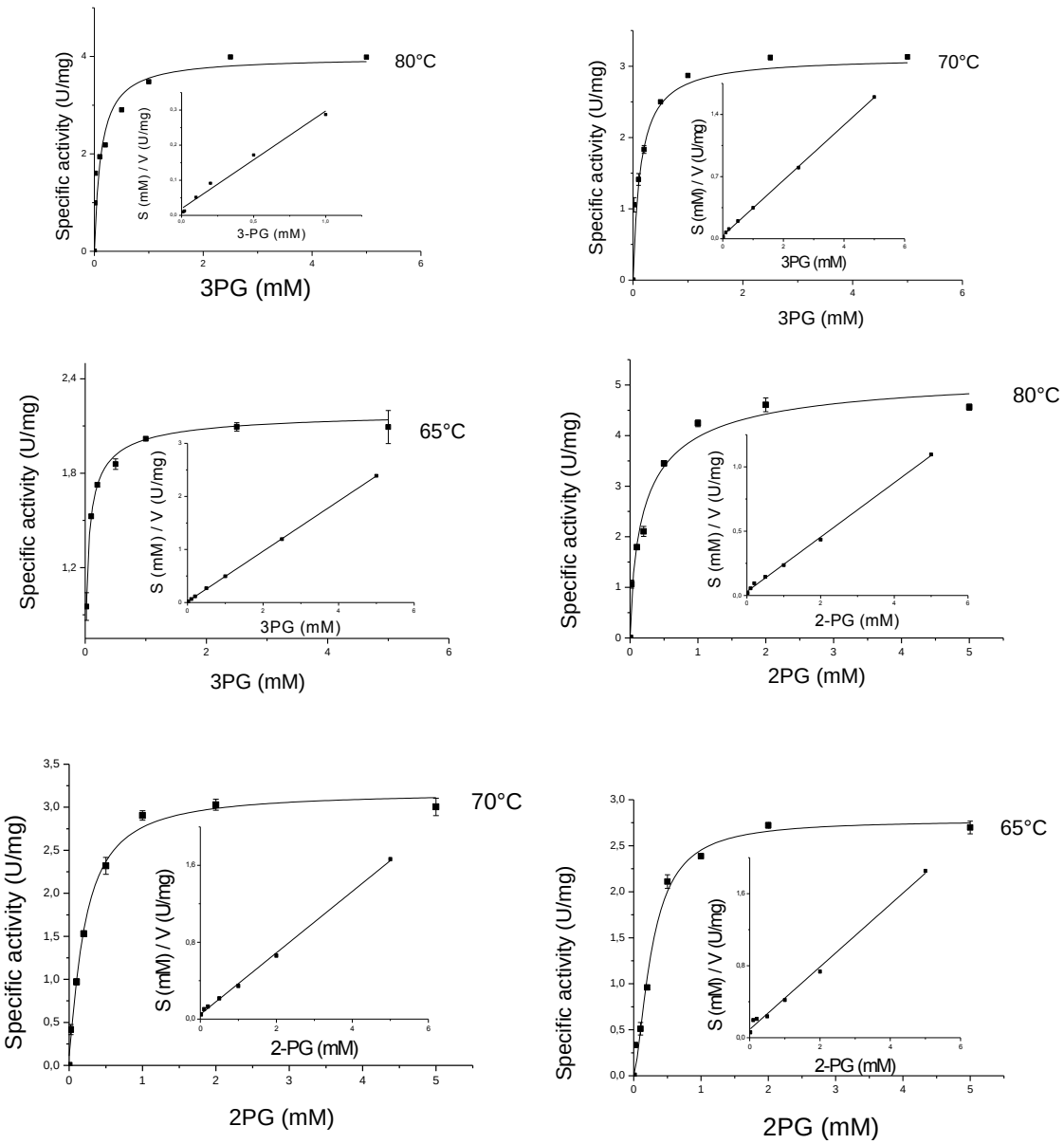

Fig.9: iPGAM (SSO0417) activity assayed at 65°C, 70°C, 80°C with either 3-PG or 2-PG as variable substrate. Insets show the respective Hanes-Woolf plots. All measurements were performed as triplicates and are means ± S.D.. Kinetic parameters are given in Tab. 2 and 3.

The highest specific activity (V_{max}) for both the anabolic (5.32 U/mg) and the katabolic (3.99 U/mg) reaction was determined at 80°C. The V_{max}-values at 70°C and 65°C are in the anabolic direction 3.04 U/mg and 2.71 U/mg and catabolic direction 2.89 U/mg (70°C) and 2.01 U/mg (65°C), respectevely. The determined K_m-values for 2-PG, (anabolic reaction), are decreasing from 0.26mM at 65°C over 0.15mM at 70°C to 0.11mM at 80°C, whereas in the catabolic direction K_m-values for 3-PG are increasing with rising temperature with 0.04 mM at 65°C, 0.10 mM at 70°C and 0.11 mM at 80°C. In the gluconeogenic reaction the catalytic efficiency rises from

7.84 $mM^{-1}s^{-1}$ determined at 65°C over 15.4 $mM^{-1}s^{-1}$ at 70°C to 36.45 $mM^{-1}s^{-1}$ at 80°C. In contrast, in the glucolytic reaction the highest catalytic efficiency was determined with 35.95 $mM^{-1}s^{-1}$ at 65°C followed by 19.81 $mM^{-1}s^{-1}$ at 70°C and 27.36 $mM^{-1}s^{-1}$ at 80°C. Observed differences regarding the catalytic efficiency are predominantly owed to changes of the K_m-values (Tab. 3; 4) at the different temperatures, the increase of the V_{max} values is in the order of 1.8-fold with the temperature rising 10°C. The katabolic reaction, with 3-PG as substrate, shows the highest catalytic efficiency at 65°C compared to 70°C and 80°C whereas the anabolic reaction shows the opposite trend with the highest determined catalytic efficiency at 80°C compared to 70°C and 65°C (Tab. 3).

Tab. 3: Kinetic parameters of SSO PGAM with **3-PG** as substrate (65°C, 70°C and 80°C).

Temp	K_m (mM)	V_{max} (U/mg)	K_{cat} (s^{-1})	K_{cat}/K_m ($mM^{-1}s^{-1}$)
65°C	0.04	2.01	1.51	35.95
70°C	0.10	2.89	2.18	19.81
80°C	0.11	3.99	3,01	27.36

Tab. 4: Kinetic parameters of SSO PGM with **2-PG** as substrate (65°C, 70°C and 80°C).

Temp	K_m (mM)	V_{max} (U/mg)	K_{cat} (s^{-1})	K_{cat}/K_m ($mM^{-1}s^{-1}$)
65°C	0.26	2.71	2.04	7.84
70°C	0.15	3.04	2.31	15.4
80°C	0.11	5.32	4.01	36.45

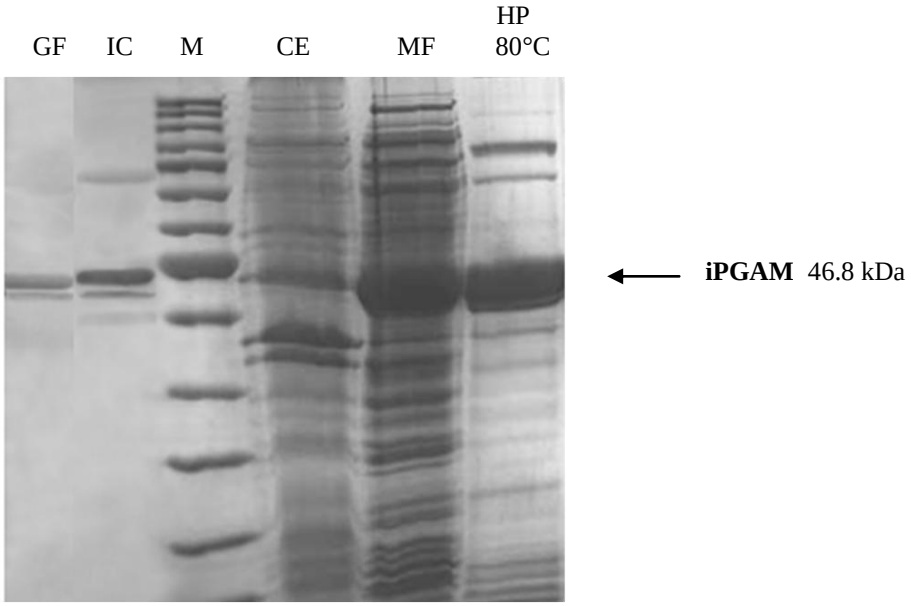

Fig. 10: Purification of the recombinant iPGAM from *S. solfataricus*; gel after SDS-PAGE coomassie stained; M, protein marker; CE (10 µg), crude extracts; MF, membrane fraction; HP (5µg), heat preciptation; IC (2µg): iPGAM containing fractions after ion exchange chromatography; GF (1µg): PGAM containing fractions after gel filtration;

3.3.3 Pyruvate kinase:

PK catalyzes the irreversible conversion of PEP to pyruvate:

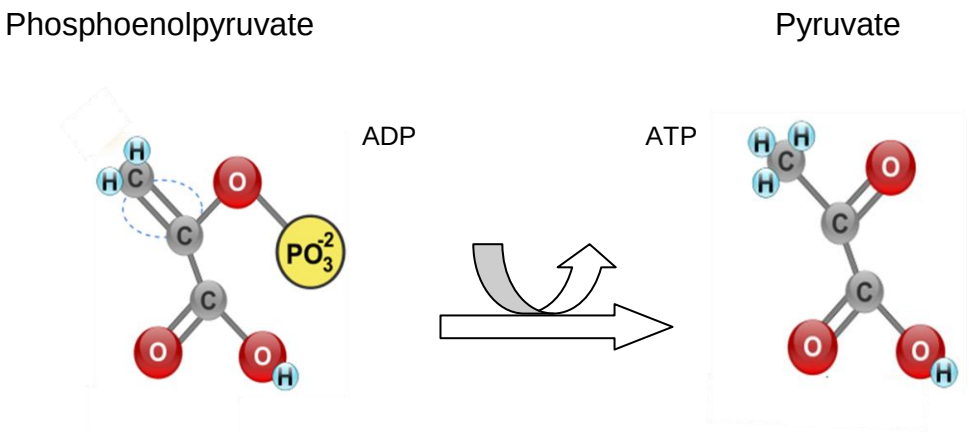

Fig. 11: Conversion of PEP to pyruvate by PK

The ORF SSO0981 is annotated as putative PK in the *S. solfataricus* genome and was cloned into the vector pET324. The enzyme was expressed heterologously in *E. coli* using the pET expression system. The protein was purified by heat precipitation (20 min 80°C) and ion exchange chromatography. As visible in Fig. 15 the protein showed high purity after the heat precipitation step (90°C) and was sufficiently purified after ion-exchange chromatography (elution at 360 mM NaCl). As shown in Fig. 12 PK (SSO0981) exhibits a molecular mass of approximately 50 kDa which matches the calculated molecular mass of 49.8 kDa. The total yield of protein was 3 mg out of 9.5 g of cell mass (wet weight).

PK activity could be confirmed and the enzyme was characterized in detail. The *S. solfataricus* PK follows classical Michaelis-Menten kinetics for PEP (0-6 mM) and ADP (0-6 mM). In order to elucidate the role of PK in the biological network, e.g. the branched ED pathway, enzymatic parameters , K_m, V_{max} and K_{cat}, were determined at 65°C,70°and 80°C (Fig.12; 13).

The highest specific activity (V_{max}) for the substrate PEP was determined at 80°C with 88.68 U/mg. Accordingly, the V_{max}-values at 70°C and 65°C are 70.37 U/mg and 60.39 U/mg. The determined K_m-values for PEP are decreasing from 0.225 mM at 50°C over 0.119 at 65°C to 0.093 mM at 70°C. Only at 80°C an increased K_m-value 0.26 mM at 80°C is observed. The catalytic efficiency rises from 137.31 $mM^{-1}s^{-1}$ at

50°C over 435.82 $mM^{-1}s^{-1}$ at 65°C to 627.95 $mM^{-1}s^{-1}$ at 70°C. At a temperature of 80°C the catalytic efficiency is noticeably reduced with 280.92 $mM^{-1}s^{1}$. These significant differences regarding the catalytic efficiency are mainly due to changes of the K_m-values (Tab. 2; 3) at the different temperatures. The V_{max}-values only increase about 1.25 fold at a temperature change of 10°C. The catalytic efficiency for the co-substrate ADP shows a similar trend with 244.26 $mM^{-1}s^{-1}$ at 50°C, 385.76 $mM^{-1}s^{-1}$ at 65°C, 851.88 $mM^{-1}s^{-1}$ at 70°C and 710.53 $mM^{-1}s^{-1}$at 80°C.

Product inhibition by ATP was observed and studied in presence of half-saturating concentrations of ADP and PEP (Fig. 14). The amount of ATP required for 50% inhibition (50% residual activity) is at all three temperatures approximately 0.8 mM. The inhibition could not be reversed by the addition of PEP or ADP. Additionally, well known activators of classical bacterial and eukaryal AMP and FBP were tested as possible effectors, but both showed no effect and did not reverse the inhibition of ATP. Further PK activity was determined in cell free S.*solfataricus* crude extracts grown at 65°C, 70°and 80°C (Tab. 10).

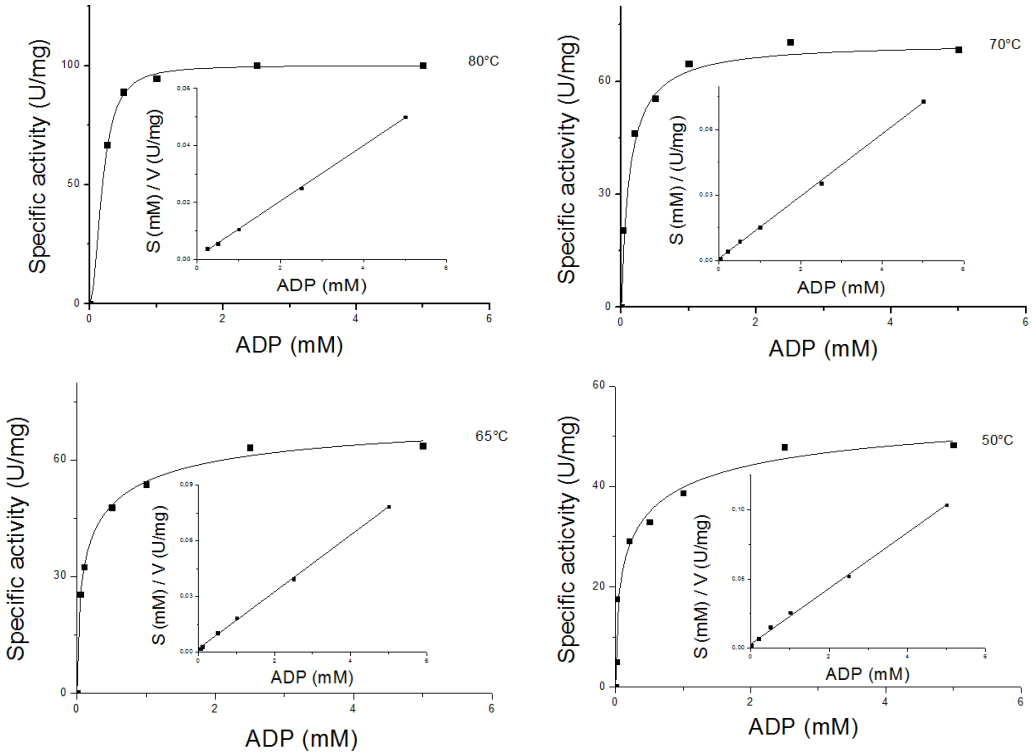

Fig.12: PK (SSO0981) activity with ADP assayed at 50°C, 65°C, 70°C and 80°C. The enzyme follows classical Michaelis-Menten Kinetics for the co-substrate ADP. Insets show the respective Hanes-Woolf plots. All measurements were performed as triplicates and are means ± S.D. Kinetic parameters are given in Tab. 5.

However, activity in crude extracts is observed to be a thousand fold lower than for the recombinant Enzyme (0.0497 U/mg). The enzyme is active over a range of temperatures (50°C-80°C; Fig.12; 13; Tab. 4; 5) with the highest specific activity at 80°C (K_m (PEP):0.26 mM; V_{max} (PEP): 88.68 U/mg). V_{max} values for both substrates increase, and K_m values decrease with rising temperatures (Tab.4; 5). At 80°C the enzyme does not follow classical Michaelis Menten kinetics for PEP concentrations below 1mM. Despite that the enzyme follows Michaelis Menten kinetics for ADP.

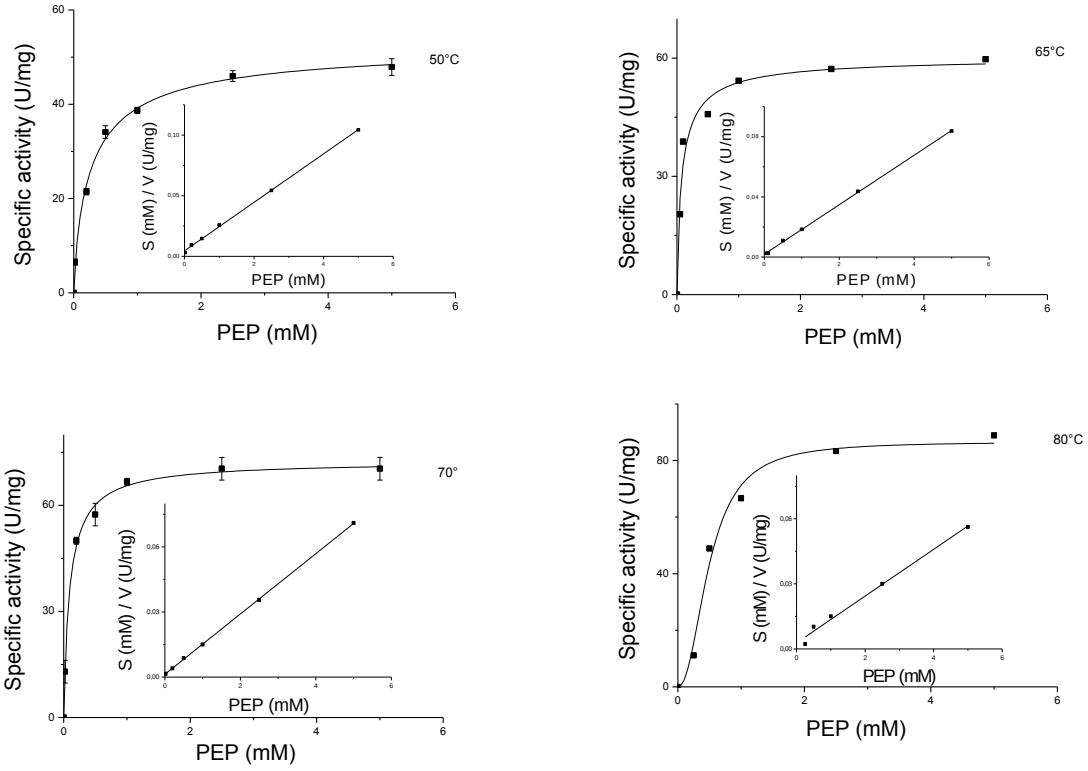

Fig. 13: Rate dependence of PK (SSO0981) on PEP concentration assayed at 50°C, 65°C, 70°C and 80°C. The enzyme follows Michaelis-Menten Kinetics for the substrate PEP with an exception at 80°C. Insets show the respective Hanes-Woolf plots. All measurements were performed as triplicates and are means ± S.D. Kinetic parameters are given in Tab. 4.

Tab. 5: Kinetic parameters of SSO PK for PEP assayed at 50°C, 65°C, 70°C and 80°C.

Temp (°C)	v_{max} (U/mg)	k_m (mM)	k_{cat} (s^{-1})	k_{cat}/k_m ($mM^{-1}s^{-1}$)
50	47.89	0.225	39.67	137.31
65	60.39	0.115	50.12	435.82
70	70.37	0.093	58.40	627.95
80	88.68	0.26	73.04	280.92

Tab. 6: Kinetic parameters of SSO PK for the co-substrate ADP assayed at 50°C, 65°C, 70°C and 80°C.

Temp (°C)	v_{max} (U/mg)	k_m (mM)	k_{cat} (s^{-1})	k_{cat}/k_m ($mM^{-1}s^{-1}$)
50	48.27	0.164	40.06	244.26
65	63.68	0.137	52.85	385.76
70	70.83	0.069	58.78	851.88
80	96.74	0.113	80.29	710.53

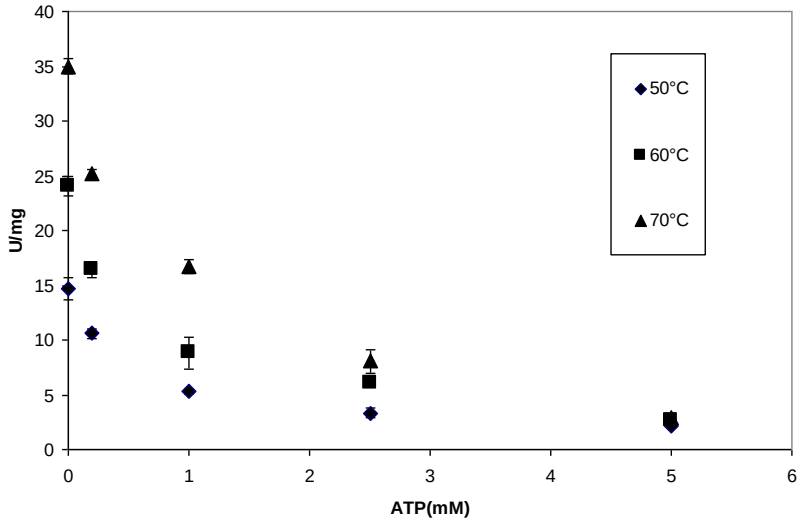

Fig. 14: The inhibition of PK activity by ATP was determined at half saturating conditions of ADP and PEP for different temperatures (50°C,60° and 70°C);

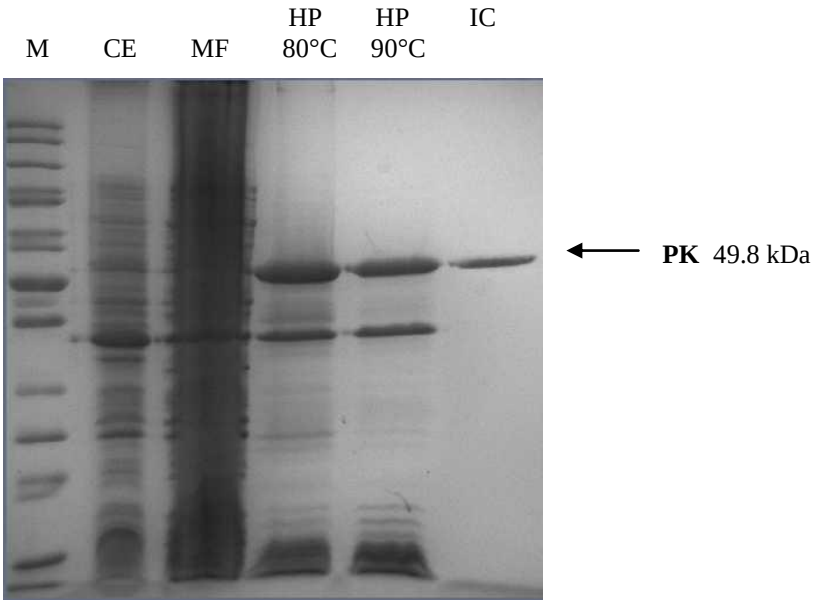

Fig. :15 SDS-PAGE **(**Comassie stained) of the purification of PK from *S. solfataricus* heterologously expressed in *E. coli*; M, protein marker; CE (10µg), crude extracts; MF, membrane fraction; HP (5µg), heat preciptation; IC (2µg): PK containing fractions after ion exchange chromatography;

3.3.4 Enolase

The ORF SSO0913, which is annotated as an enolase, was heterologously expressed in *E.coli* and the respective activity was analyzed in this study.

The gene encoding the *S.solfataricus* enolase (SSO0931) was cloned into the vector pET11c and heterologously expressed in *E. coli* Rosetta (DE3) using the pET expression system. The enzyme was purified, first by heat precipitation (20 min at 80°C) followed by ion-exchange chromatography and gel filtration. Enolase did not bind to the ion-exchange chromatography column but was found in the flow-through fraction. As most of the *E.coli* proteins bound to the column the protein was significantly enriched to be applied to the next step. After gel filtration the enzyme was sufficiently purified. As shown in Fig. 18 enolase exhibits a molecular mass of 48-52 kDa which matches approximately the calculated molecular mass of 46.7 kDa. The total yield of protein was 3.3 mg out of 10.2 g of cell mass (wet weight). Enzyme characterization was performed with enzyme fractions after gel filtration.

The *S.solfataricus* enolase catalyzes the reversible conversion of 2-PG to PEP. Like most enolases, SSO0913 is a homodimer of two approximately 50 kDa subunits (46745 Da) (Pal-Bhowmick et al., 2004). The activity was determined in a continuous assay following the formation or decrease of PEP at of 240 nm (Pal-Bhowmick et al., 2006). Enzymatic parameters like K_m, K_{cat} and V_{max} were determined at temperatures from 60°C to 88°C for the substrates PEP and 2-PG.

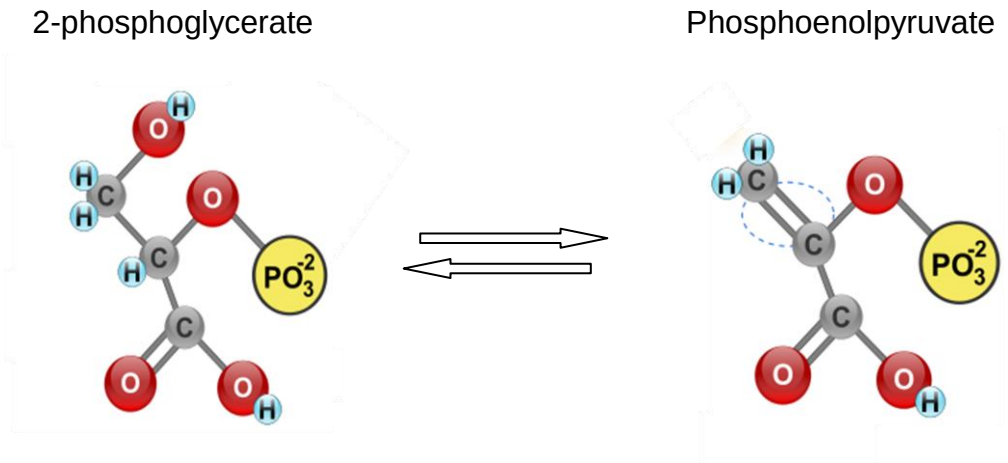

Fig. 16: Reversible interconversion of 2-PG and PEP

The highly conserved glycolytic enzyme shows classical Michaelis-Menten kinetics for 2-PG (0-6 mM) and PEP (0-2mM) (Fig. 18). The enzyme (Figure 3.5 A) exhibits increasing activity with rising assay temperature. The specific activity of the catabolic reaction increased 3-fold from 74.26 U/mg (± 3.50 U/mg) at 65°C to 232.87 U/mg (± 12.52 U/mg) at 88°C. The K_m-values increase significantly with higher assay temperature from 0.06 mM at 65° to 0.18 mM at 80°C in the catabolic direction (Fig. 17,Tab. 7), while for the anabolic reaction the K_m-values decrease with higher temperature from at 0.538 mM 65°C to 0.392 mM at 80°C (Fig. 8). The catalytic efficiency in the catabolic direction does not change significantly with the temperature with 909.53 $mM^{-1}s^{-1}$ at 70°C, 831.54 $mM^{-1}s^{-1}$ at 80°C and 941.89 $mM^{-1}s^{-1}$ at 88°C. In the anabolic direction the catalytic efficiency is in the order of 10-fold lower and changes significantly with the assay temperature from 58.44 $mM^{-1}s^{-1}$ at 65°C over 91.88 $mM^{-1}s^{-1}$ at 70°C to 110.79 $mM^{-1}s^{-1}$ at 80°C, almost 2-fold. Although the recombinant expressed enzyme shows activity in the common range, activity for the enolase reaction could not be detected in *S. solfataricus* crude extracts. Further, no interfering or inhibiting effects of *S.solfataricus* crude extracts on the activity of the recombinant expressed enzyme could be detected.

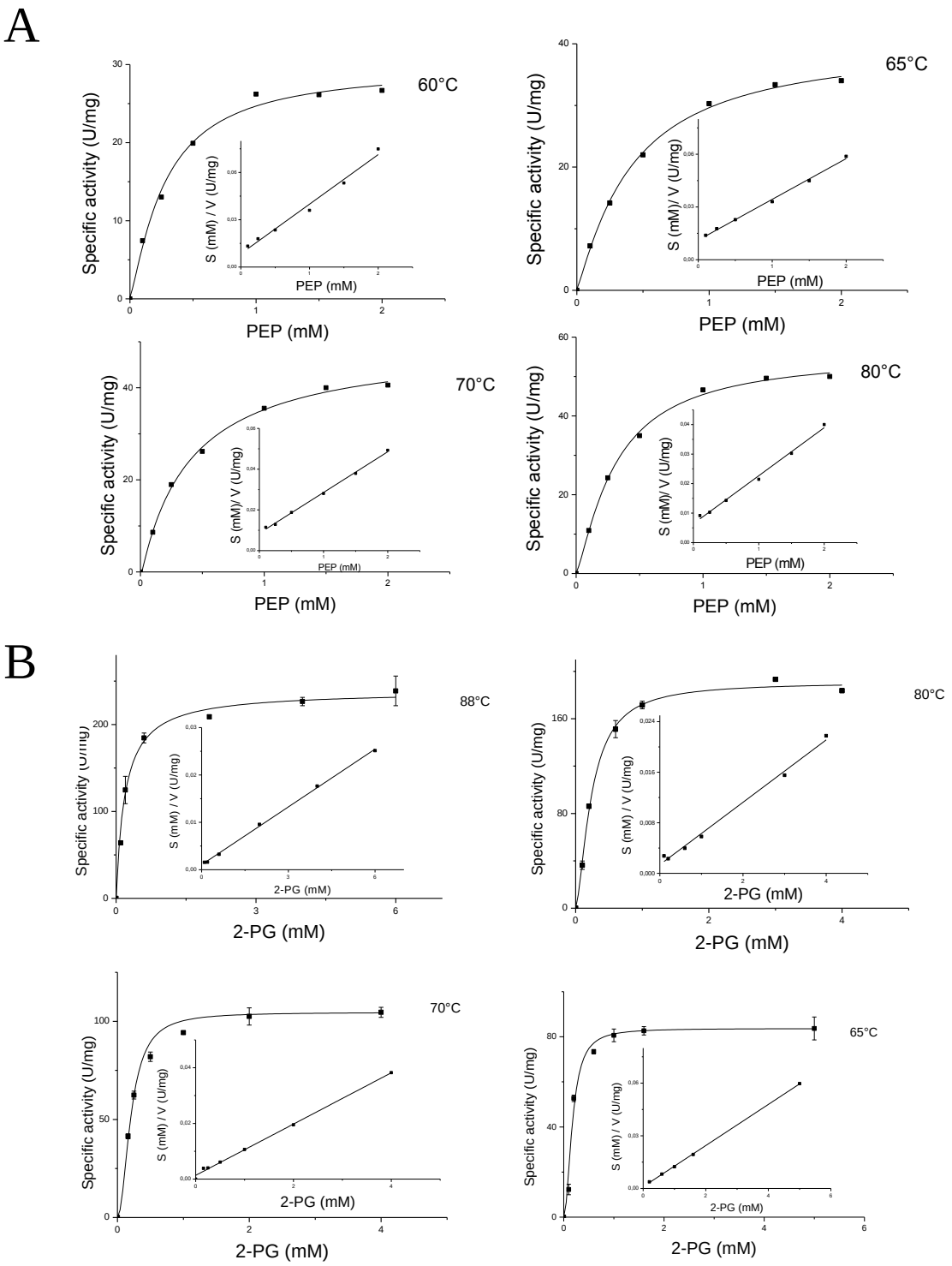

Fig. 17: Enolase (SSO0931) activity assayed at different temperatures (60°C, 65°C, 70°C, 80°C and 88°C) with either PEP (A) or 2-PG (B) (Kipper T., Master Thesis) as substrate. Insets show the respective Hanes –Woolf plot. All measurements were performed in triplicate and are means ± S.D. Kinetic parameters are given in Table 6.

Tab. 7: Kinetic parameters of SSO enolase (catabolic) for the substrate 2PG assayed at 65°C, 70°C, 80°C and 88°C (Kipper T., Master Thesis).

Temp (°C)	v_{max} (U/mg)	k_m (mM)	k_{cat} (s^{-1})	k_{cat}/k_m ($mM^{-1}s^{-1}$)
65	82.36	0.06	64.17	1069.45
70	105.07	0.09	81.86	909.53
80	192.12	0.18	149.68	831.54
88	229.71	0.19	178.96	941.89

Tab. 8: Kinetic parameters of SSO enolase (anabolic) for the substrate PEP assayed at 60°C, 65°C, 70°C and 80°C.

Temp (°C)	v_{max} (U/mg)	k_m (mM)	k_{cat} (s^{-1})	k_{cat}/k_m ($mM^{-1}s^{-1}$)
60	29.73	0.451	23.15	50.99
65	40.37	0.538	31.44	58.44
70	49.74	0.419	38.50	91.88
80	55.75	0.392	43.43	110.79

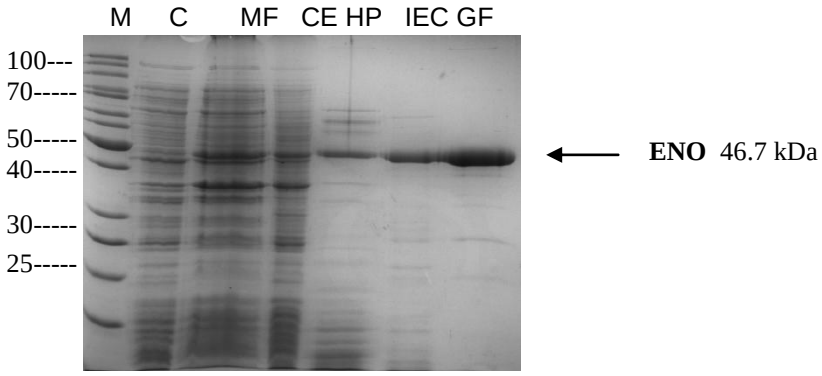

Figure 18: SDS-PAGE **(**Comassie stained) of the purification of enolase from *S. solfataricus* heterologously expressed in *E. coli*; M: Marker PageRulerTM Unstained Protein Ladder; C: Whole cells before induction; MF: Membrane fraction; CE: Crude extract (10 µg); HP80: fraction after 80°C heat precipitation (5µg); IEC: fraction after ion exchange chromatography (1µg); GF: fraction after gel filtration (1µg);

3.3.5 Phosphoenolpyruvate synthase and pyruvate dikinase

The ORF SSO0883 was annotated as PEPS in the *S. solfataricus* genome and was cloned into the vector pET11c. The enzyme was expressed heterologously in *E. coli* using the pET expression system. The enzyme was purified, first by heat precipitation (20 min at 80°C) and further by ion-exchange chromatography (elution at 420 mM NaCl) followed by gel filtration. After gel filtration the enzyme was sufficiently purified. PEPS exhibits a molecular mass of 89-92 kDa which matches approximately the calculated molecular mass of 89.3 kDa. The total yield of protein was 3.2 mg out of 14 g of cell mass (wet weight).

PEPS catalyzes the ATP dependent irreversible formation of PEP. The PEPS activity was assayed in the anabolic direction of PEP formation using a discontinuous assay at 65°C, 70°C and 80°C according to Eyzaguirre et al. (1982). The assay couples the formation of the produced PEP to the oxidation of $NADH^+$ via PK and LDH (2.4.5. / 2.4.3.). The enzyme follows classical Michaelis Menten kinetics for pyruvate and ATP. Kinetic properties could not be determined at 80°C properly due to the heat instability of the product PEP. No significant differences can be observed between the determined properties at 65°C and at 70°C. Compared to other EMP and ED-enzymes the overall activity and the catalytic efficiency are relatively low.

The putative PPDK gene SSO 2820 was cloned into the vector pET11c and the recombinant protein was heterologously expressed in *E. coli* Rosetta (DE3) using the pET expression system. The predicted PPDK (SSO2820) was purified by heat precipitation (30 min at 80°C) of *E.coli* crude extracts to confirm the respective enzyme activity. For the predicted PPDK (SSO2820) no interconversion of PEP and pyruvate could be detected under different tested conditions (2.5 PPDK, PK and PEPS assay), suggesting the gene encoding SSO2820 does not exhibit PPDK, PEPS or PK activity.

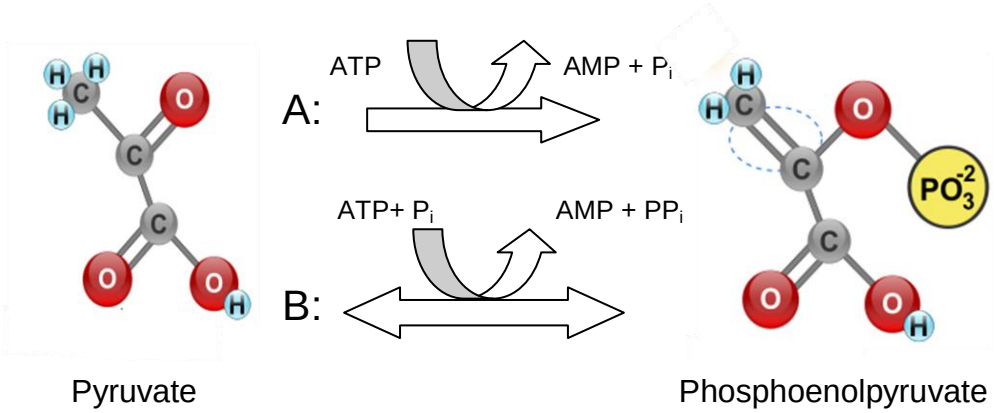

Fig. 19: Conversion of pyruvate to PEP by PEPS (A) and interconversion of pyruvate and PEP by PPDK (B).

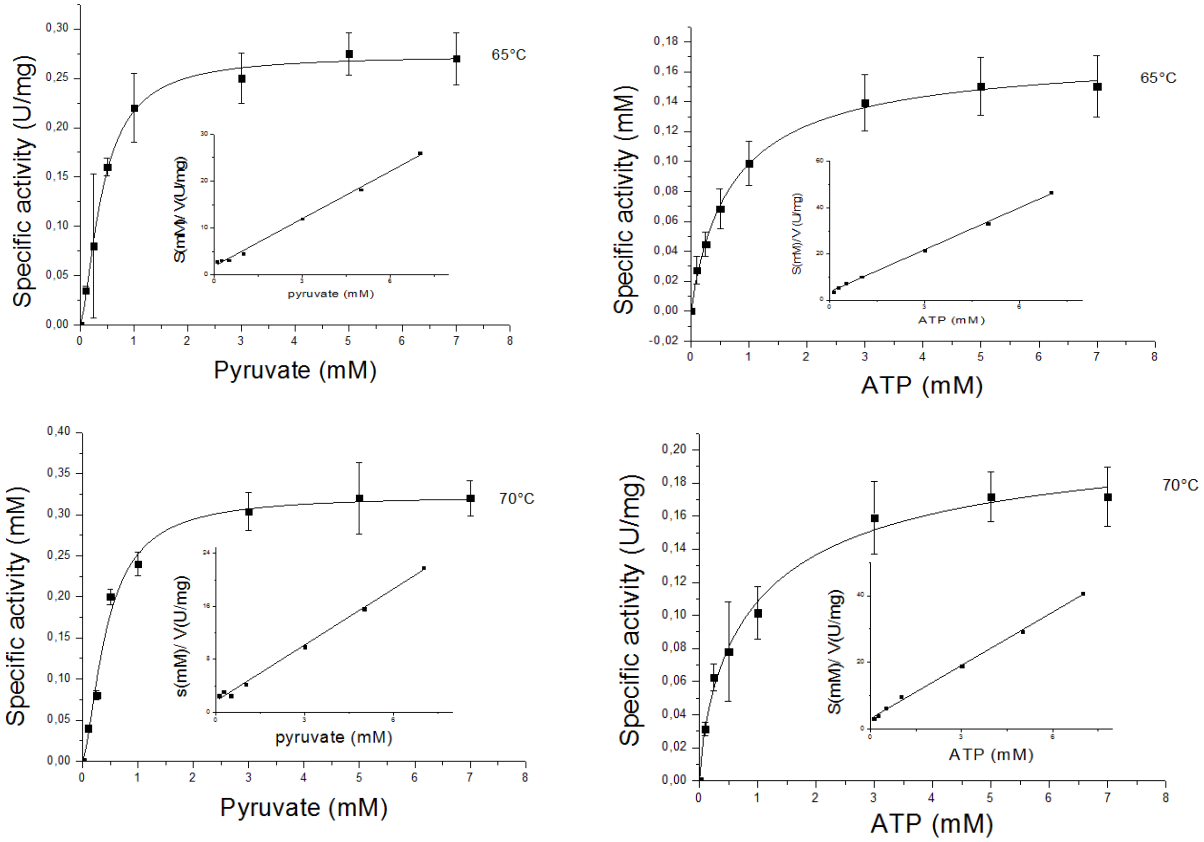

Fig. 20: Rate dependence of PEPS on pyruvate and ATP assayed at different temperatures (65°C, 70°C) with pyruvate as substrate and ATP as co-substrate. Insets show the respective Hanes –Woolf plot. All measurements were performed in triplicate and are means +/-S.D. Kinetic parameters are given in Table 9.

Tab. 9: Kinetic parameters of SSO PEPS for the substrate pyruvate and co-substrate ATP assayed at 65°C and 70°C.

Temp (°C)/ Substrate	v_{max} (U/mg)	k_m (mM)	k_{cat} (s^{-1})	k_{cat}/k_m ($mM^{-1}s^{-1}$)
Pyruvate				
65	0.273	0.54	0.41	0.75
70	0.323	0.46	0.48	1.04
ATP				
65	0.172	0.47	0.25	0.53
70	0.219	0.61	0.326	0.53

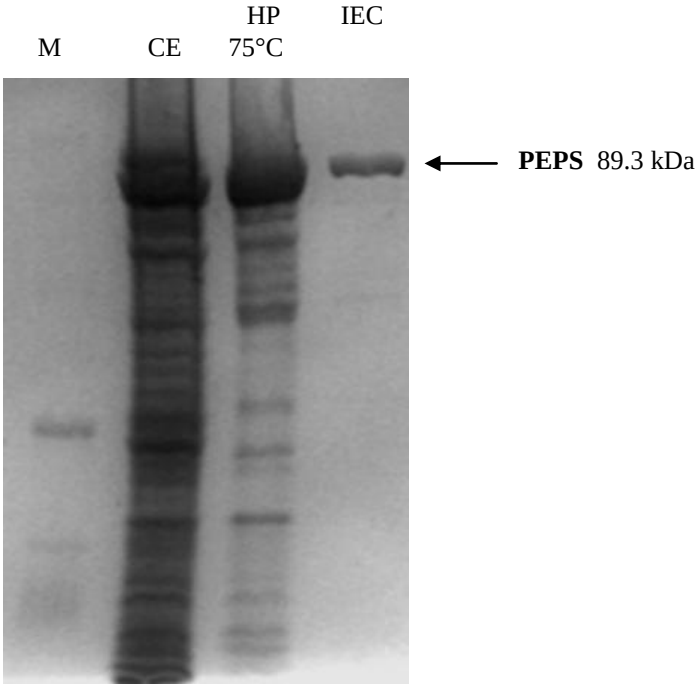

Fig. 21: SDS-PAGE **(**Comassie stained) of the purification of PEPS from *S. solfataricus* heterologously expressed in *E. coli*; M, protein marker; CE (5µg), crude extracts; MF, membrane fraction; HP (10µg), heat preciptation; IEC (4µg): PEPS containing fractions after ion exchange chromatography;

3.4 Crude Extracts Studies

Besides studying the effect of temperature variation at the enzyme level by characterization of the recombinant proteins, measurements of the respective enzyme activities in crude extracts of *S. solfataricus* grown at different temperatures were performed. The established enzyme assays were modified (2.4) and applied to crude extracts from *S. solfataricus* cells grown at 65, 70 and 80°C (provided by the Van der Oost Group, Wageningen University) and specific activities (V_{max}) of ED enzymes were determined for each cell charge at 65°C, 70°C and 80°C (Tab. 10). Specific activities are given in units/mg protein, where one unit refers to a conversion rate of 1 µM/min. In crude extracts of *S.solfataricus* enzyme activities of GDH, PGK, PGAM and PK were identified, strikingly no ENO and PEPS activity was detected despite high amounts of CE. Since, the ENO and PEPS assays have been approved for the respective available recombinant enzyme and inhibition by crude extracts was excluded, the activity appears to be below the detection limit. The enzymatic activities were measured in independent biological replicates (three different 80°C cells and two different 65°C, 70°C cells charges) independent biological replicates (*S. solfataricus* cultivations Tab. 10). In general the determined activities in *S. solfataricus* crude extracts were relatively low and the standard deviation between the cell charges was relatively high. In the case of the first charge of cells, grown at 80°C, no PGAM activity could determind, whereas the second and the third charge show activites in the range of the other activities. The GDH activity determined for the substrate galactose and the co-substrate NAD^+ varies from the second charge of cells, grown at 80°C, to the third one from 0.38 U/mg to 0.84 U/mg with a factor of approx. 2. Although there is a noticeable difference between the cell charges a trend of substrate and co-substrate preference can be observed for the GDH reaction. The highest activity was determined for the combination glucose with NAD^+, followed by galactose with NAD^+. The reaction with the substrates glucose and $NADP^+$ revealed a 50% lower activity and the reaction galactose and $NADP^+$ exhibits only 30% of the activity compared with glucose NAD^+ (Tab.10).

Tab. 10: Specific activities (V_{max} values) of ED enzymes determined at 80°C in crude extracts of *S. solfataricus* grown at 65, 70 and 80°C, respectively.

U/mg	80°C Cells			70°C Cells		65°C Cells	
	1	2	3	1	2	1	2
PK[1]	0.027 +/- 0.001	0.054 +/- 0.005	0.041 +/-0.004	0.035 +/-	0.026 +/- 0.002	0.034 +/-0.001	0.043 +/-0.008
PGAM	X	0.008 +/- 0.001	0.006 +/- 0.002	0.005 +/- 0.0013	0.007 +/- 0.001	0.006 +/- 0.001	0.007 +/-0.001
PGK	0.044 +/-0.003	0.098 +/- 0.059	0.083 +/-0.005	0.035 +/- 0.004	0.043 +/- 0.001	0.052 +/-0.006	0.066 +/-0.003
GDH NAD^+/Glu	0.911 +/- 0.023	0.742 +/- 0.025	1.384 +/- 0.038	1.155 +/- 0.032	1.006 +/- 0.033	1.751 +/- 0.130	1.445 +/-0.0507
GDH NAD^+/Gal	0.571 +/- 0.025	0.382 +/- 0.012	0.840 +/- 0.031	0.716 +/- 0.041	0.644 +/- 0.023	0.885 +/- 0.007	0.770 +/-0.023
GDH $NADP^+$/Glu	0.448 +/- 0.007	0.287 +/- 0.009	0.682 +/- 0.014	0.609 +/- 0.022	0.473 +/- 0.020	0.762 +/- 0.028	0.671 +/-0.01
GDH $NADP^+$/Gal	0.344 +/- 0.001	0.221 +/- 0.002	0.388 +/- 0.036	0.4173 +/- 0.009	0.432 +/- 0.029	0.610 +/- 0.016	0.567 +/-0.049

[1] due to heat instability of PEP no determination of PK activity at 80°C was possible;
X : no enzyme activity detected in this charge

3.5 Metabolite stabilities

The half-lifes of metabolic intermediates of glycolysis were analysed under the respective enzyme assay conditions that were used (Zaparty et al., 2010). The intermediates were incubated at various temperatures and the residual amounts were determined by enzyme assays described in the established SOPs (Zaparty et al., 2010). The intermediates 2-PG (half life 19h at 88°C) and 3-PG (half life 18h at 88°C) showed no considerable decay at the assayed temperatures. While the compounds PEP, $NADH^+$ and $NADPH^+$ are heat instable and show only a half-life of 11 min, 17.4 min and 2.7 min at 88°C respectively (Tab. 11).

Tab. 11: Half life of heat instable intermediates of *S.solfatarticus* glycolysis at 65- 88°C.

Heat instable Compound	Temp. [°C]	Half life [min]
PEP	65	210
	70	89
	80	22
	88	11
NADH	65	128.4
	70	50.7
	80	26
	88	17.4
NADPH	65	37.5
	70	26.5
	80	5.4
	88	2.7
3-PG	88	1080 (18h)
2-PG	88	1140 (19h)

4 Discussion

In this work the following ED/EMP-enzymes: GDH-2, iPGAM, ENO, PK, PPDK, dPGAM and PEPS of *S. solfataricus* were cloned, heterologously expressed in *E.coli*, analyzed for the predicted activity and characterized regarding temperature change. Further, analyses with *S.solfataricus* crude extracts were conducted, as well as the stability of metabolic intermediates were determined.

4.1 Glucose dehydrogenase

The enzyme (GDH-2, SSO3204, EC 1.1.1.47) catalyzes the irreversible oxidation of D-glucose forming gluconate with dual co-substrate (NAD^+/$NADP^+$) specificity. In contrast to GDH-1, which was previously characterized and catalyzes the oxidation of miscellaneous C5 and C6 sugars (Lamble et al., 2003; Milburn et al., 2006) GDH-2 seemed to be specific for D-glucose. More recent studies indicate additional activity with D-xylose and D-galactose (Bräsen et al. Unpublished data). D-allose, D-mannose, L-arabinose, D-ribose, D-lyxose, D-arabinose, L-xylose, D-glucosamine, 2-deoxy-D-glucose, D-fucose, D-lactose, D-maltose, D-fructose and ethanol were not used as substrates. The oxidation rate of the different sugars by GDH-1 depends significantly upon the available co-substrate (e.g. relative rates D-glucose (100% $NADP^+$, 83% NAD^+); L-arabinose, (99% NAD^+, 95% $NADP^+$); D-galactose (53% NAD^+, 12% $NADP^+$); D-xylose (72% NAD^+, 8% $NADP^+$). This seems to be also true for GDH-2, which follows classical Michaelis-Menten kinetics for glucose with NAD^+ and $NADP^+$ (10 mM) (Fig.5, Tab. 1).

Both isoenzymes, GDH-1 and GDH-2, catalyze the NAD^+/$NADP^+$ dependent oxidation of D-glucose. For both enzymes higher activity (GDH-1: 1.6-fold; GDH-2: 3.5-fold) was observed in the presence of NAD^+. However, in the presence of $NADP^+$ GDH-2 exhibits a significant (27-fold) higher affinity towards glucose (0.17 mM ($NADP^+$); 4.59 mM (NAD^+)), whereas GDH-1 shows no difference in respect to co-substrates (1.3 mM ($NADP^+$); 1.5 mM (NAD^+)). Therefore, in comparison to GDH-1 the catalytic efficiency in the presence of $NADP^+$ is significantly increased (K_{cat}/K_m: GDH-2: 115.17 $s^{-1}mM^{-1}$; GDH-1: 36.7 $s^{-1}mM^{-1}$), suggesting that GDH-2 is the preferred enzyme in glucose catabolism. However, GDH-1 seems to be slightly preferred in the presence of NAD^+ (GDH-1: 49.9 $s^{-1}mM^{-1}$; GDH-2: 14.86 $s^{-1}mM^{-1}$) and at high glucose concentration. Both isoenzymes, GDH-1 and GDH-2, catalyze the NAD^+/$NADP^+$ dependent oxidation of D-glucose.

Beside kinetic parameters, the major difference between both isoenzymes is their substrate specificity. To address the molecular basis why GDH-1 catalyzes the oxidation of a range of different five and six carbon sugars and GDH-2 seemed to be more specific regarding the substrate a bioinformatic modelling approach was chosen. The comparison of the vicinity of the sugar substrate in the crystal structure of GDH-1 and in the molecular model of GDH-2 shows a number of differences between both enzymes, including residues at positions that have been identified by (Milburn et al., 2006) as critical for the interaction with the sugar (see also Fig. 22). In the following, these differences are discussed and their likely effects on binding of substrates.

A

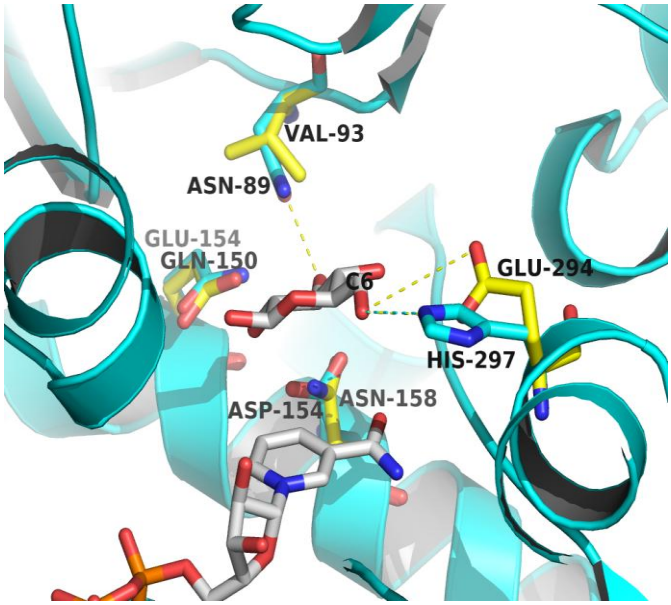

B

GDH-1 SSO3003	**GDH-2** SSO3204
C39	C40
A41	T42
N89*	**V93**
R90	R94
E114*	E118
I117	I121
Q150*	E154
D154*	N158
F279	-
V306	V303
N307*	N304
G308	A305
H297*	**E294**

Fig. 22: Comparison of sugar binding sites.
(A) Superposition of the glucose (centre,grey and red)-binding pocket of the crystal structure of GDH-1 (SSO3003, cyan) and model of the pocket in GDH-2 (SSO3204).(B) Amino acids within 0.5 nm of glucose in the crystal structure GDH-1 (PDB code 2CDB) and the amino acids at corresponding positions in the model of GDH-2. Asterisks mark key interactions with glucose according to Milburn et al., 2006. The residues in the last row are provided by neighbouring polypeptide chain of the tetramer (Haferkamp et al., 2011).

The first important change is from Asn89 in GDH-1 to Val93 in GDH-2. This will probably result in a loss of a hydrogen bond between the sugar ring (C3-hydroxyl group) and the enzyme and thus, will weaken the affinity to β-glucose (pyranose) and to α/β-xylose (pyranose). Secondly, changes from Gln150 to Glu154, and from Asp154 to Asn158 were observed (Fig. 22). These changes could be rather neutral

with respect to substrate binding as in both cases the residues are exchanged for similar ones and the total charge is not affected. A more drastic change is that from the neutral or basic His297 in GDH-1 to the more acidic Glu294 in GDH-2, both contributed by a neighbouring polypeptide chain of the respective tetrameric enzymes. While the histidine nitrogen ε2 is involved in a hydrogen bond to the C6-hydroxyl group of the glucose, it is plausible that the longer and more acidic glutamate group could lead to a stronger hydrogen bond to the same hydroxyl group. This could compensate the weaker interaction with the pyranose ring of glucose due to the transition of Asn89 to Val93 discussed above, so that GDH-2 uses glucose more efficiently as substrate than D-xylose (Haferkamp et al. 2011).

According to their enzymatic properties GDH-2 seems to play the major role in D-glucose catabolism via the branched ED pathway, although GDH-1 might acquire important function at higher D-glucose concentrations and in the presence of NAD^+. Whereas GDH-2 is specialized for D-glucose degradation, GDH-1 seems to have additional functions in the catabolism of D-galactose, D-xylose, L-arabinose and various other sugars (Lamble et al., 2003; Milburn et al., 2006; Nunn et al., 2010).

D-galactose is degraded in *S. solfataricus* via the promiscuous ED pathway (Fig.23), while the metabolism of D-xylose is still unclear.

In *Haloferax volcanii* D-xylose is degraded to α-ketoglutarate using the Weimberg pathway (via xylose dehydrogenase, xylonolactonase, xylonate dehydratase, 2-keto-3-deoxyxylonate dehydratase and α-ketoglutarate-semialdehyde dehydrogenase) and therefore, enters directly the citric acid cycle (Johnsen et al., 2009). Further on *in vivo* NMR studies in *S. acidocaldarius* revealed that D-xylose is degraded in parallel via the Weimberg pathway, which omits aldol cleavage (Nunn et al. 2010). For L-arabinose degradation the pathway (i.e. the specific L-arabinonate dehydratase) still has to be confirmed. A homolog of xylose dehydrogenase is present in the genome of *S. solfataricus* (SSO3015; Haferkamp et al. 2011), however, the respective activity is not confirmed. In addition, a similar pathway has been reported for D-arabinose degradation in this organism and the arabinose-1-dehydrogenase has been characterized recently (Brouns et al., 2006; SSO1300 see Fig. 21). The enzyme SSO1300 exhibits high affinity for D-arabinose (K_m: 0.04, k_{cat}/K_m: 595 $s^{-1}mM^{-1}$), also some other sugars, i.e. L-fucose (6-desoxy-L-galactose), D-ribose and L-galactose are oxidized. Among others arabinose-1-dehydrogenase was significantly up-

regulated at gene- (3.6-fold) and at protein (> 20-fold) level in the presence of D-arabinose compared to D-glucose (Brouns et al., 2006).

More recently a new pathway for D-xylose and L-arabinose degradation was reported (Nunn et al., 2010). The pathway has been reported to proceed via the multifunctional GDH-1, a substrate specific dehydratase (D-xylonate dehydratase (SSO2665)) and aldol cleavage of 2-keto-3-deoxy pentonate to pyruvate and glycolaldehyde via the multifunctional KD(P)G aldolase, which exhibits like GDH-1 broad substrate specificity (Lamble et al., 2003). Glycolaldehyde is converted to glyconate, glyoxylate and finally malate, which enters the citric acid cycle (Fig. 23).

Due to the presence of several uncharacterized members of the pyridine nucleotide dependent alcohol/polyol/sugar dehydrogenase family in *S. solfataricus* the role of GDH-1 in L-arabinose as well as D-xylose catabolism still remains to be elucidated (Fig.23). Possibly, the multifunctional GDH-1 might function as a more flexible "standby" enzyme, which could be involved in different sugar degradation pathways in *S. solfataricus* in addition to the pathway-specific sugar dehydrogenases. This scenario would allow a quick adaptation to different carbon sources, thus to the fine-tuning of the metabolism. This hypothesis is supported by a new D-glucose catalyzing GDH-2, which is presented in this work. Interestingly, a recent phospho-proteom approach comparing on glucose and tryptone grown cells (Esser et al. manuscript in preparation) revealed the phosphorylation of GDH-1, which is strong evidence for a regulation at that point.

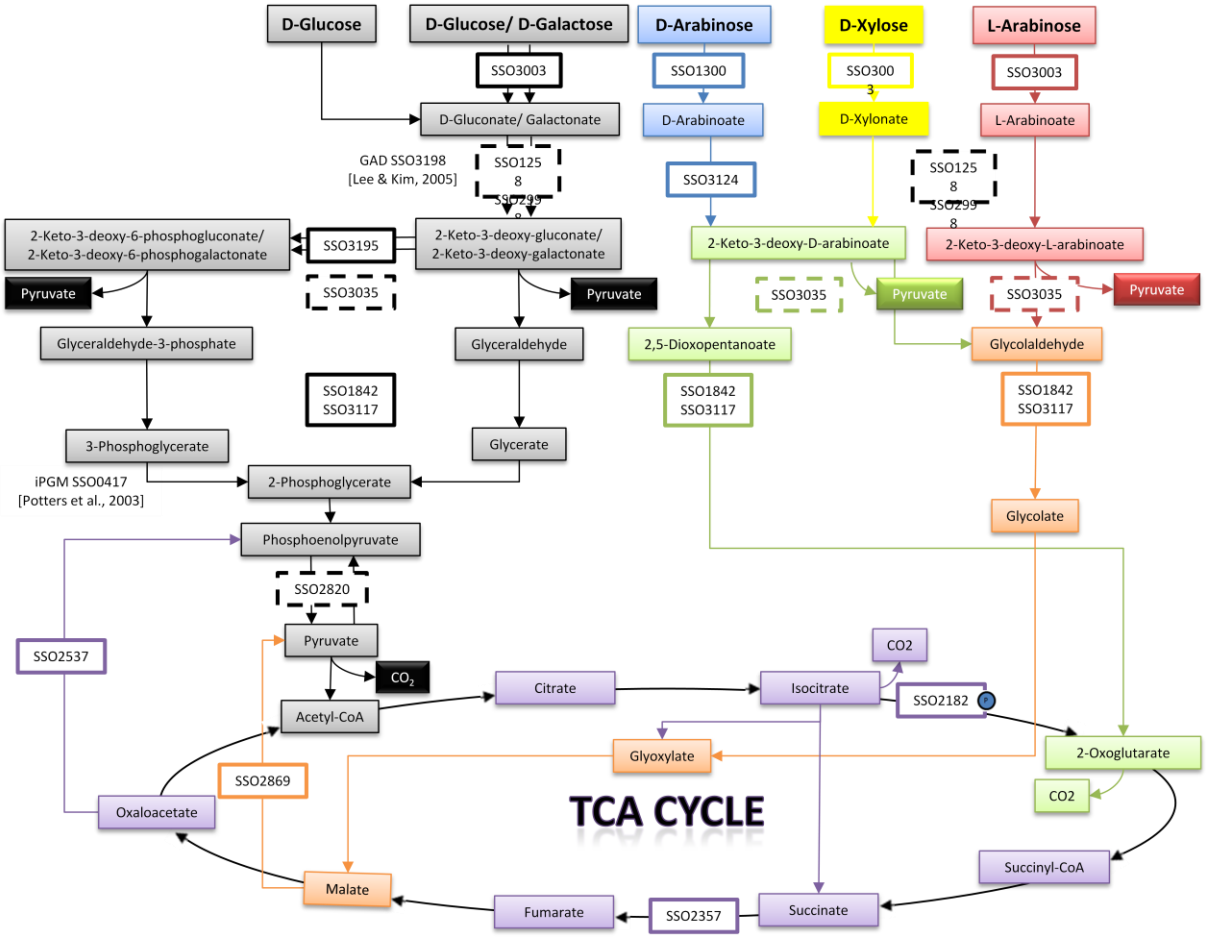

Fig. 23: Current understading of hexose and pentose degradation tricarboxylic acid cycle and C4/C3 interconversion in *S.solfataricus* P2.
Branched Entner Doudoroff pathway for glucose and galactose degradation as well as pathways for D-arabinose, D-xylose and L-arabinose catabolism. Dashed lines indicate candidates of unknown functions (Esser et al., 2011 manuscript in preparation).

4.2 Enolase

Enolase catalyzes the reversible interconversion of 2-PG and PEP. Regarding *S. solfataricus*, this enzyme is essential for growth on glucose and galactose. In this work enolase from *S. solfataricus* P2, heterologously expressed in *E. coli*, was characterized for the first time. Enolase characterization was performed at four different temperatures: 65, 70, 80, 88°C. Temperatures of 65 and 70°C were chosen to simulate cold-, 88°C to simulate heat-shock conditions. PEP formation catalyzed by enolase was detected spectrophotometrically in a continuous enzyme assay (see 2.4). In recent years a continuous spectrophotometric detection of PEP formation has become established in enolase characterization (Lee et al., 2006; Antikainen et al., 2007; Seweryn et al., 2008), which omits the use of auxiliary enzymes and allows for continuous measurement, independent of assay temperature.

In general, enolase (SSO0913) substrate affinity is higher in the catabolic direction compared to the anabolic direction independent of temperature (Tab. 6; 7). Thus, the catalyzed conversion of 2-PG to PEP (catabolic direction) is favoured over the anabolic direction. This does not apply to all bidirectional enzymes in the glycolytic pathways. While, for example, glycolysis in *S. cerevisiae* is also preferential for phosphoglycerate kinase (McHarg et al., 1999; Hurth et al., 2007), PGAM of the protozoan parasite *Leishmania mexicana* favours the anabolic direction (Fothergill-Gilmore and Watson, 1990; Guerra et al., 2004).

Enolase (SSO0913) characterization revealed decreasing substrate affinity with increasing temperature in the catabolic direction. K_m-values for 2-PG increase from 0.060 mM at 65°C to 0.192 mM at 88°C. Nevertheless, the catalytic efficiency only decreases in the temperature range of 65°C to 80°C from 1069 to 766 $mM^{-1}s^{-1}$ but increases to 945 $mM^{-1}s^{-1}$ at 88°C. This is due to comparably large increase of enolase specific activity (182 U/mg to 233 U/mg) and low decrease in substrate affinity (0.185 mM to 0.192 mM) from 80°C to 88°C.

As there is only one enzyme with enolase functionality annotated in *S. solfataricus*, the described temperature dependent substrate affinity seems to point to a metabolic adaptation mechanism: faster conversion of PEP in comparison to 2-PG at higher temperatures. A plausible explanation to this assumption may be provided by the thermal stability of the substrates of the bidirectional enolase. Thermal stability experiments at 88°C revealed a half life of 19.25 h for 2-PG (see 3.5) and only 11 min for PEP (Tab. 11). High temperature stability of 2-PG could be the reason for a

reduced PEP synthesis, so that PEP loss due to thermal degradation can be minimized.

The high temperature stability of 3-PG (half life: 57.76 h) supports the assumption of a metabolic regulation on PEP level in hyperthermophilic organisms. PGAM converts 3-PG to 2-PG, thus providing the substrate of enolase in the catabolic direction. Like enolase, PGAM is part of the lower shunt of the commen EMP-pathway and the semi-phosphorilative ED-branch.

Enolase K_m-values of other Archaea (also Bacteria and Eukarya) were obtained and compared in respect to their optimal growth temperature (Tab. 13). The K_m-values of 0.19 mM (2-PG) and 0.39 mM (PEP) for enolase (SSO0913), obtained in this study are in the range of those determined for other organisms (2-PG: 0.04 – 0.21 mM; PEP: 0.24 – 0.95 mM). There are no obvious differences in the presented values from Table 13 regarding the belonging to the three domains of life. Enolases from mesophilic organisms show the highest (*S. cerevisiae*: V_{max} = 430 U/mg; K_m = 0.04 mM) as well as the lowest (*C. albicans*: V_{max} = 35 U/mg; K_m= 0.38 mM) specific activity and substrate affinity, respectively, for 3-PG, in the catabolic direction. Kinetic data obtained for *S. solfataricus* and *T. maritima*, the two hyperthermophilic organisms in this comparison (Tab. 13), are similar. The specific activity as well as the substrate affinity (V_{max} = 192 U/mg; K_m = 0.18 mM) of *S. solfataricus* enolase are similar to those of *T. maritima* (V_{max} = 250 U/mg; K_m = 0.07 mM) at 80°C in contrast to the kinetic parameters of the other presented organisms (Tab. 13). Altogether, the enolase affinity for 2-PG is higher than for PEP. Additionally, enolase SSO0913 specific activity in the catabolic direction (192 U/mg) is more than three times higher as compared to the anabolic direction (56 U/mg). For T. brucei the difference is 10-fold and for C. albicans about 8 times higher. In conclusion, catalysis in catabolic direction is favoured by the enzyme.

Tab. 12: Kinetic parameters of enolase from various organisms.
The K_m-values of enolases from different organisms measured at the individual temperature and the respective substrate is given. Enolase recombinantly expressed in *E. coli* is marked by the letter ***R*** behind the respective organism's name. If deviating from the assay temperature, the optimum growth temperature of the respective organism is added in brackets. Domains are separated by dashed lines.

Organism	Domain	K_m	V_{max}	Substrate	Reference
Thermotoga maritima	Bacteria	0.07 mM 75°C (80°C)	250.00 U/mg 40°C (80°C)	2-PG	(Schurig *et al.*, 1995); (Huber *et al.*, 1986)
Bacteroides fragilis ***R***	Bacteria	0.21 mM 37°C	-	2-PG	(Sijbrandi *et al.*, 2005); (Tamimi *et al.*, 1960)
Saccharomyces cerevisiae (wt) ***R***	Eukarya	0.04 mM 25°C	429.50 U/mg 21.7°C	2-PG	(Sims *et al.*, 2006) (Brewer *et al.*, 2003)
Saccharomyces cerevisiae ***R***	Eukarya	0.05 mM 25°C	-	2-PG	(Sims *et al.*, 2006)
Trypanosoma brucei ***R***	Eukarya	0.05 mM 25°C (37°C)	63 U/mg 25°C (37°C)	2-PG	(Hannaert *et al.*, 2003) (Duszenko *et al.*, 1985)
Candida albicans	Eukarya	0.38 mM 30°C (25 – 37°C)	35.31 U/mg 30°C (25 – 37°C)	2-PG	(Kustrzeba-Wójcicka and Golczak, 2000); (Mattia and Cassone, 1979)
Pyrrococcus furiosus	Archaea	0.40 mM	13.8 U/mg 90°C	2-PG	M.J. Peak et al. 1994
Sulfolobus solfataricus ***R***	Archaea	0.18 mM 80°C	192.21 U/mg 80°C	2-PG	This work
Trypanosoma brucei ***R***	Eukarya	0.24 mM 25°C (37°C)	6.3 U/mg 25°C (37°C)	PEP	(Hannaert *et al.*, 2003) (Duszenko *et al.*, 1985)
Candida albicans	Eukarya	0.95 mM 30°C (25 – 37°C)	-	PEP	(Kustrzeba-Wójcicka and Golczak, 2000); (Mattia and Cassone, 1979)
Sulfolobus solfataricus ***R***	Archaea	0.39 mM 80°C	55.75 U/mg 80°C	PEP	This work

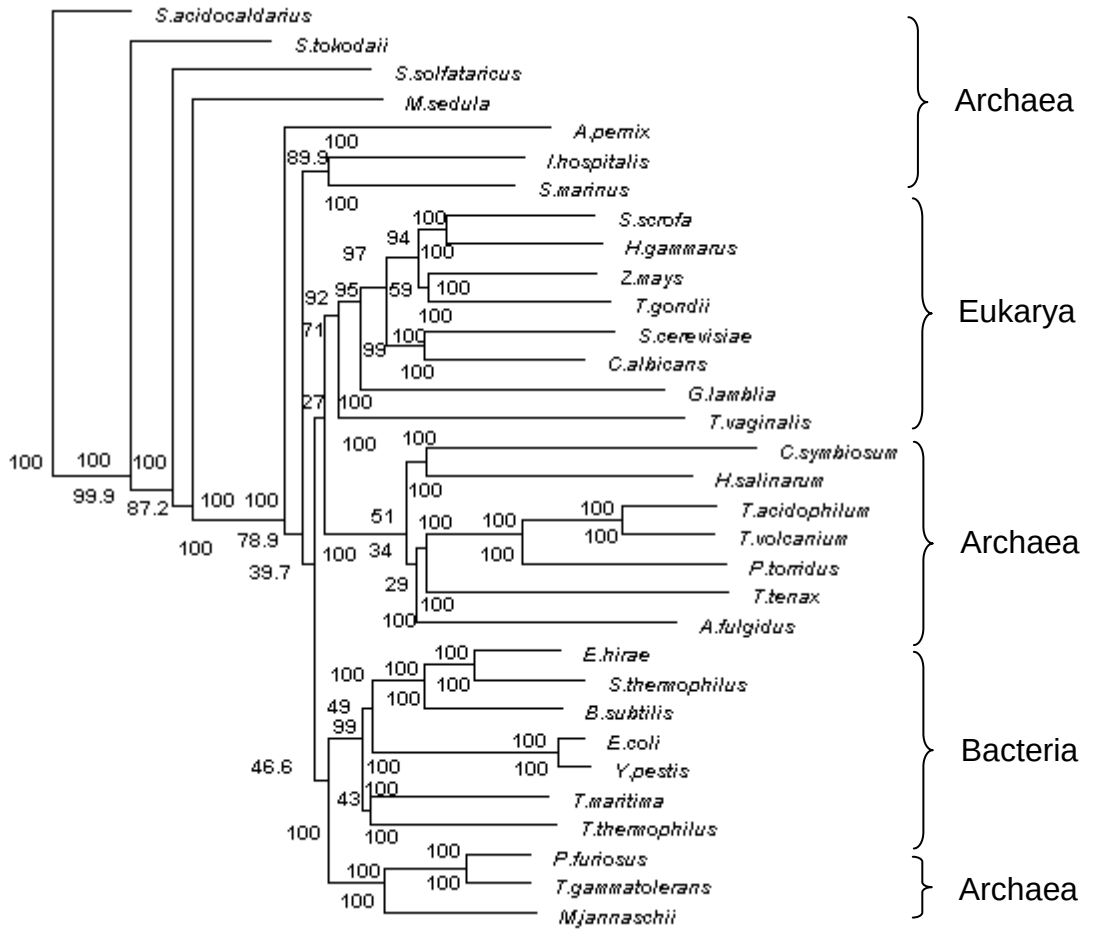

Fig. 24: Unrooted phylogenetic tree of enolase generated with the neighbor joining method from 32 organisms covering the three domains of life (Fig. 1).Unrooted phylogenetic network was calculated by the use of Software SplitsTree4 (Huson and Bryant, 2006). 0.1 changes per nucleotide.

In order to unravel evolutionary relationships between enolases an unrooted phylogenetic tree was constructed using SplitsTree4 (Huson and Bryant, 2006). The phylogenetic tree shows a close relation of all enolases that were included in the analysis. Enolase from *S. solfataricus* shows sequence identities in a range of 29.5 % to 99 % to enolases from organisms presented in Fig. 23. Enolase sequence identities show a classification according to the domain of life although the lowest as well as the highest enolase sequence identities were found for enolases from other Archaea. Sequence identities of archaeal, eukaryotic and bacterial organisms towards enolase SSO0913 range from 29.5% - 99%, 40.0 % - 43.0 % and 41.0 % - 44.5 %, respectively (Fig. 23). A bacterial and a eukaryal cluster are clearly evident, whereas the archaeal sequences seem to be devided into several clusters. Furthermore, the degree of enolase sequence identity seems not to be influenced by lifestyle conditions such as temperature or salt adaptation. No clustering according to growth conditions is observed. Also a devision by taxa in crenarchaeota or

eurarchaeota is not visible. While enolase from the hyperthermophile *T. tenax* exhibits a sequence identity as low as 33.9 %, those of hyperthermophile *M. jannaschii* exhibits similar high sequence identity (45.3 %) towards enolase SSO0913, as the two following hyperthermophilic organisms, Archaeaon, *P.furiosus* with 45.1% and the bacterium, *T.maritima* with 44.5%. Corresponding to the comparably high sequence identity of enolases from hyperthermophiles to *S. solfataricus*, enolases from the psychrophilic Archaeon *C. symbiosum* reveals the lowest sequence identity (29.5 %) (Fig. 23). Thus, enolases are universally present in hyperhermophiles and are highly conserved and widely distributed among all organisms. Brown and Doolittle (1997) found that for enzymes from the lower shunt of glycolysis, including GAPDH, PGK and enolase, the bacterial and eukaryal sequences were closer and the archaeal sequences more distant. Concluding, the high degree of conservation and universal distribution of the enzymes of the lower shunt of glycolysis enable them to be used as viable and important molecular chronometers to investigate the origins of metabolism and life itself. As discussed previously by Ronimus et al., evolutionary history of enzymes from hyperthermophilic microorganisms, points to a gluconeogenic origin for the Embden-Meyerhof-Parnas pathway. This contrasts with the upper portion of the pathway, which is characterized by multiple origins for the enzymatic activities present in hyperthermophiles and other archaea (Ronimus et al. 2002).

4.3 Phosphoglycerate mutase

Phosphoglycerate mutase (PGAM SSO0417, SSO2236) belongs to the branch I histidine phosphatase superfamily. PGAM catalyses the interconversion of 2-PG and 3-PG and is a key enzyme of glycolytic pathways as it takes part in glycolysis and gluconeogenesis.

There was no enzyme activity detected for the 2.3 BPG dependent dPGM under the given assay conditions (3.3.2), and further tests with the addition of 2.3-BPG did not show activity as well. However, as the positive control with the enzyme from *A.fulgidus* did not work it is still unclear if the enzyme SSO2236 is active under different conditions and needs further testing. So far, dPGM from A. fulgidus is the only characterized dPGM in the domain Archaea (Johnsen et al. 2007).

The recombinant expression of *S.solfataricus* iPGAM yielded 2.2 mg protein out of 7.8 g cells (wet weight). The incubation of iPGAM with phosphate containing intermediates was performed to investigate whether the visible double band (Fig. 9) can be explained by phosphorylation. Apparently, the tested substances (ATP, ADP, AMP, 3-PG, 2-PG, PP_i) have no influence on the band pattern on the SDS-PAGE.

As the optimal growth temperature for *S.solfataricus* is 80°C it might be expected that the enzyme is also most efficient at 80°C. For the iPGAM (SSO0417) this could be confirmed for the anabolic reaction, but not for the catabolic reaction. It is suggested that the CCM network of *S.solfataricus* is adapted to high temperatures by controlling the flux of thermolabile metabolic intermediates (Albers et al., 2009). Both, 3-PG and 2-PG are heat stable for at least 18 hours at 80°C, but 2-PG is converted by enolase to the heat instable PEP (Halflife 22min 80°C; Tab. 10; 2.5) and 3-PG is converted to the extremely heat instable 1.3BPG (halflife 60°C 1.6 min) by PGK, thus implicating a secondary role of the iPGAM in the temperature dependent flux control. The glycolytic reaction exhibits a noticeable low K_m at 65°C that leads to an even higher catalytic efficiency (Tab. 2; 3) compared to 80°C, which might be explained as compensation strategy to keep the metabolism on a similar or higher level under low temperature conditions. It seems that hyperthermophilic archaea are not only adapted to high temperatures, but also have to be equipped with strategies to cope with low temperature conditions, compared to their optimal growth temperature. These results show how changes in temperature have a significant impact on the catalytic properties of enzymes, like for example a shift from 80°C to 65°C results in a change of the K_m from 0.11 mM 3-PG to 0.26 mM 3-PG (*S.solfataricus* iPGAM) .

Recombinantly expressed PGAM from *P. furiosus* (PF1959) and *M. jannaschii* (MJ1612), were previously described by Van der Oost et al. (2002) at a temperature of 50°C. Compared to the completely purified PGAM from *P. furiosus* (V_{max} = 2.34 U/mg) and *M. jannaschii* (V_{max} = 1.15 U/mg) (Van Der Oost et al., 2002), iPGAM SSO0417 revealed a specific activity in the same range with a V_{max} of 2.01 U/mg, determined at 65°C. The archaeal iPGAM (SSO0417) was previously analyzed as a 46 kDa homotetrameric enzyme exhibiting a specific activity of 0.182 U/mg (25°C) (Potters et al., 2003) and thus is similar to characterized iPGAMs from *P. furiosus* (V_{max}: 2.34 U/mg at 50°C), ORF PF1959, and from *M. jannaschii* (V_{max}:1.15 U/mg at 50°C, ORFMJ1612, Van der Oost et al., 2002).The results determined in this study are in a similar range with a V_{max} of 3.99 U/mg in the catabolic direction at 80°C. For 3-PG a K_m of 0.04mM could be determined at 65°C which is a factor 10 lower compared to the K_m of 0.45 mM for *P.furiosus* measured at 50°C (van der Oost et al., 2002), however, its optimal growth temperature is around 100°C. Therefore considering the different growth optima, the iPGAM from A. fulgidus shows the highest activity at 70°C (Johnsen et al. 2007), which is in accordance with the growth temperature of the organism (Stetter et al., 1988). RT-PCR analysis showed that AF1751, encoding *A. fulgidus* iPGAM, was transcribed in vivo during growth of the organism on lactate/sulfate suggesting a role in gluconeogenesis (Johnsen et al., 2006).

4.4 Posphoenolpyruvate synthetase, pyruvate phosphate dikinase and pyruvate kinase

It was shown that the ORF SSO0981 is coding for a 49.8 kDa protein and as annotated, pyruvate kinase activity was confirmed. The enzyme was characterized at temperatures from 50°C to 80°C. The enzyme shows activity in a commen range with a $V_{max(PEP)}$ of 70.37 U/mg determined at 70°C compared with PKs from other organisms (Tab. 14) and also other ED/EMP enzymes in *S. solfataricus* (ENO $V_{max(PEP)}$ 49.74 U/mg; GDH-2 $V_{max(glucose,\ NADP)}$: 42.94 U/mg) . It was observed that V_{max} -values increase and K_m-values decrease with higher temperatures. This could be expected as the optimum growth temperature for *S.solfataricus* is 80°C (Zillig et al., 1980) and chemical reactions are accelerated according to van't Hoff's rule, which states that a temperature increase by 10°C will increase a rate constant by a factor of approx. 2. This explains the raising V_{max}-values and for most enzymes also an effect on the K_m-values, with increased affinity at higher temperature, was observed.

PK activity in *S. solfataricus* crude extracts (0.0497 U/mg) was 1000-fold lower than from the recombinant enzyme. This is a general effect observed in crude extracts possibly due to the low expression and the resulting low amount of protein. Surprisingly, the SSO PK shows significant inhibition by ATP. Inhibition by ATP is a well characterized form of regulation for PKs from Bacteria and Eukarya, while for PKs in Archaea only a few regulating effectors are known (Siebers and Schönheit, 2005) and the PK from *A.fulgidus* is the only archaeal enzyme known to be inhibited by ATP so far. For *A.fulgidus* ATP inhibition could be reversed by high PEP concentrations suggesting a competitive inhibition (Johnsen et al., 2003; Potter et al., 1992). In the case of the *S. solfataricus* PK inhibition could not be reversed by AMP or FBP which are activators for many bacterial and eukaryotic PKs or by higher PEP or ADP concentrations. So the mechanism of regulation has to be either non- or uncompetitive. In Eukarya and Bacteria the PK is a major control point of the glycolysis as it catalyzes its last step and is highly regulated. The regulative properties in Archaea are reduced, but the, for Archaea, unique form of product inhibition by ATP indicates an important role as a control point of the CCM in *S. solfataricus*.

Tab. 13: Kinetic parameters of PKs from various organisms.
The K_m-values and V_{max}-values of PKs from different organisms are given. If the assay temperature deviates from the optimal growth temperature, the temperature is added in brackets. Eu.: Euryarchaeota; Cr. : Crenarchaeota;

Organism	Domain	K_m(PEP)	V_{max}(PEP)	Growth temp.	Reference
T. acidophilum	Archaea (Eu.)	0.04 mM (60°C)	201 U/mg (60°C)	56°C	Potter et al. 1992
A. fulgidus	Archaea (Eu.)	0.4 mM (65°C)	1000 U/mg (65°C)	80°C	Johnsen et al. 2003
A. pernix	Archaea (Cr.)	0.26 mM (65°C)	53 U/mg (65°C)	95°C	Johnsen et al. 2003
P. aerophilum	Archaea (Cr.)	1.31 mM (65°C)	46 U/mg (65°C)	100°C	Johnsen et al. 2003
T. tenax	Archaea (Cr.)	0.7 mM (50°C)	46 U/mg (50°C)	85°C	Schramm et al. 2000
S. solfataricus	Archaea (Cr.)	0.09 mM (70°C)	70.37 U/mg (70°C)	80°C	This work
S. cerevisiae	Eukarya	0.09 mM	250 U/mg	30°C	Kayne et al. 1973
G. stearo-thermophilus	Bacteria	0.11 mM	330 U/mg	30°C	Sakai et al. 1986
T. maritima	Bacteria	0.1 mM	320 U/mg	80°C	Johnsen et al. 2003

The ORFs SSO2820 and SSO0883 are annotated as putative PPDK and PEPS, respectively. In the branched ED and EMP pathways these enzymes catalyze the conversion of pyruvate and PEP. As mentioned above, also the ORF SSO0981 was analyzed and confirmed as functional catabolic PK, which catalyzes the counterreaction of the classical anabolic PEPS (PEP to pyruvate). When compared in an alignment (Fig. 25) the aminoacid sequence of SSO2820 shows a relatively high similarity to known PEPS and PPDKs from other organisms but does not match the typical size of the sequence. As shown in Fig. 25 and Fig. 26 the aminoacid sequence of SSO2820 is only a third of the size compared with functional confirmed enzymes like the *S. solfataricus* PEPS. Only the conserved region of the PPDK_N (PF01326) superfamily (as indicated) is represented by the sequence, but the residual expected conserved regions for PEP-utilizer (PF0396) and the malat

synthase (PF01274) superfamily are missing. Both ORFs were heterologuously expressed in *E.coli* and analyzed. The ORF SSO0883 showed the annotated PEPS activity and no PPDK activity, while the expressed protein of ORF SSO2820 showed neither PEPS nor PPDK activity.

```
SSO2820      MNYTYLLDEVS-------------LSMVSIVGRKSAYLGELYKMGFNIPK
SSO0883      MGSFLLVEAISSEEDLILDVSQVTKDMVQLAGGKGANLGELTSIGVRVPP

SSO2820      GFIISSRGVN--EAIKDLDDEIRGILSSVNLNDTTDLEKRSEMIKSMIIA
SSO0883      AFILTSKAFKYFLEYNNLFDKIRDTLSSS---ETS--EEASEKIKQLIKN

SSO2820      SKLPNEMEKEIYERFSQLGSKY-----VAVRATATSP-LSGASFAGEYET
SSO0883      AKMPDKLSSMIYQAYDELSKKVGKEILVAVRSSATAEDIETASFAGQQDT

SSO2820      DLFVTQENLIPSIKRVIASYFNPRAIAYRILTHNEAG---MAILVQTMIN
SSO0883      YLNVTKDELIDRIKDVWASLYNARAMEYRKSKGIDDLSILIAVVVQKMVN

SSO2820      PVSAGTAFSIHPITEEPDYVVIESSFGLGESVTKGMVTPDQYVVSKATRS
SSO0883      SRSAGVMFTLHPVTGDEKYIMIESNWGLGESVVGGKVTPDEVLIEKSTLR

SSO2820      LVSKRISEKVMKLTYDFAEKKIKSIELSKEEALAESLSDNDAIRIANMAI
SSO0883      IVEKKVSNKNIKIVYDKQLKKNVTITLDEKESRLMSITDEEAIELAKLAL

SSO2820      AIESIFKRNINIEWAIED-----KKVYLLEVR-----------------
SSO0883      KIEEHYKRPMDIEWAIDNDLSFPENIFIVQARPETFWSSKRKENKNIAEK

SSO2820      ----G----IRRLYP---------------------EF------------
SSO0883      SAPIGGKVLVRGLAASPGIAFGKAKIILDIKDPKVHEFQKGEILVTKMTD

SSO2820      --------------------------------------------------
SSO0883      PDWVPLMKIAGAIITDEGGMTSHAAIVSRELGIPAIVGSREATKIIRDNQ

SSO2820      --------------------------------------------------
SSO0883      EITVDAIRGIVYEGKVLQTSETVSQQAQPSIGIQGISREVLLSLYPVTAT

SSO2820      --------------------------------------------------
SSO0883      KIYMNLGEPDVIDKYLDLPFDGIGLMRIEFIVSEWVRYHPLYLIKIGNAE

SSO2820      --------------------------------------------------
SSO0883      LFVDKLAEGIAKVASAIYPRPVVVRFSDFKTNEYKKLIGGEEFEPDERNP

SSO2820      --------------------------------------------------
SSO0883      MIGWRGVSRYVSKEYEPAFRLEAKAIRKVREEMGLKNVWVMFPFVRTTWE

SSO2820      --------------------------------------------------
SSO0883      LEKAIKIMEEEGLRRDSDFKVWIMAEVPSVVVLAEEFAKIVDGFSVGSND

SSO2820      --------------------------------------------------
SSO0883      LAQLTLGVDRDSELLARMGYYDERDPAVLESIRKLIKAAHKYGKTVSICG

SSO2820      --------------------------------------------------
SSO0883      QAPSVYPAVVEYLVKAGIDSISVNPDAVINVRRQVASIEQQIILRNLNGK

SSO2820      ----
SSO0883      RKNK
```

Fig. 25: Pairwise alignment of the PEPS SSO0883 and the annotated PPDK SSO282 Conserved residues involved in PEP binding are marked red.

As the conserved PPDK region (Fig. 25/26) is involved in PEP/ pyruvate binding it can be speculated that the protein SSO2820 exhibits an unknown function, possibly in the regulation of the PEP/ pyruvate interconversion. Also, a study of the phosphoproteom of *S.solfataricus* by Esser et al. (unpublished) showed that the protein SSO2820 is phosphorylated under glucose growth conditions, which additionally indicates a role the regulation of glycolysis.

It can be speculated, that the above mentioned inhibition of the *S. solfataricus* PK by ATP (50% residual activity at 0.8 mM ATP at 70°C) fits to the relatively high K_m for ATP (0.61 mM at 70°C) of the PEPS, suggesting a regulation at this level. With high amounts of ATP in the cell the glycolytic reaction of the PK would be slowed down and the gluconeogenic reaction of the PEPS would be favoured.

The determined PEPS activity is relatively low with a V_{max} of 0.323 U/mg for pyruvate, compared to the counterreaction of the PK with 70.37 U/mg for PEP (both determined at 70°C). Also, no glycolytic activity with the substrates PEP, AMP and ADP can be detected. However, the measured activities of the *S. solfataricus* PEPS are in a similar range compared with the *T.tenax* enzyme with a V_{max} of 0.45 U/mg for pyruvate determined at 70°C (Tjaden et al., 2006; Tab. 15) as are the determined K_m-values of 0.4 mM and 0.47 mM pyruvate.

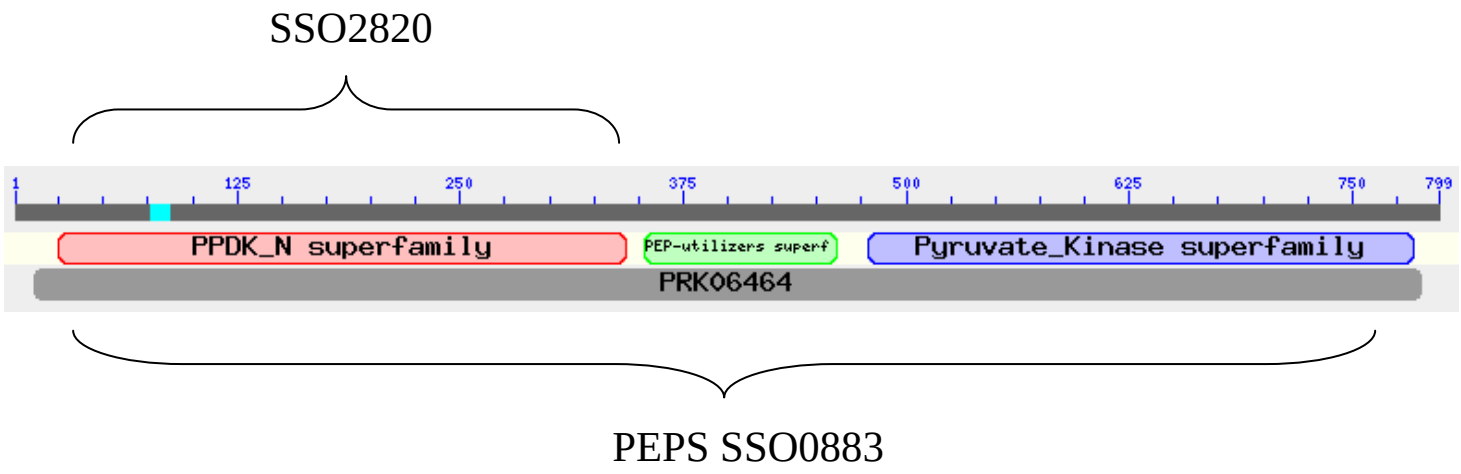

Fig. 26: PPDK / PEPS- gene conserved domains

Tab. 14: Kinetic parameters of PEPSs (PPDK only in *T.tenax*) from various organisms.
The K_m-values and V_{max}-values of PEPSs from different organisms are given. If the assay temperature deviates from the optimal growth temperature, the temperature is added in brackets. ND: not detected;

PEPS					
anabol	*T. tenax (85°C)* (Tjaden 2006)	*P. furiosus (90°C)* (Hutchins2001)	*M. thermoauto-trophicum (56°C)* (Eyzaguirre 1982)	*S. solfataricus (80°C) This study*	*E. coli (37°C)* (Berman 1970)
K_m(mM) pyruvate	0.4 (70°C)	0.11 (80°C)	0.36 (50°C)	0.46 (70°C)	0.08 (25°C)
K_m(mM) ATP	1 (70°C)	0.39 (80°C)	ND	0.61 (70°C)	0.028 (25°C)
V_{max} (U/mg) pyruvate	0.45 (70°C)	14.9 (80°C)	0.29 (50°C)	0.32 (70°C)	8.9 (25°C)
V_{max} (U/mg) ATP	ND	12.9 (80°C)	ND	0.219 (70°C)	ND
catabol					
K_m(mM) PEP	ND	0.4 (50°C)	ND	ND	ND
K_m(mM) AMP	ND	1 (50°C)	ND	ND	ND
V_{max} (U/mg) PEP	ND	0.14 (50°C)	ND	ND	ND
V_{max} (U/mg) AMP	ND	0.059 (50°C)	ND	ND	ND
PPDK					
K_m(mM) pyruvate	0.8 (70°C)				
K_m(mM) ATP	8 (70°C)				
V_{max} (U/mg) pyruvate	1.1 (70°C)				
V_{max} (U/mg) ATP	ND				
catabol					
K_m(mM) PEP	0.5 (55°C)				
K_m(mM) AMP	0.02 (55°C)				
V_{max} (U/mg) PEP	2.5 (70°C)				
V_{max} (U/mg) AMP	ND				

There are significant differences regarding the last step of the glycolysis, the interconversion of PEP and pyruvate, in different archaeal species (Fig. 27).

T.tenax uses three enzymes for this step: PK, PEPS, and PPDK. PK and PEPS are only unidirectional, whereas the PPDK is bidirectional but is more efficient in the glycolytic direction. In this case the PPDK is a standby enzyme which allows for fine tuning of the energy level in the last step of gylcolysis (Tjaden et al 2006).

In *T. kodakarensis* and *P. furiosus* no PPDK homolog is present according to the genome sequence information, but functional PK and PEPS were described. Strikingly, the PEPS of T.kodakarensis and P. furiosus is bidirectional (Fig. 27). In the case of *T. kodakarensis* PEPS is the essential enzyme for both the glycolytic and the gluconeogenic conversion of PEP and PK is used in addition at high energy levels as derived from a mutational approach (Imanaka et al. 2006).

In *P.furiosus* Tuininga et al. (2003) determined $\Delta G^{0'}$ -values for enzyme rections, -20 kJ/mol for the PK reaction and -8.75 kJ/mol for the PEPS reaction, which indicates that the PEPS reaction in the glycolytic direction is thermodynamically feasible. Additionally it was shown that with the addition of AMP K_m-value of PK for ADP rises and the K_m-value of PEPS is lower for AMP (1 mM; Tab. 14) suggesting that PEPS is favoured over the PK reaction in the case of a high intracellular AMP level (Huttschins et al 2001; Tuininga et al 2003).

In *S. solfataricus* the situation is different once more (Fig. 27), three candidate genes were annotated: PPDK, PEPS and PK. The PPDK sequence is unusually short and the recombinant protein shows no PK, PEPS or PPDK activity. PEPS and PK are in this case unidirectional: (I) PK is only active in glycolytic direction with a catalytic efficiency of 627.95 $mM^{-1}s^{-1}$ for (PEP, 70°C; Tab.14) and is allosterically regulated by ATP, which is well known for bacterial and eucaryal PKs but is unusual in Archaea so far. (II) PEPS is only active in gluconeogenic direction, but exhibits a much lower catalytic efficiency of 1.04 $mM^{-1}s^{-1}$ for pyruvate at 70°C. Therefore, suggesting the presence of an alternative pathway for the formation of PEP. The already mentioned study of the phosphoproteom of *S. solfataricus* (Esser et al., manuscript in preperation) revealed that the putative PEP-carboxykinase SSO2537 is phosphorylated and probably regulated by post-translational modification and could convert oxaloacetate to PEP *S. solfataricus*. It is still unclear if the small, as PPDK annotated, protein has a role in the regulation of PK or PEPS or the PEP/ pyruvate conversion as it shows high homology to the PEP/ pyruvate binding site of PEPS and PPDK enzymes it can be speculated that it might have regulative relevance.

The detailed study of the regulation of the lower shunt of glycolysis in *S.solfataricus*

In comparison to other archaea reveals different strategies for regulation at the level of PEPS/ pyruvate conversion. However, as well known for bacteria and eukarya this seems to be an important regulation point also in archaeal metabolism.

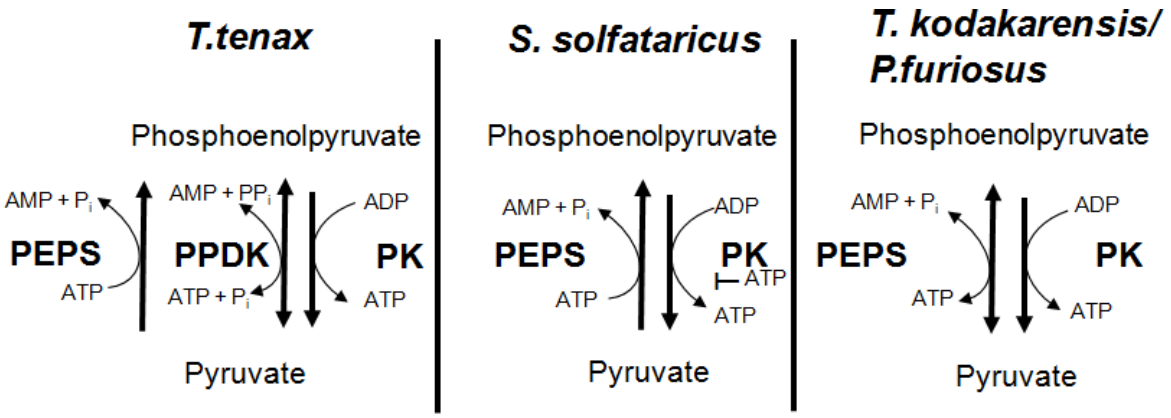

Fig. 27: PEP / pyruvate conversion in the archaeal species *T.tenax, S. solfataricus, P. furiosus* and *T. kodekarensis*

4.5 Crude extracts and model implications

In order to unravel the effect of temperature variation at enzyme level, V_{max}-values of enzymes of the ED-pathway and the common lower shunt of the EMP-pathway were determined at 80°C (optimal growth temperature) in crude extracts of *S. solfataricus* cells grown at different temperatures (65°C, 70°C and 80°C; Tab. 10).

As described in this study there are at least two GDH isoenzymes (SSO3003, SSO3204) with different substrate and co-substrate preferences. The crude extract measurements were performed with glucose and galactose as substrates and NAD^+ and $NADP^+$ as cosubstrates. Unfortunately, it is not possible to compare the kinetic properties of recombinant enzymes with those determined in crude extracts. But when the general trend of substrate and co-substrate usage of the GDH reaction is considered it can be suggested that at least a third GDH isoenzyme or a specific galactose dehydrogenase is present in the *S. solfataricus* genome. GDH-2 does not catalyze galactose with high efficiency and GDH-1 does not show big differences in kinetic properties between galactose with NAD^+ and with $NADP^+$ (Milburn et al., 2006). There seems to be a gap that could be filled by a galactose dehydrogenase that prefers NAD^+ as cosubstrate or another GDH isoenzyme which catalyzes multiple substrates, similar to GDH-1. A relatively high GDH activity with 0.57 U/mg with the substrate galactose and the co-substrate NAD^+ compared with 0.91 U/mg with glucose and NAD^+ was determined in *S. solfataricus* crude extracts. Indeed, there are several members of the alcohol/polyol/sugar dehydrogenase superfamily annotated in the *S. solfataricus* genome (Fig. 21), which could be candidates for arabinose dehydrogenases, xylose dehydrogenases and galactose dehydrogenases (Fig. 23).

One of the challenges in Systems Biology is to obtain experimental data for the different rate parameters for a reaction kinetic model. An important part of the SulfoSYS –project (Albers et al., 2010) is the determination of rate parameters both from extracts and from recombinant enzymes. From the relative abundances of protein levels in *S. solfataricus* recently determined by Snijders et al. (2006), and from an absolute concentration estimate of glyceraldehyde-3-phosphate dehydrogenase performed by Russo et al. (1995), concentrations were estimated by Ruoff et al. (2011, manuscript in preparation). The collected kinetic data of activities in crude extracts, as well as of recombinant expressed enzymes was used to establish the first kinetic CCM model for an archaeal thermoacidophilic organism (Ruoff et al., manuscript in preparation; Kouril et al., manuscript accepted). The

preliminary established model can be found under the following link: http://jjj.biochem.sun.ac.za/sysmo/models/Sulfo-Sys/index.html

Compared with a similar model established for the organism *S.cerevisiae* (http://jjj.biochem.sun.ac.za/database/index.html) a basic insight during the construction of the model which uses transcriptotomic, proteomic, metabolomic and kinetic data, is that the capacity of regulation of the CCM in *S. solfataricus* is lower than expected. This raises questions about how the metabilc network is then regulated. This study shows how the properties of enzymes, like the K_m and the catalytic efficiency, are considerably influenced by the change of temperatures and the effect at each enzyme is different (K_m: ENO 65°C 0.538mM PEP 80°C 0.392 mM PEP, PGAM 65°C 0.04 mM 3-PG 80°C 0.11 mM 3-PG).

This leeds to the assumtion that a metabolic network can adapt to high temperatures specifically challenged by instability of intermediates by regulating the amount of intermediates and the flux through the pathway, mainly by the kinetic properties of enzymes. These experiments show that not only protein and membrane stability plays an important role for the adaptation of life at high temperatures, but also stability of metabolic intermediates is essential. As some substrates, like PEP, GAP, DHAP and 1.3BPG decrease rapidly at 80°C, an adjustment of the metabolic network can achieve that these intermediate are only present for a short time or in small amounts, so its decay can be minimized.

Results summarized in Table 16 reveal insights into the relationship of substrate affinity and temperature of other glycolytic SSO enzymes, e.g. GAPN SSO3194 and GAPDH SSO0528 towards GAP. Both enzymes metabolize GAP in catabolic direction of the branched ED pathway. At optimum growth conditions of *S. solfataricus* (80°C) (Zillig et al., 1980) substrate affinity of GAPDH is almost 80 % lower as compared to that of GAPN, suggesting a preference of GAP catalysis by GAPN (Kouril et al., unpublished data; Esser et al., unpublished data).

In this study, which focuses on PEP, it was analyzed to which compounds the ED intermediate degrades at high temperatures and it could be reveald that the only product of PEP decay is pyruvate, which is basically the same reaction that is catalyzed by the enzyme PK but without gaining ATP. *S. solfataricus* relies on aerobic respiration and therfore most of the energy in the ED-pathway of *S. solfataricus* is gained in form of NADH and NADPH, however, it is hard to believe that the organism would sacrify the energy of one ATP for each PEP molecule.

Tab. 16: Substrate affinity (K_m (mM)) of GAPDH SSO0528, GK SSO0666, PK SSO0981 and GAPN SSO3194 in the catabolic direction and enolase SSO0913 and iPGAM SSO0417 in the catabolic and anabolic direction. All enzymes originated from *S. solfataricus* and were recombinantly expressed in *E. coli.* To date unpublished K_m-values of SSO0528, SSO0666, SSO0981 and SSO3194 were supplied by Esser et al., and Kouril et al., respectively. Arrows indicate decreasing substrate affinity.

	K_m (mM) catabolic direction						**K_m (mM) anabolic dir.**		
Temp.	**GAPDH**	**Enolase**	**PGAM**	**PK**	**GK**	**GAPN**	**Enolase**	**PGAM**	**PEPS**
	SSO0528	**SSO0913**	**SSO0417**	**SSO0981**	**SSO0666**	**SSO3194**	**SSO0913**	**SSO0417**	SSO0883
50°C	-	-	-	0.225	-	-	-		
60°C	1.000	-		-	-	1.430	0.451		
65°C	1.130	0.060	0.04	0.115	2.340	1.460	0.538	0.26	0.273
70°C	1.870	0.167	0.10	0.093	1.300	1.510	0.419	0.15	0.323
80°C	4.900	0.185	0.11	0.260	0.700	1.000	0.392	0.11	
88°C	7.800	0.192		-	-	0.660	-		

More importantly, table 16 also shows the trend of K_m-values obtained from different recombinant enzymes of *S. solfataricus*. Enolase SSO0913 characterization revealed increasing K_m-values and therefore reduced affinity for its substrate 2-PG with increasing assay temperature. Most other enzymes of the *S. solfataricus* ED pathway characterized so far glycerate kinase (GK) SSO0666, PK SSO0981 and GAPN SSO03194 including enolase SSO0913 (in anabolic direction) show opposite or fluctuant behaviour (Tab. 16). Enolase therefore takes an exceptional position among *S. solfataricus* glycolytic enzymes with respect to substrate affinity under temperature variation in the catabolic direction. Interestingly, the catalytic efficiency of enolase in catabolic direction is not influenced significantly by temperature change, but rises with factor two from 58.88 $mM^{-1}s^{-1}$ at 65°C to 110.79 $mM^{-1}s^{-1}$ at 80°C.

The idea in this case is that the PEP producing step (ENO) is slowed down at higher temperatures while the PEP consuming step (PK) is accelerated at the same time, resulting in a relatively low concentration of PEP at high temperatures. The analyzed properties of the presented enzymes show, how metabolic thermoadaptation is achieved and the studied intermediate stabilities show that a mechanism to protect these intermediates from heat dependent decay is essential.

5 Summary

Within the *Sulfolobus* Systems Biology (“SulfoSYS”) project the effect of temperature on a metabolic network is investigated at transcriptomic, metabolomic, proteomic and enzyme level. *S. solfataricus* utilizes an unusual branched Entner-Doudoroff (ED) pathway for sugar degradation that is promiscuous for glucose and galactose.

As a part of the SulfoSYS project, this work focuses on the characterization of the following enzymes: glucose dehydrogenase (GDH-2, SSO3204), phosphoglycerate mutases (iPGAM, SSO0417 and dPGM, SSO2236), enolase (ENO, SSO0913), pyruvate kinase (PK, SSO0981), phosphoenolpyruvate synthetase (PEPS, SSO0831), pyruvate dikinase (PPDK, SSO2820) comprising cloning, expression and detailed analysis at different temperatures ranging from 50°C to 88°C. Furthermore, cell free extracts of *S.solfataricus* cells, grown at the temperatures 65°C, 70°C and 80°C, were prepared and analyzed for activity. In addition, temperature dependent stability of metabolic intermediates was detrmined. GDH-2, ENO, PK and PEPS, only annotated as putative enzymes in the *S. Solfataricus* genome, were confirmed as functional enzymes and characterized in detail.

S. solfataricus iPGAM was confirmed to exhibit activity in the anabolic direction in addition to the already known catabolic direction. The comparison of kinetic parameters suggests that GDH-2 might represent the major player in glucose catabolism via the branched ED pathway, while GDH-1 might have a role in the degradation of a variant of different sugars. The kinetic parameters of iPGAM, ENO, PK and PEPS show interesting trends regarding temperature change. Each enzyme behaves differently to changing temperature. It was shown that the metabolic intermediates PEP, NADH and NADPH are heat instable. Therefore a metabolic thermoadaptation strategy is essential for the organism.

These findings, combined with the fact that the enzymes ENO and iPGAM have a different preference for the anabolic and the catabolic direction of the respective reaction, suggests a metabolic thermo adaptation by the control of flux of intermediates. The PEP producing step (ENO) is slowed down at higher temperatures while the PEP consuming step (PK) is accelerated at the same time, resulting in a relatively small amount of PEP at higher temperatures. Additionally, the PEP conversion to 2-PG by ENO is preferred at high temperatures. With changing

catalytic parameters at different temperatures, this might allow the organism to keep pools of heat instable compounds small in order to avoid their decay.

Furthermore, cell free extracts of *S. solfataricus* cells, grown at the temperatures 65°C, 70°C and 80°C, were analyzed for activity and in addition the temperature dependent stability of metabolic intermediates was investigated. Considering the general trend of substrate and co-substrate usage of the GDH reaction in *S. solfataricus* crude extracts it can be suggested that at least a third GDH isoenzyme or a specific galactose dehydrogenase is present in SSO.

Kinetic data of activities in crude extracts, as well as of recombinant expressed enzymes were used to establish the first kinetic CCM model for an archaeal thermoacidophilic organism, which can be found at the following link:

http://jjj.biochem.sun.ac.za/sysmo/models/Sulfo-Sys/index.html

Zusammenfassung:

Im Rahmen des Sulfosys-Projekts wird die Auswirkung von Temperaturänderung auf ein metabolisches netzwerk auf Transcriptom, Metabolom, Proteom und Enzymebene untersucht. *S. solfataricus* nutzt einen ungewöhnlich verzweigten Entner-Doudoroff (ED) Weg für den Zuckerabbau, der sowohl Glukose als auch Galaktose verarbeitet. Als Teil des SulfoSYS-Projekts konzentriert sich diese Arbeit auf die Charakterisierung der folgenden Enzyme Glucose-Dehydrogenase (GDH-2, SSO3204), Phosphoglycerat Mutasen (iPGAM, SSO0417 und dPGM, SSO2236), Enolase (ENO, SSO0913), Pyruvatkinase (PK, SSO0981), Phosphoenolpyruvat-Synthetase (PEPS, SSO0831), Pyruvat Dikinase (PPDK, SSO2820), bestehend aus Klonierung, Expression und detallierter Analyse der Aktivität bei verschiedenen Temperaturen zwischen 50°C bis 88°C. Darüber hinaus wurden zellfreie Extrakte aus *S. solfataricus* Zellen hergestellt die bei den Temperaturen 65°C, 70°C und 80°C gewachsen sind und auf Enzymaktivitäten hin untersucht. Des Weiteren wurden temperaturabhängige Stabilitäten von Intermediaten bestimmt. GDH-2, ENO, PK und PEPS waren nur als putative enzyme im *S. solfataricus* Genom annotiert, diese wurden im Detail charakterisiert und konnten in dieser Arbeit als funktionelle Enzyme bestätigt werden. Für die *S. solfataricus* iPGAM konnte gezeigt werden dass diese zusätzlich zur bereits bekannten katabolen auch in die anabole Richtung aktiv ist. Der Vergleich kinetischer Parameter zeigt, dass GDH-2 den Grossteil der Verarbeitung von Glukose übernimmt, während GDH-1 flexibler ist und eine ganze Reihe an verschiedenen Zuckern als Substrat nutzt. Die kinetischen Parameter von iPGAM, ENO, PK und PEPS weisen interessante Trends bezüglich der Temperaturänderung auf und zeigen dass jedes der untersuchten Enzyme unterschiedlich auf die Änderung der Temperatur reagiert. Es konnte gezeigt werden, dass die Intermediate PEP, NADH und NADPH hitzelabil sind, wodurch eine metabolische Thermoadaptionsstrategie für den Organismus *S. solfataricus* notwendig ist. Diese Erkentnisse und die Tasache, dass iPGAM und ENO unterschiedliche Präferenzen in anaboler und kataboler Richtung der Enzymreaktion aufweisen, legt eine Anpassung an hohe Temperaturen nahe, bei der der Flux von hitzelabilen Intermediaten gesteuert wird. Die Produktion von PEP durch ENO wird bei hohen Temperaturen verlangsamt und gleichermassen die umwandlung von PEP zu pyruvat beschleunigt, wodurch kleinere Mengen des hitzelabilen Intermdiats PEP der hohen Temperatur ausgesetzt sind. Darüber hinaus wird die anabole Reaktion

von PEP hin zum hitzestabilen 2-PG bei höheren Temperaturen bevorzugt. Die Untersuchungen der zellfreien Extrakte von *S. solfataricus* Zellen weist eine Substrat und Co-substratnutzung der GDH-Reaktion auf, die vermuten lässt das noch ein weiteres Enzym an dieser Reaktion beteiligt ist, möglicherweise eine Galaktose Dehydrogenase oder ein drittes GDH-Isoenzym.

Die kinetischen Parameter aus zellfreien Extrakten und rekombinant exprimierten Enzymen wurden zur erstellung des ersten kinetischen ZKM Modell für einen thermoacidophilen Archaeum verwendet. Ziel des Projektes ist, eine ausreichend präzise Nachbildung des ZKM von *S. solfataricus* („Silicon Cell“) zu erstellen, die es erlaubt, die Robustheit des Netzwerkes gegenüber Temperaturveränderungen zu berechnen und modellieren.

Das Modell ist unter folgendem Link zu finden:

http://jjj.biochem.sun.ac.za/sysmo/models/Sulfo-Sys/index.html

6 Literature

Ahmed, H., T. J. Ettema, et al. (2005). "The semi-phosphorylative Entner-Doudoroff pathway in hyperthermophilic archaea: a re-evaluation." Biochem J **390**(Pt 2): 529-540.

Albers, S. V., N. K. Birkeland, et al. (2009). "SulfoSYS (Sulfolobus Systems Biology): towards a silicon cell model for the central carbohydrate metabolism of the archaeon Sulfolobus solfataricus under temperature variation." Biochem Soc Trans **37**(Pt 1): 58-64.

Anemuller, S. and G. Schafer (1990). "Cytochrome aa3 from Sulfolobus acidocaldarius. A single-subunit, quinol-oxidizing archaebacterial terminal oxidase." Eur J Biochem **191**(2): 297-305.

Antikainen, J., Kuparinen V., et al (2007). „Enolases from Gram-positive bacterial pathogens and commensal lactobacilli share functional similarity in virulence-associated traits. FEMS Immunol Med Microbiol 2007, **51**: 526-534

Barns, S. M., C. F. Delwiche, et al. (1996). "Perspectives on archaeal diversity, thermophily and monophyly from environmental rRNA sequences." Proc Natl Acad Sci U S A **93**(17): 9188-9193.

Bernhardt, G., R. Jaenicke, et al. (1988). "High Pressure Enhances the Growth Rate of the Thermophilic Archaebacterium Methanococcus thermolithotrophicus without Extending Its Temperature Range." Appl Environ Microbiol **54**(5): 1258-1261.

Boyer, P. D., M. Deluca, et al. (1962). "Identification of phosphohistidine in digests from a probable intermediate of oxidative phosphorylation." J Biol Chem **237**: PC3306-PC3308.

Bradford, M. M. (1976). "A rapid and sensitive method for the quantitation of microgram quantities of protein utilizing the principle of protein-dye binding." Anal Biochem **72**: 248-254.

Brochier-Armanet, C., B. Boussau, et al. (2008). "Mesophilic Crenarchaeota: proposal for a third archaeal phylum, the Thaumarchaeota." Nat Rev Microbiol **6**(3): 245-252.

Brouns, S. J., J. Walther, et al. (2006). "Identification of the missing links in prokaryotic pentose oxidation pathways: evidence for enzyme recruitment." J Biol Chem **281**(37): 27378-27388.

Budd, G. E. (2001). "Why are arthropods segmented?" Evol Dev **3**(5): 332-342.

Chong, P. K., A. M. Burja, et al. (2007). "Proteome and transcriptional analysis of ethanol-grown *Sulfolobus solfataricus* P2 reveals ADH2, a potential alcohol dehydrogenase." J Proteome Res **6**(10): 3985-3994.

Cooper, R. A. and H. L. Kornberg (1965). "Net formation of phosphoenolpyruvate from pyruvate by Escherichia coli." Biochim Biophys Acta **104**(2): 618-620.

Eyzaguirre, C. and L. Monti-Bloch (1982). "Nicotinic and muscarinic reactive sites in mammalian glomus cells." Brain Res **252**(1): 181-184.

Fothergill-Gilmore, L. A. and H. C. Watson (1990). "Phosphoglycerate mutases." Biochem Soc Trans **18**(2): 190-193.

Gerlt, J. A. and P. C. Babbitt (2001). "Divergent evolution of enzymatic function: mechanistically diverse superfamilies and functionally distinct suprafamilies." Annu Rev Biochem **70**: 209-246.

Giardina, P., M. G. de Biasi, et al. (1986). "Glucose dehydrogenase from the thermoacidophilic archaebacterium *Sulfolobus solfataricus*." Biochem J **239**(3): 517-522.

Gribaldo, S. and C. Brochier-Armanet (2006). "The origin and evolution of Archaea: a state of the art." Philos Trans R Soc Lond B Biol Sci **361**(1470): 1007-1022.

Grogan, D. W. (1989). "Phenotypic characterization of the archaebacterial genus Sulfolobus: comparison of five wild-type strains." J Bacteriol **171**(12): 6710-6719.

Guerra, D. G., D. Vertommen, et al. (2004). "Characterization of the cofactor-independent phosphoglycerate mutase from Leishmania mexicana mexicana. Histidines that coordinate the two metal ions in the active site show different susceptibilities to irreversible chemical modification." Eur J Biochem **271**(9): 1798-1810.

Haferkamp, P., S. Kutschki, et al. (2011). "An additional glucose dehydrogenase from *Sulfolobus solfataricus*: fine-tuning of sugar degradation?" Biochem Soc Trans **39**(1): 77-81.

Huber, H., M. J. Hohn, et al. (2002). "A new phylum of Archaea represented by a nanosized hyperthermophilic symbiont." Nature **417**(6884): 63-67.

Hurth, C., C. Tassius, et al. (2007). "Enzymatic activity of immobilized yeast phosphoglycerate kinase." Biosens Bioelectron **22**(11): 2449-2455.

Huson, D. H. and D. Bryant (2006). "Application of phylogenetic networks in evolutionary studies." Mol Biol Evol **23**(2): 254-267.

Hutschins, A. H., Holden, J.F., et al. (2001). “Phosphoenolpyruvate synthase from the hyperthermophilic archaeon *Pyrococcus furiosus*.” J Bacteriol 183, 709-715

Imanaka, H. A. Yamatsu et al. (2006). “Phosphoenolpyruvate synthase plays an essential role for glycolysis in the modified Embden-Meyerhof pathway in *Thermococcus kodakarensis*.“ Mol Microbiol **61** (4): 898-909

Jedrzejas, M. J., M. Chander, et al. (2000). "Structure and mechanism of action of a novel phosphoglycerate mutase from Bacillus stearothermophilus." EMBO J **19**(7): 1419-1431.

Johnsen, U., M. Dambeck, et al. (2009). "D-xylose degradation pathway in the halophilic archaeon Haloferax volcanii." J Biol Chem **284**(40): 27290-27303.

Johnsen, U., T. Hansen, et al. (2003). "Comparative analysis of pyruvate kinases from the hyperthermophilic archaea Archaeoglobus fulgidus, Aeropyrum pernix, and Pyrobaculum aerophilum and the hyperthermophilic bacterium Thermotoga maritima: unusual regulatory properties in hyperthermophilic archaea." J Biol Chem **278**(28): 25417-25427.

Johnsen, U. and P. Schonheit (2007). "Characterization of cofactor-dependent and cofactor-independent phosphoglycerate mutases from Archaea." Extremophiles **11**(5): 647-657.

Kardinahl, S., C. L. Schmidt, et al. (1999). "The strict molybdate-dependence of glucose-degradation by the thermoacidophile Sulfolobus acidocaldarius reveals the first crenarchaeotic molybdenum containing enzyme--an aldehyde oxidoreductase." Eur J Biochem **260**(2): 540-548.

Kastarinen, M., R. Antikainen, et al. (2009). "Prevalence, awareness and treatment of hypertension in Finland during 1982-2007." J Hypertens **27**(8): 1552-1559.

Kates, M., N. Moldoveanu, et al. (1993). "On the revised structure of the major phospholipid of Halobacterium salinarium." Biochim Biophys Acta **1169**(1): 46-53.

Kehrer, D., H. Ahmed, et al. (2007). "Glycerate kinase of the hyperthermophilic archaeon Thermoproteus tenax: new insights into the phylogenetic distribution and physiological role of members of the three different glycerate kinase classes." BMC Genomics **8**: 301.

Koonin, E. V. (2003). "Horizontal gene transfer: the path to maturity." Mol Microbiol **50**(3): 725-727.

Lamble, H. J., N. I. Heyer, et al. (2003). "Metabolic pathway promiscuity in the archaeon *Sulfolobus solfataricus* revealed by studies on glucose dehydrogenase and 2-keto-3-deoxygluconate aldolase." J Biol Chem **278**(36): 34066-34072.

Lamble, H. J., A. Theodossis, et al. (2005). "Promiscuity in the part-phosphorylative Entner-Doudoroff pathway of the archaeon *Sulfolobus solfataricus*." FEBS Lett **579**(30): 6865-6869.

Lee, D. S., J. Park, et al. (2008). "The implications of human metabolic network topology for disease comorbidity." Proc Natl Acad Sci U S A **105**(29): 9880-9885.

Londei, P. (2005). "Evolution of translational initiation: new insights from the archaea." FEMS Microbiol Rev **29**(2): 185-200.

McHarg, J., S. M. Kelly, et al. (1999). "Site-directed mutagenesis of proline 204 in the 'hinge' region of yeast phosphoglycerate kinase." Eur J Biochem **259**(3): 939-945.

Milburn, C. C., H. J. Lamble, et al. (2006). "The structural basis of substrate promiscuity in glucose dehydrogenase from the hyperthermophilic archaeon Sulfolobus solfataricus." J Biol Chem **281**(21): 14796-14804.

Nunn, C. E., U. Johnsen, et al. (2010). "Metabolism of pentose sugars in the hyperthermophilic archaea *Sulfolobus solfataricus* and Sulfolobus acidocaldarius." J Biol Chem **285**(44): 33701-33709.

Pal-Bhowmick, I., K. Sadagopan, et al. (2004). "Cloning, over-expression, purification and characterization of Plasmodium falciparum enolase." Eur J Biochem **271**(23-24): 4845-4854.

Pal-Bhowmick, I., H. K. Vora, et al. (2006). "Generation and characterisation of monoclonal antibodies specific to Plasmodium falciparum enolase." J Vector Borne Dis **43**(2): 43-52.

Potter, S. and L. A. Fothergill-Gilmore (1992). "The pyruvate kinase of Thermoplasma acidophilum: purification, kinetic characterisation & use as a phylogenetic marker." Biochem Soc Trans **20**(1): 11S.

Potters, M. B., B. T. Solow, et al. (2003). "Phosphoprotein with phosphoglycerate mutase activity from the archaeon *Sulfolobus solfataricus*." J Bacteriol **185**(7): 2112-2121.

Qin, J., G. Chai, et al. (2006). "Fluoride inhibition of enolase: crystal structure and thermodynamics." Biochemistry **45**(3): 793-800.

Rigden, D. J. (2008). "The histidine phosphatase superfamily: structure and function." Biochem J **409**(2): 333-348.

Riveros-Rosas, H., A. Julian-Sanchez, et al. (2003). "Diversity, taxonomy and evolution of medium-chain dehydrogenase/reductase superfamily." Eur J Biochem **270**(16): 3309-3334.

Ronimus R. and H.W. Morgan (2002). " Distribution and phylogenies of enzymes of the Embden-Mayerhof-Parnas pathway from archaea and hyperthermophilic bacteria support a gluconeogenic origin of metabolism." Archaea **1**: 199-221

Russo, A. D., R. Rullo, et al. (1995). "Glyceraldehyde-3-phosphate dehydrogenase in the hyperthermophilic archaeon *Sulfolobus solfataricus*: characterization and significance in glucose metabolism." Biochem Mol Biol Int **36**(1): 123-135.

Sanger, F., S. Nicklen, et al. (1977). "DNA sequencing with chain-terminating inhibitors." Proc Natl Acad Sci U S A **74**(12): 5463-5467.

Schramm, A., B. Siebers, et al. (2000). "Pyruvate kinase of the hyperthermophilic crenarchaeote Thermoproteus tenax: physiological role and phylogenetic aspects." J Bacteriol **182**(7): 2001-2009.

Selig, M., K. B. Xavier, et al. (1997). "Comparative analysis of Embden-Meyerhof and Entner-Doudoroff glycolytic pathways in hyperthermophilic archaea and the bacterium Thermotoga." Arch Microbiol **167**(4): 217-232.

Seweryn, E., I. S. Bednarz-Misa, et al. (2008). "Distribution of beta-enolase in normal and tumor rat cells." Folia Histochem Cytobiol **46**(4): 519-524.

She, Q., R. K. Singh, et al. (2001). "The complete genome of the crenarchaeon *Sulfolobus solfataricus* P2." Proc Natl Acad Sci U S A **98**(14): 7835-7840.

Siebers, B. and P. Schonheit (2005). "Unusual pathways and enzymes of central carbohydrate metabolism in Archaea." Curr Opin Microbiol **8**(6): 695-705.

Sims, P. A., T. M. Larsen, et al. (2003). "Reverse protonation is the key to general acid-base catalysis in enolase." Biochemistry **42**(27): 8298-8306.

Snijders, A. P., J. Walther, et al. (2006). "Reconstruction of central carbon metabolism in *Sulfolobus solfataricus* using a two-dimensional gel electrophoresis map, stable isotope labelling and DNA microarray analysis." Proteomics **6**(5): 1518-1529.

Szymona, M. and M. Doudoroff (1960). "Carbohydrate metabolism in Rhodopseudomonas sphreoides." J Gen Microbiol **22**: 167-183.

Theodossis, A., H. Walden, et al. (2004). "The structural basis for substrate promiscuity in 2-keto-3-deoxygluconate aldolase from the Entner-Doudoroff pathway in *Sulfolobus solfataricus*." J Biol Chem **279**(42): 43886-43892.

Tjaden, B., A. Plagens, et al. (2006). "Phosphoenolpyruvate synthetase and pyruvate, phosphate dikinase of Thermoproteus tenax: key pieces in the puzzle of archaeal carbohydrate metabolism." Mol Microbiol **60**(2): 287-298.

Tuininga, J. E., et al (2003). “Pyruvate kinase and phosphoenolpyruvate synthase from Pyrococcus furiosus and their role in the modified Embden-Mayerhof pathway.” Enzymology and bioenergetics of the glycolytic pathway of *Pyrococcus furiosus* CH.**5** 73-100

van der Oost, J., M. A. Huynen, et al. (2002). "Molecular characterization of phosphoglycerate mutase in archaea." FEMS Microbiol Lett **212**(1): 111-120.

Woese, C. R., O. Kandler, et al. (1990). "Towards a natural system of organisms: proposal for the domains Archaea, Bacteria, and Eucarya." Proc Natl Acad Sci U S A **87**(12): 4576-4579.

Zaparty, M., D. Esser, et al. (2010). ""Hot standards" for the thermoacidophilic archaeon *Sulfolobus solfataricus*." Extremophiles **14**(1): 119-142.

Zhang, G., J. Dai, et al. (2005). "Catalytic cycling in beta-phosphoglucomutase: a kinetic and structural analysis." Biochemistry **44**(27): 9404-9416.

Zillig, W., K. O. Stetter, et al. (1979). "DNA-dependent RNA polymerase from the archaebacterium Sulfolobus acidocaldarius." Eur J Biochem **96**(3): 597-604.

7 Appendix

7.1 Abbreviations

A. bidest	Aqua bidestillata = two times distilled water
aa	Amino acid
APS	Ammonium persulfate
bp	Base pair
BSA	Bovine serum albumin
ca.	circa = about, around
CE	Crude extract fraction
CIP	Calf intestinal phosphatase
DMSO	Dimethyl sulfoxide
DNA	Deoxyribonucleic acid
dNTP	Desoxy-nucleotide triphosphate
DTT	dithiothreitol
ε	Extension coefficient
ED	Entner-Doudoroff pathway
EDTA	Ethylene diamine tetraacetic acid
EMP	Embden-Meyerhof-Parnas pathway
et al.	et alii = and the others
etc.	et = cetera and so on
F1,6P	Fructose-1,6-bisphosphate
F6P	Fructose-6-phosphat
Fig	Figure
g	Gram
G1P	Glucose-1-phosphate
G6P	Glucose-6-phosphate
GA	Glyceraldehyde
GAD	Gluconate dehydratase
GAP	Glyceraldehyde 3-phosphate
GAPN	Non-phosphorylating glyceraldehyde-3-phosphate dehydrogenase
GAPOR	Glyceraldehyde-3-phosphate oxidoreductase
GDH	Glucose dehydrogenase
GF	Gel filtration fraction
h	Hour
HP	Heat precipitation fraction
i.e.	id est = that is, that is to say
IPTG	Isopropyl-ß-D-thiogalactopyranoside
Kb	Kilobase
kDa	Kilodalton
KDG	2-keto-3-deoxygluconate
KDGA	KDG aldolase
KDGal	2-keto-3-deoxygalactonate
KDGK	KDG kinase
KDPG	2-keto-3-deoxy-6-phosphogluconate
KD(P)GA	KD(P)G aldolase
KDPGal	2-keto-3-deoxy-6-phosphogalactonate
K_m	Michaelis constant

L	Liter
LB	Luria-Bertani
LDH	Lactate dehydrogenase
m	milli (10-3)
M	molar (mol/l)
mA	Milliampere
min	Minute
MW	Molecular weight
NAD+	Nicotinamid-adenin-dinucleotid (oxidized)
NADH	Nicotinamid-adenin-dinucleotid (reduced)
NADP+	Nicotinamid-adenin-dinucleotid-phosphate (oxidized)
NADPH	Nicotinamid-adenin-dinucleotid-phosphate (reduced)
NCBI	National Center for Biotechnology Information
OD	Optical density
PAGE	Polyacrylamide gel electrophoresis
PCR	polymerase chain reaction
PEP	Phosphoenolpyruvate
PEPS	Phosphoenolpyruvate Synthetase
pH	Negative logarithm of the hydrogen ion (H+) concentration
Pi	Inorganic Phosphate
PK	Pyruvate Kinase
PPDK	Pyruvate, Phosphate Dikinase
PPi	Inorganic Pyrophosphate
Psi	Pounds per square inch
RNA	ribonucleic acid
Rnase	Ribonuclease
rRNA	ribosomal RNA
RT	Room temperature
SDS	sodiumdodecylsulfate
Sec	Seconds
Sp.	Species
Tab	Table
TAE	Tris-Acetat-EDTA-buffer
Taq-Polymerase	DNA-Polymerase from Thermus aquaticus
TEMED	N,N,N',N'-Tetramethylethylenediamine
Tris	Tris-(hydroxymethyl)-aminomethane
U	Unit = Enzyme activity
UV	Ultraviolet
v	Velocity
V	Volt
V_{max}	Maximal velocity
Vol	Volume
W	Watt
x g	Gravitational acceleration
µ	micro (10^{-6})

7.2 Publikationsliste

Haferkamp P, Kutschki S, Treichel J, Hemeda H, Sewczyk K, Hoffmann D, Zaparty M, Siebers B. (2011) An additional glucose dehydrogenase from *Sulfolobus solfataricus*: fine-tuning of sugar degradation? Biochem Soc Trans. Jan 19;39(1): 77-81.

Zaparty M, Esser D, Gertig S, Haferkamp P, Kouril T, Manica A, Pham TK, Reimann J, Schreiber K, Sierocinski P, Teichmann D, van Wolferen M, von Jan M, Wieloch P, Albers SV, Driessen AJ, Klenk HP, Schleper C, Schomburg D, van der Oost J, Wright PC, Siebers B. (2010) "Hot standards" for the thermoacidophilic archaeon *Sulfolobus solfataricus*. Extremophiles. 14(1):119-42. Epub 2009 Oct 4.

Albers SV, Birkeland NK, Driessen AJ, Gertig S, Haferkamp P, Klenk HP, Kouril T, Manica A, Pham TK, Ruoff P, Schleper C, Schomburg D, Sharkey KJ, Siebers B, Sierocinski P, Steuer R, van der Oost J, Westerhoff HV, Wieloch P, Wright PC, Zaparty M. (2009) SulfoSYS (Sulfolobus Systems Biology): towards a silicon cell model for the central carbohydrate metabolism of the archaeon *Sulfolobus solfataricus* under temperature variation.Biochem Soc Trans. 37(Pt 1):58-64.

Mentel M, Zimorski V, Haferkamp P, Martin W, Henze K. (2008) Protein import into hydrogenosomes of *Trichomonas vaginalis* involves both N-terminal and internal targeting signals: a case study of thioredoxin reductases. Eukaryot Cell. 7(10):1750-7.

Vorträge

24.11.2008 SulfoSYS-Meeting (Essen,Germany)
"Silicon Cell Model for the central carbohydrate metabolism of the archaeon *Sulfolobus solfataricus* under temperature variation: Unravelling the central carbohydrate metabolism of *S. solfataricus"*
P.Haferkamp (AG Siebers)

Poster

01.-02.07.2008 Evaluation Conference SysMO (Bad Honnef)

SulfoSYS- Biochemical and kinetic characterization of enzymes in the central carbohydrate metabolism of *Sulfolobus solfataricus*: Temperature effect on enzyme regulation
M. Zaparty, T. Kouril, P. Haferkamp, P. Sierocinski, J. Van der Oost and B. Siebers

13.9.2008	Annual Retreat of the DFG Graduaten Training Programm (Dormagen-Zons) Biochemical analyses of the central carbohydrate metabolism of *Sulfolobus solfataricus* in response to temperature change Thomas Kipper, Patrick Haferkamp, Melanie Zaparty, Bettina Siebers & SulfoSYS consortium
19- 20.05.2009	2nd Evaluation Conference SysMO (Vienna, Austria) SulfoSYS- Identification of players in the CCM network of *S. solfataricus* T. Kouril, D. Esser, M. Zaparty, P. Haferkamp, J. Reimann, S.-V. Albers and B. Siebers
19- 20.05.2009	2nd Evaluation Conference SysMO (Vienna, Austria) The effect of temperature change on CCM enzyme activities in crude extracts of *S.solfataricus* P. Haferkamp, T. Kouril, M. Zaparty, P. Sierocinski, J. von der Oost B. Siebers
28- 31.03.2010	VAAM Hannover „Hot spots“ of thermoadaptation the central carbohydrate metabolism of *Sulfolobus solfataricus* P. Haferkamp, T. Kipper, M. Zaparty, B. Siebers& SulfoSYS consortium

Der Lebenslauf ist in der Online-Version aus Gründen des Datenschutzes nicht enthalten.

7.4 Erklärung

Hiermit versichere ich, dass ich die vorliegende Arbeit mit dem Titel

„Biochemical studies of enzymes involved in glycolysis of the thermoacidophilic crenarchaeon *S. solfataricus* "

selbst verfasst und keine außer den angegebenen Hilfsmitteln und Quellen benutzt habe, und dass die Arbeit in dieser oder ähnlicher Form noch bei keiner anderen Universität eingereicht wurde.

Essen, im August 2011

7.8 Danksagung

Frau Prof. Dr. Bettina Siebers danke ich, für die Bereitstellung des Arbeitsplatzes im Institut für Molekulare Enzymtechnologie und Biochemie und des interessanten Themas und für die gute Bertreuung dieser Arbeit.

Herrn Prof. Dr. Daniel Hoffmann danke ich für die Übernahme des Korreferats.

Ich danke allen Mitarbeitern der AG Siebers für ihre Unterstützung, da mir jeder einzelne bei dem einen oder anderen Problem geholfen hat. Insbesondere danke ich Melanie Zaparty für die quasi Betreuung und meinen Büronachbarn Theresa Kouril, Dominik Esser und Kohei Matsubara für die entspannte und unterhaltsame „Arbeits“-atmosphäre.

Ich danke auch Jeanette Marrero für die Unterstützung bei der Laborarbeit.

Ich danke allen, die mir durch Korrekturlesen, Hilfestellungen, Diskussionen oder Ratschläge beim erstellen dieser Arbeit geholfen haben.